CHAPTER 22

RADIATION COMBINED WITH CONDUCTION AND CONVECTION

22.1 INTRODUCTION

In our analyses of radiative transfer in participating media we have, up to this point, always assumed that there was no interaction with other modes of heat transfer, i.e., we have limited ourselves to cases of radiative equilibrium and cases of specified temperature fields. In practical systems, of course, it is nearly always the case that radiation occurs in conjunction with conduction and/or convection, and two or three heat transfer modes must be accounted for simultaneously. In such cases overall conservation of energy, equation (10.72), needs to be solved, which always leads to a nonlinear integro-differential equation.

Many important applications of interactions between radiation and other modes of heat transfer have been reported in the literature. Discussion of all of these could easily, by itself, fill a book as voluminous as this one. We will therefore limit ourselves here to the discussion of a few very basic cases (*i*) to show the basic trends of how the different modes of heat transfer interact with one another, and (*ii*) to outline some of the numerical schemes that have been used to solve such problems. We will begin with two sections that deal with combined radiation and conduction in participating media, the latter one including change-of-phase effects. Combined radiation and convection is treated in several subsequent sections, the first three dealing with simple external and internal flows, as well as natural convection. Separate sections have been devoted to more advanced topics, such as radiation in chemically reacting flows, numerical interfacing between convection, chemical reactions and radiation, and turbulence–radiation interactions.

For much of this chapter we will limit our theoretical developments to a simple plane-parallel geometry with a gray medium, since our aim is to investigate only the general trends of the interaction among the different modes of heat transfer. More advanced topics and applications, such as the multidimensional interaction of radiation with convection, turbulence, and chemical reactions will be outlined in order to understand the nature of such interactions, and a list of references for more in-depth study will be given.

22.2 COMBINED RADIATION AND CONDUCTION

Throughout the remainder of this chapter we will deal with the interaction of radiation with conduction and/or convection within an absorbing, emitting, and scattering medium. We start

in this section by discussing the interaction between radiation and conduction in a stationary, radiatively participating medium. Since we are primarily interested in general trends and in evaluation methods, we will limit ourselves here to the relatively simple example of steady-state heat transfer through a one-dimensional, absorbing–emitting (but not scattering) gray medium, confined between two parallel, isothermal, gray, diffusely emitting and reflecting plates.

The energy equation for simultaneous conduction and radiation in a participating medium is, from equation (10.72),

$$\rho c_v \frac{\partial T}{\partial t} = \nabla \cdot (k \nabla T) + \dot{Q}''' - \nabla \cdot \mathbf{q}_R. \tag{22.1}$$

For a one-dimensional, planar medium at steady state and without internal heat generation, this reduces to equation (10.73), or

$$\frac{d}{dz}\left(k\frac{dT}{dz} - q_R\right) = 0, \tag{22.2}$$

subject to the boundary conditions

$$z = 0: \quad T(0) = T_1, \tag{22.3a}$$

$$z = L: \quad T(L) = T_2. \tag{22.3b}$$

The radiative heat flux, or its divergence

$$\frac{dq_R}{dz} = \int_0^\infty \kappa_\eta (4\pi I_{b\eta} - G_\eta)\, d\eta, \tag{22.4}$$

may be obtained by any of the methods discussed in the preceding chapters.

For simplicity, we will assume that all properties are constant (i.e., thermal conductivity k, absorption coefficient κ, and refractive index n) and gray. Note that the assumption of a semitransparent medium implies that the absorptive index (also denoted by the letter k)—although directly related to the absorption coefficient—is negligible[1] in the evaluation of the blackbody intensity, i.e., $I_b = n^2\sigma T^4/\pi$. Introducing the nondimensional variables and parameters

$$\xi = \frac{z}{L}, \quad \theta = \frac{T}{T_1}, \quad \Psi_R = \frac{q_R}{n^2\sigma T_1^4}, \quad g = \frac{G}{4n^2\sigma T^4};$$

$$\tau_L = \kappa L, \quad \theta_L = \frac{T_2}{T_1}, \quad N = \frac{k\kappa}{4\sigma T_1^3},$$

reduces equations (22.2) through (22.4) to

$$\frac{d^2\theta}{d\tau^2} = \frac{1}{4N}\frac{d\Psi_R}{d\tau}, \tag{22.5}$$

$$\frac{d\Psi_R}{d\tau} = 4(\theta^4 - g), \tag{22.6}$$

$$\theta(0) = 1, \quad \theta(\tau_L) = \theta_L. \tag{22.7}$$

Here τ_L is the optical thickness of the medium, and N is known as the *conduction-to-radiation parameter*. For optically thick slabs ($\tau_L \gg 1$) N gives a good estimate of the relative importance of conductive and radiative heat fluxes: From equations (15.17) and (15.18),

$$\tau_L \gg 1: \quad \frac{q_C}{q_R} = \frac{-k\,\partial T/\partial z}{-k_R\,\partial T/\partial z} = \frac{k}{k_R} = \frac{3}{4}\frac{k\kappa}{4n^2\sigma T^4},$$

[1] See the discussion on the value of k in Section 3.5.

which gives the ratio of heat fluxes in terms of a *local* temperature. The situation is a little more complicated for optically thin situations ($\tau_L \ll 1$), for which the temperature field of the entire enclosure must be considered. For example, for an optically thin slab bounded by two black walls at T_1 and T_2, respectively, from equation (15.7),

$$\begin{aligned} \tau_L \ll 1: \quad q_R &\simeq n^2\sigma(T_1^4 - T_2^4) = 4n^2\sigma T_{\text{av}}^3(T_1 - T_2), \\ q_C &= -k\frac{\partial T}{\partial z} \simeq k(T_1 - T_2)/L, \\ \frac{q_C}{q_R} &\simeq \frac{k/L}{4n^2\sigma T_{\text{av}}^3} = \frac{1}{\tau_L}\frac{k\kappa}{4n^2\sigma T_{\text{av}}^3}. \end{aligned}$$

If, in an optically thin slab, emission from within the slab (rather than from its boundaries) dominates the radiative heat flux, then q_R becomes proportional to κ [cf. equation (10.54)], and

$$\tau_L \ll 1 \text{ (emission dominated)}: \frac{q_C}{q_R} = \mathcal{O}\left(\frac{N}{\tau_L^2}\right).$$

As representative examples for combined radiation and conduction in a slab, we will discuss here solutions for the radiative heat flux using the exact integral formulation (as presented in Chapter 14) and the differential or P_1-approximation (described in Sections 15.4 and 16.5). Similarly, equation (22.2) may be solved by a variety of numerical techniques. Since the equation is nonlinear (because of the T^4-dependence for the radiative heat flux), analytical solutions are not possible, and numerical schemes require an iterative solution. For illustrative purposes we will limit ourselves here to a finite-difference solution of equations (22.2) and (22.3).

Exact Formulation

The exact formulation for incident radiation G and radiative heat flux q_R for a one-dimensional slab with specified temperature distribution has been given by equations (14.53) and (14.54). For a nonscattering medium the radiative source term reduces to $S(\tau) = I_b(\tau) = n^2\sigma T^4(\tau)/\pi$ [as given by equation (14.52)], and the radiative heat flux, as given by equation (14.54), becomes, in nondimensional form,

$$\Psi_R(\tau) = 2\left\{\mathscr{J}_1 E_3(\tau) - \mathscr{J}_2 E_3(\tau_L - \tau) + \int_0^\tau \theta^4(\tau')E_2(\tau - \tau')\,d\tau' - \int_\tau^{\tau_L} \theta^4(\tau')E_2(\tau' - \tau)\,d\tau'\right\}, \quad (22.8)$$

where we have introduced the nondimensional radiosities $\mathscr{J}_i = J_i/n^2\sigma T_1^4$. Equation (22.8) may be integrated by parts, using the recursion relations of Appendix E, leading to

$$\begin{aligned} \Psi_R(\tau) = 2\Bigg\{&(\mathscr{J}_1 - 1)E_3(\tau) - (\mathscr{J}_2 - \theta_L^4)E_3(\tau_L - \tau) \\ &- \int_0^\tau \frac{d\theta^4}{d\tau'}(\tau')E_3(\tau - \tau')\,d\tau' - \int_\tau^{\tau_L} \frac{d\theta^4}{d\tau'}(\tau')E_3(\tau' - \tau)\,d\tau'\Bigg\}, \end{aligned} \quad (22.9)$$

and, using Leibniz's rule [1], as given by equation (3.107),

$$\begin{aligned} \frac{d\Psi_R}{d\tau} = 2\Bigg\{&(1 - \mathscr{J}_1)E_2(\tau) + (\theta_L^4 - \mathscr{J}_2)E_2(\tau_L - \tau) \\ &+ \int_0^\tau \frac{d\theta^4}{d\tau'}(\tau')E_2(\tau - \tau')\,d\tau' - \int_\tau^{\tau_L} \frac{d\theta^4}{d\tau'}(\tau')E_2(\tau' - \tau)\,d\tau'\Bigg\}. \end{aligned} \quad (22.10)$$

Equation (22.10) must be solved simultaneously with equation (22.5) and its boundary conditions (22.7). For nonblack surfaces two additional relations are required for the determination

of the radiosities $\mathscr{J}_1$ and $\mathscr{J}_2$. These may be obtained by applying equation (22.9) (evaluation of the radiative heat flux in terms of radiosities and medium temperature) at the two boundaries, eliminating the radiative heat flux through equation (14.48) (relating heat flux to radiosity and surface temperature). For the illustrative purposes of our present discussion, we will limit ourselves to black surfaces, i.e., $\mathscr{J}_1 = 1$ and $\mathscr{J}_2 = \theta_L^4$, and

$$\frac{d\Psi_R}{d\tau} = 2\left\{\int_0^{\tau} \frac{d\theta^4}{d\tau'}(\tau')E_2(\tau-\tau')\,d\tau' - \int_{\tau}^{\tau_L} \frac{d\theta^4}{d\tau'}(\tau')E_2(\tau'-\tau)\,d\tau'\right\}. \tag{22.11}$$

For this simple case, substitution of equation (22.11) into (22.5) gives a single nonlinear integro-differential equation for the unknown temperature, θ. Once the temperature field has been determined, the total heat flux follows as

$$q = -k\frac{dT}{dz} + q_R = \text{const},$$

or, in nondimensional form,

$$\Psi = \frac{q}{n^2\sigma T_1^4} = -4N\frac{d\theta}{d\tau} + \Psi_R = \text{const}. \tag{22.12}$$

Example 22.1. An absorbing–emitting medium is contained between two large, parallel, isothermal, black plates at temperatures T_1 and $T_2 = 0.5\,T_1$, respectively. Determine the steady-state temperature distribution within the medium and the total heat flux between the two plates, if heat is transferred by conduction and radiation. Discuss the influence of the conduction-to-radiation parameter, N, and of the optical thickness of the layer, τ_L.

Solution

The numerical solution to the governing equation may be found in a number of ways. We will employ here $J+1$ equally spaced nodes $\tau = 0, \Delta\tau, 2\Delta\tau, \ldots, J\Delta\tau = \tau_L$ with nodal temperatures θ_i $(i = 0, 1, 2, \ldots, J)$ and simple finite-differencing for the conduction term,

$$\frac{d^2\theta}{d\tau^2} \simeq \frac{\theta_{i+1} - 2\theta_i + \theta_{i-1}}{\Delta\tau^2} + \mathscr{O}(\Delta\tau^2),$$

with a truncation error of order $\Delta\tau^2$. The divergence of the radiative heat flux, equation (22.11), will be calculated by approximating the emissive power, θ^4, by a spline function, followed by analytical evaluation of the piecewise integrals. In order to obtain the same truncation error as for the conduction term, $\mathscr{O}(\Delta\tau^2)$, the prediction of $d\theta^4/d\tau'$ must be accurate to $\mathscr{O}(\Delta\tau)$ [since the piecewise integration decreases the truncation error by $\mathscr{O}(\Delta\tau)$]. Thus, for the emissive power a linear spline is sufficient, or

$$\begin{aligned}
\theta^4(\tau) &= \theta_i^4 + B_i(\tau-\tau_i) + \mathscr{O}(\Delta\tau^2) = \frac{\theta_i^4(\tau_{i+1}-\tau) + \theta_{i+1}^4(\tau-\tau_i)}{\Delta\tau} + \mathscr{O}(\Delta\tau^2),\\
\frac{d\theta^4}{d\tau}(\tau) &= \frac{\theta_{i+1}^4 - \theta_i^4}{\Delta\tau} + \mathscr{O}(\Delta\tau),\\
&\qquad\qquad \tau_i < \tau < \tau_{i+1}, \quad i = 0, 1, 2, \ldots, J-1.
\end{aligned}$$

Substituting this into equation (22.11) leads to

$$\begin{aligned}
\left(\frac{d\Psi_R}{d\tau}\right)_i &\simeq 2\sum_{j=1}^{i} \frac{\theta_j^4 - \theta_{j-1}^4}{\Delta\tau}\int_{\tau_{j-1}}^{\tau_j} E_2(\tau_i-\tau')\,d\tau' - 2\sum_{j=i+1}^{J} \frac{\theta_j^4 - \theta_{j-1}^4}{\Delta\tau}\int_{\tau_{j-1}}^{\tau_j} E_2(\tau'-\tau_i)\,d\tau'\\
&= \frac{2}{\Delta\tau}\sum_{j=1}^{i}\left(\theta_j^4 - \theta_{j-1}^4\right)\left[E_3(\tau_i-\tau_j) - E_3(\tau_i-\tau_{j-1})\right] + \frac{2}{\Delta\tau}\sum_{j=i+1}^{J}\left(\theta_j^4 - \theta_{j-1}^4\right)\left[E_3(\tau_j-\tau_i) - E_3(\tau_{j-1}-\tau_i)\right]\\
&= \frac{2}{\Delta\tau}\sum_{j=1}^{J}\left(\theta_j^4 - \theta_{j-1}^4\right)\left[E_3\left(|i-j|\Delta\tau\right) - E_3\left(|i+1-j|\Delta\tau\right)\right].
\end{aligned}$$

Equating both sides of equation (22.5), we find

$$\theta_{i-1} - 2\theta_i + \theta_{i+1} = \frac{\Delta\tau}{2N}\sum_{j=1}^{J}(\theta_j^4 - \theta_{j-1}^4)\left[E_3\left(|i-j|\Delta\tau\right) - E_3\left(|i+1-j|\Delta\tau\right)\right], \quad i = 1, 2, \ldots, J-1,$$

$$\theta_0 = 1, \quad \theta_J = \theta_L.$$

If N is relatively large ($N > 0.1$), heat transfer is dominated by conduction, and the solution proceeds as follows:

1. A temperature profile is guessed (e.g., the linear profile for pure conduction), and the $(d\Psi_R/d\tau)_i$ are calculated based on these temperatures.
2. A new temperature profile is determined by inverting the simple tridiagonal matrix for θ.
3. The temperature profile is iterated on, using underrelaxation as necessary (as discussed in the previous example).

If N is small, radiation dominates, and the process should be reversed:

1. A temperature profile is guessed, the conduction contribution is calculated, and an emissive power field is determined by inverting the full matrix for the θ_i^4 on the right-hand side.
2. A new temperature profile is deduced from the emissive powers, etc.

Once the temperature profile is known, the total heat flux follows from equations (22.9) and (22.12) as

$$\begin{aligned}\Psi_i \simeq\ & -\frac{2N}{\Delta\tau}(\theta_{i+1} - \theta_{i-1}) - \frac{2}{\Delta\tau}\left\{\sum_{j=1}^{i}\left(\theta_j^4 - \theta_{j-1}^4\right)\int_{\tau_{j-1}}^{\tau_j} E_3(\tau_i - \tau')\,d\tau' \right.\\ &\left. + \sum_{j=i+1}^{J}\left(\theta_j^4 - \theta_{j-1}^4\right)\int_{\tau_{j-1}}^{\tau_j} E_3(\tau' - \tau_i)\,d\tau'\right\}\\ =\ & -\frac{2N}{\Delta\tau}(\theta_{i+1} - \theta_{i-1}) - \frac{2}{\Delta\tau}\left\{\sum_{j=1}^{i}\left(\theta_j^4 - \theta_{j-1}^4\right)\left[E_4(\tau_i - \tau_j) - E_4(\tau_i - \tau_{j-1})\right]\right.\\ &\left. - \sum_{j=i+1}^{J}\left(\theta_j^4 - \theta_{j-1}^4\right)\left[E_4(\tau_j - \tau_i) - E_4(\tau_{j-1} - \tau_i)\right]\right\}, \qquad i = 1, 2, \ldots, J-1.\end{aligned}$$

This value for the nondimensional heat flux should be the same for all nodes.

Representative results are shown in Figs. 22-1 and 22-2. Figure 22-1 shows the nondimensional temperature variation within the slab for an intermediate optical thickness of $\tau_L = 1$, calculated by two different methods: by the integral formulation of the present example, and by the P_1-approximation. For $N = 0$ there is no conduction, and the temperature profile is discontinuous at the walls, as first indicated in Fig. 14-3. For very small values of N the temperature profile remains similar except near the walls, where the medium temperature must rapidly approach the surface temperatures. As N increases, the influence of conduction increases, and the temperature profile rapidly becomes linear. For optically thin situations (not shown) the effect is even more pronounced: larger temperature jumps at the wall for $N = 0$ and an already near-linear temperature profile for $N = 0.01$. This behavior may be explained by noting that—for small τ_L—little emission and absorption takes place inside the medium; radiative heat flux travels directly from surface to surface.

Representative nondimensional heat fluxes are shown in Fig. 22-2 and are compared with approximate methods, which will be discussed a little later. Since the optical thickness of a slab acts as a radiative barrier between two surfaces at different temperatures, the net heat flux increases with decreasing τ_L. That $q/n^2\sigma T_1^4$ increases with increasing N may be interpreted in two opposite ways: If the increase of N is due to an increase in thermal conductivity k, then the conductive and total heat fluxes increase. However, if the increase in N is due to a decrease in T_1, the radiative and total heat fluxes *decrease* due to the decreasing temperature levels (since $q/n^2\sigma T_1^4$ increases less rapidly than N).

Simple combined conduction–radiation problems such as this were first treated by Viskanta and Grosh [2, 3] and Lick [4]. More recent investigations for nonscattering media have looked

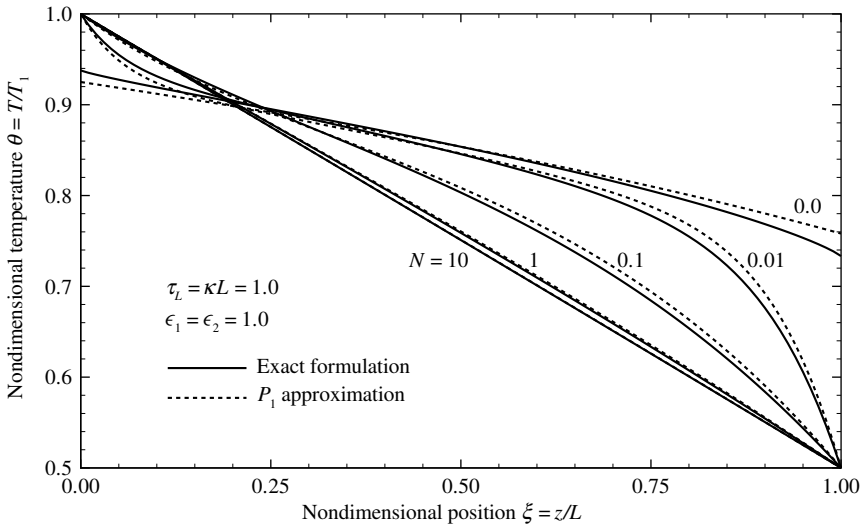

FIGURE 22-1
Nondimensional temperature distribution for combined radiation and conduction across a gray slab of optical thickness $\tau_L = 1$, bounded by black plates with a temperature ratio of $\theta_L = T_2/T_1 = 0.5$.

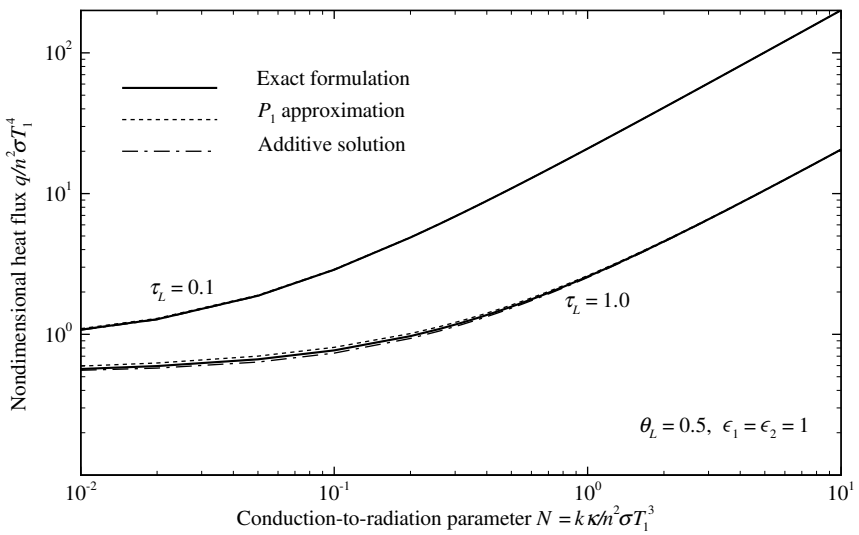

FIGURE 22-2
Nondimensional total heat flux for combined radiation and conduction across a gray slab, bounded by black plates with a temperature ratio of $\theta_L = T_2/T_1 = 0.5$.

at laser flash diffusivity measurements of semitransparent materials [5], and several nongray problems such as heat transfer through aerogels [6], plastics [7], and combustion gases [8]. Several other one-dimensional investigations have also used exact radiation formulations in the presence of isotropic [9–11] and even anisotropic scattering [12], all using gray and constant radiation properties. Two-dimensional problems have been considered by Wu and Ou [13], who looked at a gray rectangular medium with isotropic scattering, and by Tuntomo and Tien [14], who applied Maxwell's equations to small metallic particles irradiated by a laser. A comprehensive review of combined conduction–radiation heat transfer investigations has been given by Siegel [15].

P_1-Approximation

The governing equations for the P_1-approximation and their boundary conditions have been given by equations (15.42) through (15.44) for the one-dimensional slab, and by equations (16.50) through (16.52) for general geometries. For a one-dimensional, gray, nonscattering slab between two gray-diffuse surfaces, the relations may be summarized as

$$\frac{dq}{d\tau} = 4\pi I_b - G, \tag{22.13}$$

$$\frac{dG}{d\tau} = -3q, \tag{22.14}$$

$$\tau = 0: \qquad 2q = 4J_1 - G = \frac{\epsilon_1}{2-\epsilon_1}(4\pi I_{b1} - G), \tag{22.15a}$$

$$\tau = \tau_L: \qquad -2q = 4J_2 - G = \frac{\epsilon_2}{2-\epsilon_2}(4\pi I_{b2} - G), \tag{22.15b}$$

or, in nondimensional form (as given at the beginning of this section),

$$\frac{d\Psi_R}{d\tau} = 4(\theta^4 - g), \tag{22.16}$$

$$\frac{dg}{d\tau} = -\frac{3}{4}\Psi_R, \tag{22.17}$$

$$\tau = 0: \qquad \Psi_R = 2(\mathscr{J}_1 - g) = \frac{2\epsilon_1}{2-\epsilon_1}(1 - g), \tag{22.18a}$$

$$\tau = \tau_L: \qquad -\Psi_R = 2(\mathscr{J}_2 - g) = \frac{2\epsilon_2}{2-\epsilon_2}(\theta_L^4 - g). \tag{22.18b}$$

The radiative heat flux, Ψ_R, may be eliminated from equations (22.16) through (22.18), leading to

$$\frac{d^2g}{d\tau^2} + 3(\theta^4 - g) = 0, \tag{22.19}$$

$$\tau = 0: \qquad \frac{dg}{d\tau} + \frac{3}{2}\frac{\epsilon_1}{2-\epsilon_1}(1 - g) = 0, \tag{22.20a}$$

$$\tau = \tau_L: \qquad \frac{dg}{d\tau} - \frac{3}{2}\frac{\epsilon_2}{2-\epsilon_2}(\theta_L^4 - g) = 0. \tag{22.20b}$$

This second-order differential equation for the incident radiation is connected to the overall energy equation by combining equations (22.5) and (22.6), or

$$\frac{d^2\theta}{d\tau^2} = \frac{1}{N}(\theta^4 - g), \tag{22.21}$$

with its boundary condition (22.7). A solution is obtained by guessing a temperature field, followed by the determination of the incident radiation field from equations (22.19) and (22.20). This, in turn, is used to find an updated temperature field from equations (22.21) and (22.7). Using suitable underrelaxation (generally necessary because of the nonlinearity of the problem), an iteration is performed until converged temperature and incident radiation fields have been obtained. At that point the net heat flux may be calculated from equation (22.12) after evaluation of the radiative heat flux from equation (22.17), or

$$\Psi_R = -\frac{4}{3}\frac{dg}{d\tau}. \tag{22.22}$$

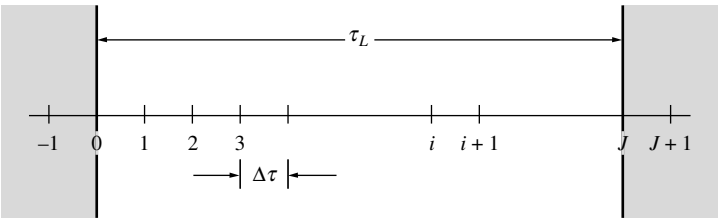

FIGURE 22-3
Nodal system for a one-dimensional slab, with artificial nodes "−1" and "$J+1$" inside the walls.

Example 22.2. Repeat the previous example, employing the P_1-approximation.

Solution
We will use a simple finite-difference method for the solution of overall energy as well as the P_1-approximation. As before, we will break up the optical thickness τ_L into $J+1$ equally spaced nodes: $i = 0, 1, \ldots, J$ with $\tau_i = i\Delta\tau$ and $\Delta\tau = \tau_L/N$. Thus, equation (22.21) becomes

$$\theta_{i-1} - 2\theta_i + \theta_{i+1} = \varphi_i = \frac{\Delta\tau^2}{N}(\theta_i^4 - g_i), \qquad i = 1, 2, \ldots, J-1,$$
$$\theta_0 = 1, \quad \theta_J = \theta_L.$$

Similarly, equation (22.19) transforms to

$$g_{i-1} - (2 + 3\Delta\tau^2)\, g_i + g_{i+1} = -3\Delta\tau^2\theta_i^4, \qquad i = 1, 2, \ldots, J-1.$$

Two more relations are needed at the two walls. The two boundary conditions for g are of the *third kind*, i.e., they contain both the dependent variable and its normal derivative. In order to retain the overall truncation error of $\mathcal{O}(\Delta\tau^2)$ for all relations, and to retain the tridiagonal nature of the finite-difference equations, it is best to use the *method of artificial nodes* [16]. In this method hypothetical nodes outside the medium (i.e., inside the walls) are introduced on each side, as indicated in the sketch of Fig. 22-3, and equations (22.19) and (22.20) are finite-differenced at the walls as if the boundary nodes were well inside the medium. Thus, with

$$\left(\frac{dg}{d\tau}\right)_0 \simeq \frac{g_1 - g_{-1}}{2\Delta\tau},$$

we obtain

$$g_{-1} - (2 + 3\Delta\tau^2)\, g_0 + g_1 = -3\Delta\tau^2,$$
$$-g_{-1} - 3\Delta\tau\, g_0 + g_1 = -3\Delta\tau.$$

Adding,

$$-[2 + 3\Delta\tau(1 + \Delta\tau)]\, g_0 + 2g_1 = -3\Delta\tau(1 + \Delta\tau).$$

Similarly, at the other boundary,

$$g_{N-1} - (2 + 3\Delta\tau^2)\, g_N + g_{N+1} = -3\Delta\tau^2\theta_L^4,$$
$$-g_{N-1} + 3\Delta\tau\, g_N + g_{N+1} = 3\Delta\tau\theta_L^4,$$

and, after subtracting,

$$2g_{N-1} - [2 + 3\Delta\tau(1 + \Delta\tau)]\, g_N = -3\Delta\tau(1 + \Delta\tau)\,\theta_L^4.$$

Therefore, we have two simultaneous tridiagonal systems for the unknown θ_i and g_i. These systems are readily solved by guessing a distribution for the φ_i (say, $\varphi_i = 0$) and inverting the tridiagonal matrix for θ_i. With this the right-hand side for the g_i can be calculated, and the tridiagonal matrix for g_i can be inverted. At this point new values for φ_i may be determined, etc. Once the iteration has converged, the net heat flux is obtained from

$$\Psi_i = \frac{2N}{\Delta\tau}(\theta_{i-1} - \theta_{i+1}) + \frac{2}{3\Delta\tau}(g_{i-1} - g_{i+1}).$$

Some sample results are included in Figs. 22-1 and 22-2 for comparison with the exact results. It is observed that the accuracy of the temperature profile is as expected from the differential approximation

(cf. Chapters 15 and 16). Also as expected, the accuracy improves with increasing N, i.e., when conduction dominates more and more over radiation. Similar observations hold true for the evaluation of net heat fluxes.

Wang and Tien [17] apparently were the first ones to employ the P_1- or differential approximation for combined radiation and conduction.

Additive Solutions

Since the evaluation of simultaneous heat transfer by conduction and radiation is rather cumbersome, it is tempting to treat each mode of energy transfer separately (as if the other one weren't there), followed by adding the two resulting heat fluxes. This simple method gives the correct heat flux for the two limiting situations (when only a single mode of heat transfer is present). The question is, how accurate is the method for intermediate situations?

The energy flux by pure steady-state conduction through a one-dimensional slab of thickness L is given by

$$q_C = k\frac{T_1 - T_2}{L}, \tag{22.23}$$

while the radiative heat flux for a gray, nonscattering medium at radiative equilibrium, confined between two isothermal black plates is, from Example 15.5,

$$q_R = \frac{n^2\sigma(T_1^4 - T_2^4)}{1 + \frac{3}{4}\tau_L}, \tag{22.24}$$

where we have used the result obtained from the differential approximation, in order to make a closed-form expression possible. Adding these two heat fluxes yields the approximate net heat flux, which, in nondimensional form, may be written as

$$\Psi = \frac{q}{n^2\sigma T_1^4} \simeq \frac{4N}{\tau_L}(1 - \theta_L) + \frac{1 - \theta_L^4}{1 + \frac{3}{4}\tau_L}, \tag{22.25}$$

which is also included in Fig. 22-2. It is observed that the additive solution is surprisingly accurate. Einstein [18] and Cess [19] have shown that the method is within 10% of exact results for black plates, although somewhat larger errors are observed for strongly reflecting surfaces. Zeng and coworkers [20] have applied the method to somewhat nongray materials, and Howell [21] has demonstrated the relative accuracy of the method for concentric cylinders. Since the method has no physical foundation, it is impossible to predict its accuracy for general geometries. In addition, the method cannot be used to predict the temperature field, since pure conduction and pure radiation each predict their own—conflicting—profiles.

Other Work

Since the early 1960s numerous articles on combined conduction–radiation problems have appeared in the literature. Most of the early papers dealt with very simple one-dimensional problems [2–4, 17, 22–27]. A number of investigations dealt with the effects of scattering in a one-dimensional slab [28–51]; others considered spectral/nongray effects in varying degrees of sophistication [44, 46, 47, 52–65]. The effects of external irradiation on the combined-mode heat transfer in a one-dimensional slab have been discussed in various investigations [5, 57, 62, 66–73] and the influence of transient conduction in others [5, 34, 41, 50, 51, 62, 70–86]. Others considered variable property effects (thermal conductivity and/or radiative properties) [42, 43, 49], some studied ultrafast effects (hyperbolic conduction) [51, 73], and others again applied inverse analysis to infer properties from experimental measurements [12, 48, 87]. Various numerical

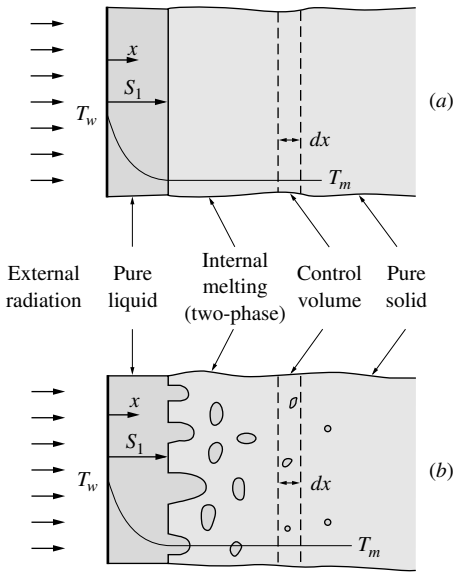

FIGURE 22-4
Melting zones within a semi-infinite body: (*a*) opaque medium, (*b*) semitransparent medium.

schemes for the solution of the governing nonlinear integro-differential equation have been employed, such as collocation with *B*-spline trial functions [88], collocation with Chebyshev polynomials [38], Galerkin methods [33,34], and finite-element methods [34]. In addition to the "exact" integral expressions, a number of different approximate methods were used to evaluate the radiative heat flux, such as the diffusion method [45,63,65,70,89], the two-flux method [29,44,47,72,77,90,91], the exponential kernel approximation [4,50,64,72], the P_N-approximation or variations of it [13,17,35,48,49,74], the discrete ordinates method [41–43,46,51,65,87,92–96], the zonal method [60], the Monte Carlo method [37, 97–99], and others. The few available experimental measurements of conduction–radiation interaction demonstrate the validity of theoretical models for glass [95, 100, 101], aerogel [6, 102], glass particles [38], fiberglass [36], porous media [103], packed spheres [46], and gases [104].

While the majority of investigations have dealt with the interaction in a one-dimensional slab, other geometries have been increasingly considered, such as one-dimensional spheres [21, 105–110], one-dimensional cylinders [91, 99, 111–116], and rectangular and other two- and three-dimensional configurations [13, 37, 63, 87, 92–96, 117–125].

22.3 MELTING AND SOLIDIFICATION WITH INTERNAL RADIATION

Melting and solidification of materials is of importance in many applications and has been studied for over a century. Until the 1950s attention had been focused exclusively on melting and solidification of opaque materials, i.e., situations where the influence of internal radiative heat transfer may be neglected. Early investigations into the effects of radiation have assumed that, as in the case of opaque bodies, there is a distinct interface between liquid and solid zones [126–136], even though meteorologists had already realized that internal melting may occur within ice (e.g., [137, 138]). Chan and coworkers [139] postulated that there exists a two-phase zone between the pure liquid and pure solid zones, as shown schematically in Fig. 22-4. The existence of such a two-phase layer in the presence of an internal radiation field may be explained as follows. Consider the melting of a semi-infinite solid, which is initially isothermal at its melting temperature T_m. A constant radiative heat flux is supplied to the face of the solid, as indicated in Fig. 22-4. If the material is opaque, the incident heat flux is absorbed by a thin surface layer at $x = 0$, and heat transfer inside the medium is by conduction alone. Melting then

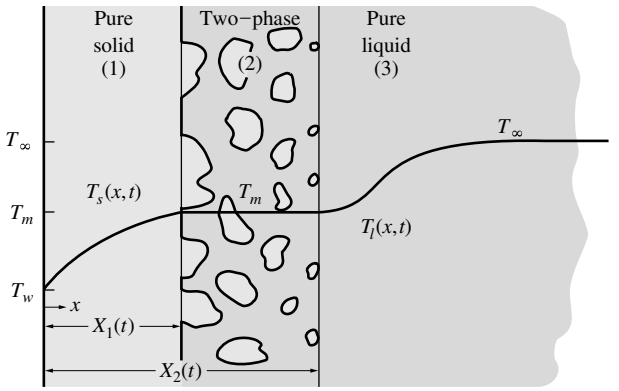

FIGURE 22-5
Solidification of a semitransparent liquid at T_∞, subjected to a cold boundary T_w ($T_w < T_m < T_\infty$).

proceeds with a distinct interface as indicated in Fig. 22-4*a*, and as described in many papers and textbooks, e.g., [140]. If the material is semitransparent the external radiation penetrates deep into the solid, and some of the energy is absorbed internally, say, in the strip dx. This absorbed energy cannot be conducted away (the solid is isothermal at T_m), nor can it raise the sensible heat without first melting the solid within the layer. Since the amount of energy absorbed over a short period of time cannot be sufficient to melt all of the material within the layer dx instantaneously, only gradual—and, therefore, partial—melting can be expected. As the amount of absorbed energy decreases for increasing distance away from the surface, the melt fraction will decrease along with it. For the more general case, if there is solid at temperatures below the melting point, absorbed radiative energy will be used first to raise the sensible heat of the material, resulting in a purely solid zone. Similar conclusions about the existence of a two-phase zone or "mushy zone" can be reached by replacing the external heat flux by a hot surface (with its surface emission), or by considering solidification rather than melting.

For the illustrative purposes of the present section, we will limit our consideration to a semi-infinite body, which is originally liquid and isothermal at temperature T_∞ ($T_\infty > T_m$, the melting temperature of the medium). For times $t > 0$ the temperature of the face at $x = 0$ is changed to, and kept at, a temperature T_w, which is lower than the melting/solidification temperature T_m. This results in a three-layer system with a qualitative temperature distribution as shown in Fig. 22-5. To keep the analysis simple, we will further assume that liquid and solid have identical and constant properties ($k_l = k_s = k$, $\kappa_l = \kappa_s = \kappa$, etc.), that the medium does not scatter, and that the face is black ($\epsilon_w = 1$). Consideration of variable properties, different boundary conditions, different geometry, and/or melting instead of freezing is straightforward (but very tedious) and will not be discussed here. In the following pages we will set up the relevant energy equations governing the three zones, and the boundary conditions that they require, following the development of Chan and coworkers [139].

Pure Solid Region If, at $t = 0$, the temperature of the face is lowered instantaneously to $T_w < T_m$, this requires the instantaneous formation of an (infinitesimally thin) layer of pure solid, which will grow with time. The governing equation for the temperature within the solid zone follows from equation (10.72) as

$$\rho c \frac{\partial T}{\partial t} = k \frac{\partial^2 T}{\partial x^2} - \frac{dq_R}{dx}, \tag{22.26}$$

which—assuming for now the location of the solid–mushy zone interface $X_1(t)$ to be known—requires an initial condition and two boundary conditions, that is,

$$t = 0: \qquad T(x,0) = T_\infty, \tag{22.27a}$$

$$x = 0: \qquad T(0,t) = T_w, \tag{22.27b}$$

$$x = X_1(t): \qquad T(X_1,t) = T_m. \tag{22.27c}$$

We defer, for the moment, the evaluation of the radiative heat flux since this is done in the same way for all three zones.

Two-Phase Region (Mushy Zone) In the presence of a two-phase region, at least a part of the solidification takes place over a finite *volume* (rather than only at a distinct interface). Since during solidification the medium releases heat in the amount of L J/kg (where L is the *heat of fusion*), this gives rise to a volumetric heat source in the amount of

$$\dot{Q}''' = L\dot{m}_s''' = L\,\rho_s \dot{V}_s''' = L\,\rho_s \frac{\partial f_s}{\partial t}, \tag{22.28}$$

where $\dot{m}_s'''$ and $\dot{V}_s'''$ are the mass and volume of solid formed per unit time and volume, respectively, ρ_s is the density of the pure solid, and f_s is the local solid fraction. Thus, with this heat source the energy equation (10.72) becomes

$$\rho c \frac{\partial T}{\partial t} = k\frac{\partial^2 T}{\partial x^2} - \frac{dq_R}{dx} + \rho L \frac{\partial f_s}{\partial t}, \tag{22.29}$$

where we have omitted the subscript s from ρ_s in the heat source term, since we assume that $\rho_s = \rho_l = \rho = \text{const}$. Since everywhere within the two-phase zone liquid and solid coexist and are assumed to be in local thermodynamic equilibrium, this implies that the temperature in the mushy zone is uniformly at the melting point, and there can be no sensible heat change ($\partial T/\partial t = 0$) and no conduction ($\partial^2 T/\partial x^2 = 0$). Thus, the energy equation simply becomes a relationship for the determination of the solid fraction, or

$$\frac{\partial f_s}{\partial t} = \frac{1}{\rho L}\,\frac{dq_R}{dx}, \tag{22.30}$$

subject to the initial condition

$$t = 0: \quad f_s(x,0) = 0. \tag{22.31}$$

Pure Liquid Region The energy equation for the pure liquid region is identical to the one for the solid, but with different boundary conditions since the zone extends from $x = X_2(t)$ to $x \to \infty$:

$$\rho c \frac{\partial T}{\partial t} = k\frac{\partial^2 T}{\partial x^2} - \frac{dq_R}{dx}, \tag{22.32}$$

$$t = 0: \qquad T(x,0) = T_\infty, \tag{22.33a}$$

$$x = X_2(t): \qquad T(X_2,t) = T_m, \tag{22.33b}$$

$$x \to \infty: \qquad T(\infty,t) = T_\infty. \tag{22.33c}$$

Radiative Heat Flux The radiative heat flux within a semitransparent, semi-infinite medium bounded by a black wall, as well as its divergence, are readily found from equations (14.54) through (14.36):

$$q_R(\tau) = 2\left[E_{bw}E_3(\tau) + \int_0^\tau E_b(\tau')E_2(\tau-\tau')\,d\tau - \int_\tau^\infty E_b(\tau')E_2(\tau'-\tau)\,d\tau'\right], \tag{22.34}$$

$$\frac{dq_R}{d\tau}(\tau) = 4E_b(\tau) - 2\left[E_{bw}E_2(\tau) + \int_0^\infty E_b(\tau')E_1(|\tau-\tau'|)\,d\tau'\right], \tag{22.35}$$

where $\tau = \kappa x$ is the usual optical coordinate, and we assume here that the absorption coefficient is constant and the same for both liquid and solid. Note that $q_R(\tau)$ and $dq_R/d\tau$ are continuous everywhere, including interfaces[2] (which is not true for the divergence of the conductive heat flux, as we will see from the interface conditions below).

[2]This is also true for variable/different absorption coefficients, for which equations (22.34) and (22.35) continue to hold with $\tau = \int_0^x \kappa(x)\,dx$.

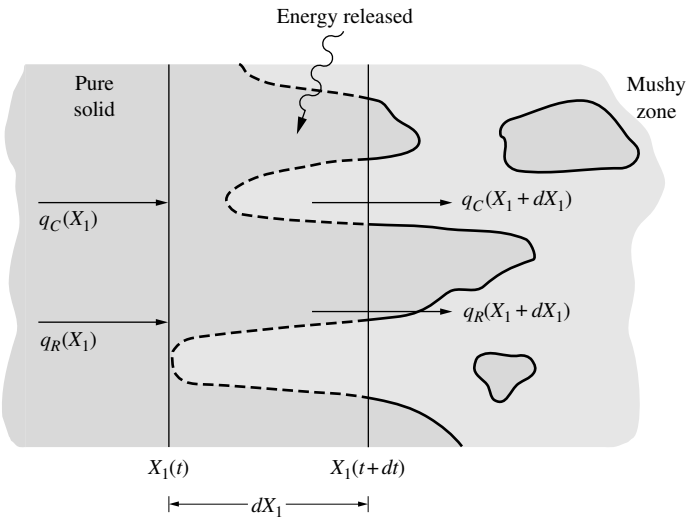

FIGURE 22-6
Energy balance at the moving interface between solid and mushy zones.

Interface Conditions Finally, we need two conditions for the determination of the location of the two interfaces between solid and mushy zones, $X_1(t)$, and between mushy zone and pure liquid, $X_2(t)$. These are obtained by performing energy balances over infinitesimal volumes adjacent to the interface, as depicted in Fig. 22-6. Consider a volume of thickness dX_1 at the solid–mushy zone interface, dX_1 being the thickness that becomes purely solid over a time period dt. An energy balance gives:

energy conducted in at $X_1(t)$ + energy radiated in at $X_1(t)$ + energy released during dt
= energy conducted out at $X_1(t+dt)$ + energy radiated out at $X_1(t+dt)$,

or

$$-k\left.\frac{\partial T}{\partial x}\right|_{X_1-0} dt + q_R(X_1)\,dt + \rho L(1-f_s)\,dX_1 = -k\left.\frac{\partial T}{\partial x}\right|_{X_1+dX_1+0} dt + q_R(X_1+dX_1)\,dt, \tag{22.36}$$

where the subscripts ±0 imply locations on the left of the interface (−0), i.e., in the solid, and on the right of the interface (+0), i.e., in the mushy zone. The heat release term contains the factor $(1 - f_s)$ because the fraction f_s is already solid. Noting that $T = T_m = \text{const}$ inside the mushy zone, it follows that $\partial T/\partial x|_{X_1+dX_1+0} = 0$. The radiative heat flux, on the other hand, is continuous and cancels out from the interface condition once dt and dX_1 are shrunk to zero, and equation (22.36) becomes simply

$$x = X_1(t): \quad -k\left.\frac{\partial T}{\partial x}\right|_{X_1-0} + \rho L(1-f_s)\frac{dX_1}{dt} = 0, \tag{22.37}$$

subject to

$$t = 0: \qquad X_1(0) = 0. \tag{22.38}$$

Note that there does not appear to be any requirement of $f_s \to 1$ at the interface (smooth transition from mushy zone to pure solid).

Similar to equation (22.36) we find for the mushy zone–liquid interface

$$-k\left.\frac{\partial T}{\partial x}\right|_{X_2-0} dt + q_R(X_2)\,dt + \rho L f_s\,dX_2 = -k\left.\frac{\partial T}{\partial x}\right|_{X_2+dX_2+0} dt + q_R(X_2+dX_2)\,dt, \tag{22.39}$$

where $(1 - f_s)$ is replaced by f_s since the fraction f_s solidifies from pure liquid. Upon shrinking dt and dX_2, the q_R cancel again, and the conduction term within the mushy zone vanishes, or

$$\rho L f_s \frac{dX_2}{dt} = -k\left.\frac{\partial T}{\partial x}\right|_{X_2+0}. \tag{22.40}$$

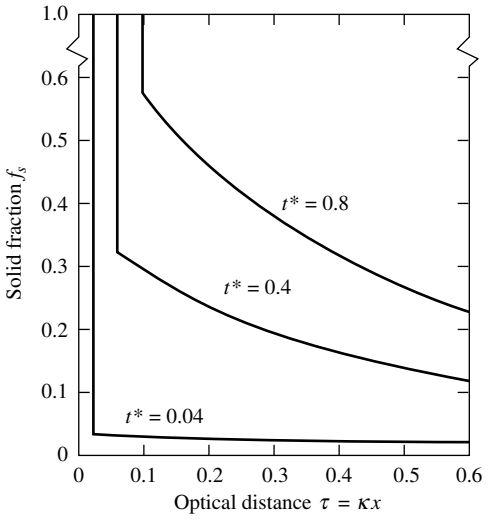

FIGURE 22-7
Solidification of a semi-infinite, semitransparent medium initially isothermal at melting temperature: development of solid and mushy zones; $\theta_w = T_w/T_m = 0.9$, $N = k\kappa/4n^2\sigma T_m^3 = 0.75$, Ste $= L/cT_m = 500$, $t^* = 2\kappa n^2\sigma(T_m^4 - T_w^4)t/\rho L$.

Now, in order for freezing to occur, we must have $dX_2/dt > 0$ and $\partial T/\partial x \geq 0$. Since the solid fraction must be nonnegative, this implies that the left-hand side of equation (22.40) should be positive and the right-hand side should be negative. This apparent contradiction can be overcome only if both sides of equation (22.40) are identically equal to zero, or,

$$x = X_2(t): \qquad f_s(X_2, t) = 0, \quad \frac{\partial T}{\partial x}(X_2, t) = 0. \tag{22.41}$$

This implies that there is no distinct interface between mushy zone and liquid: Temperature, heat flux, and solid fraction are continuous across this "interface." Mathematically, one distinguishes between mushy zone and pure liquid, since in the mushy zone f_s is the unknown variable ($T = T_m$ is known), and in the liquid zone the temperature is unknown ($f_s = 0$ is known). The location of interface X_2 is found implicitly by evaluating $f_s(x, t)$ and determining the location where $f_s = 0$.

In summary, in order to predict the solidification of a semitransparent solid, it is necessary to simultaneously solve equations (22.26) and (22.27) (solid), equations (22.30) and (22.31) (mushy zone), and equations (22.32) and (22.33) (liquid), together with the interface conditions, equations (22.37) and (22.41). Note that—for an opaque medium—the radiative source within the medium vanishes ($q_R = 0$) and, from equations (22.30) and (22.31), $f_s(x, t) = 0$; that is, the mushy zone shrinks to a point, collapsing the two interfaces as expected for pure conduction. This system of equations is nonlinear, even in the absence of radiation, making exact analytical solutions impossible to find. Chan and coworkers [139] have presented approximate results for a few simple situations. For example, Fig. 22-7 shows the development of the solid and mushy zones for the case of a liquid that is initially uniform at melting temperature.

Example 22.3. Consider a large (i.e., semi-infinite) block of clear ice exposed to solar radiation on one of its faces. The ice is initially at a uniform 0°C, i.e., at its melting temperature. Heat transfer from the surfaces of the ice (except the solar irradiation) may be neglected, as may the radiative emission from within the ice. Determine the development of the mushy zone for small times. Indicate how the movement of the liquid–mushy zone interface may be calculated.

Solution
Since the side walls are insulated, the problem is one-dimensional; and since the block is "very large," we may assume that it is essentially a semi-infinite body with solar irradiation on its (otherwise insulated) left face at $x = 0$. Since, in this example, we consider the melting of a solid, the order of zones is reversed, i.e., we have pure liquid for $0 \leq x \leq X_1$, the mushy zone for $X_1 < x < X_2$, and pure solid for $x > X_2$. In the present example $X_2 \to \infty$, since the ice is everywhere at the melting point. Also, since the face temperature is not increased abruptly, there is no instantaneous formation of a pure liquid layer and $X_1 = 0$ for some time $t > 0$. The solar irradiation is not absorbed by the surface but penetrates into the

ice, causing a local radiative heat flux—if emission from and scattering by the ice is neglected—of

$$q_R(x) = q_{\text{sol}}\, e^{-\kappa x},$$

where q_{sol} is the strength of solar irradiation penetrating into the ice (after losing some of its strength due to reflection at the interface at $x = 0$) (see Chapter 19).

The purely liquid zone is essentially described by equations (22.26) and (22.27):

$$\begin{aligned} \rho c \frac{\partial T}{\partial t} &= k \frac{\partial^2 T}{\partial x^2} + q_{\text{sol}} \kappa\, e^{-\kappa x}, \\ t = t_0: &\quad T(x, t_0) = T_m, \\ x = 0: &\quad \frac{\partial T}{\partial x}(x, t) = 0, \\ x = X_1(t): &\quad T(X_1, t) = T_m, \end{aligned}$$

where t_0 is the time at which a purely liquid zone starts to exist, and the boundary condition at $x = 0$ has been replaced to reflect the lack of heat transfer at the surface.

The heat generation term of equation (22.28) becomes a sink, and, while the expression is correct as is, it appears more logical to work with a liquid fraction, $f_l = 1 - f_s$, in the case of melting. Thus, equation (22.30) becomes

$$\frac{\partial f_l}{\partial t} = -\frac{1}{\rho L} \frac{dq_R}{dx} = \frac{q_{\text{sol}} \kappa}{\rho L}\, e^{-\kappa x},$$

$$t = 0: \quad f_l(0) = 0.$$

Finally, the interface equation at $x = X_1(t)$ must be rewritten as

$$-k \left.\frac{\partial T}{\partial x}\right|_{X_1 - 0} = \rho L (1 - f_l) \frac{dX_1}{dt},$$

$$t = t_0: \quad X_1 = 0,$$

where f_s has been replaced by f_l, and L by $-L$ (since melting *requires* heat rather than *releasing* it). Since $\partial T/\partial x = 0$ at $x = 0$, no liquid layer can grow until $f_l = 1$ at $x = 0$. After this has taken place (at time $t = t_0$) the temperature may rise at $x = 0$, and $\partial T/\partial x$ becomes negative at $x = X_1 - 0$; therefore, $f_l(X_1)$ must diminish again, and $dX_1/dt > 0$.

For times $t < t_0$, the equation for the mushy zone is readily solved, leading to

$$f_l(x, t) = \frac{q_{\text{sol}} \kappa t}{\rho L}\, e^{-\kappa x}, \qquad 0 = X_1(t) < x < \infty.$$

From this relationship it follows that a purely liquid zone starts at

$$t_0 = \frac{\rho L}{q_{\text{sol}} \kappa},$$

that is, when $f_l = 1$ at $x = 0$. For times larger than t_0, the relation for the liquid fraction, $f_l(x, t)$, within the mushy zone continues to hold, but only for $x \geq X_1 > 0$. The temperature profile within the liquid zone and the location of its interface must be determined by simultaneously solving the conduction and interface equations (with known values of f_l).

Since the original postulation by Chan and coworkers [139], the notion of a mushy zone has found widespread acceptance among other researchers [86, 141–144].

22.4 COMBINED RADIATION AND CONVECTION IN BOUNDARY LAYERS

In this section we will briefly discuss how at high temperatures the presence of thermal radiation affects the temperature distribution in a thermal boundary layer and, therefore, the heat transfer

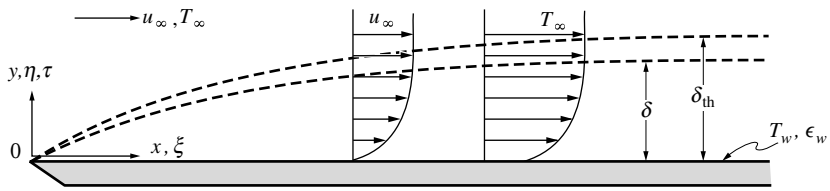

FIGURE 22-8
Laminar flow of an absorbing/emitting fluid over an isothermal gray-diffuse plate.

rate to or from a wall. Again, since we are mainly interested in the basic nature of interaction between convective and radiative heat transfer, we will limit ourselves to a single simple case, laminar flow over a flat plate.

Consider steady, laminar flow of a viscous, compressible, absorbing/emitting (but not scattering) gray fluid over an isothermal gray-diffuse plate, as illustrated in Fig. 22-8. Making the standard boundary layer assumptions [145], conservation of mass, momentum, and energy follow as

$$\frac{\partial}{\partial x}(\rho u) + \frac{\partial}{\partial y}(\rho v) = 0, \tag{22.42}$$

$$\rho\left(u\frac{\partial u}{\partial x} + v\frac{\partial u}{\partial y}\right) = \frac{\partial}{\partial y}\left(\mu\frac{\partial u}{\partial y}\right) - \frac{dp}{dx}, \tag{22.43}$$

$$\rho c_p\left(u\frac{\partial T}{\partial x} + v\frac{\partial T}{\partial y}\right) = \frac{\partial}{\partial y}\left(k\frac{\partial T}{\partial y}\right) - \frac{\partial q_R}{\partial y} + \mu\left(\frac{\partial u}{\partial y}\right)^2, \tag{22.44}$$

subject to the boundary conditions

$$x = 0: \quad u(0,y) = u_\infty, \qquad T(0,y) = T_\infty; \tag{22.45a}$$

$$y = 0: \quad u(x,0) = v(x,0) = 0, \quad T(x,0) = T_w; \tag{22.45b}$$

$$y \to \infty: \quad u(x,\infty) = u_\infty, \qquad T(x,\infty) = T_\infty. \tag{22.45c}$$

Equations (22.43) and (22.44) incorporate the standard boundary layer assumptions of $\partial u/\partial y \gg \partial u/\partial x$ and $\partial T/\partial y \gg \partial T/\partial x$ (momentum and heat transfer rates across the boundary layer are much larger than along the plate, which is dominated by convection), as well as the simplified dissipation function $(\partial u/\partial y)^2$. Similarly, one may drop the x-wise radiation term in favor of the radiative heat flux across the boundary layer. This is readily justified by using the diffusion approximation to get an order-of-magnitude estimate for the radiative heat flux: From equation (15.20), $\mathbf{q}_R = -k_R \nabla T$, and—since $\partial T/\partial y \gg \partial T/\partial x$—radiation along the plate may be neglected as compared to radiation across the boundary layer. Therefore, assuming that the radiative heat flux is one-dimensional, q_R may be approximated from equation (14.54) (with $\tau = \int_0^y \kappa\, dy$ and $\tau_L \to \infty$) as[3]

$$q_R(x,y) = 2J_w(x)E_3(\tau) + 2\int_0^\tau E_b(x,\tau')E_2(\tau-\tau')\,d\tau' - 2\int_\tau^\infty E_b(x,\tau')E_2(\tau'-\tau)\,d\tau', \tag{22.46}$$

and

$$\frac{1}{\kappa}\frac{\partial q_R}{\partial y}(x,y) = \frac{\partial q_R}{\partial \tau} = 4E_b(x,\tau) - 2J_w E_2(\tau) - 2\int_0^\infty E_b(x,\tau')E_1(|\tau-\tau'|)\,d\tau'. \tag{22.47}$$

Alternatively, the radiative heat flux may be evaluated from any of the approximate methods discussed in Chapter 15.

[3]Equations (22.46) and (22.47) are approximate since they assume that the local value of E_b is independent of x.

It should be remembered that photons carry momentum, thus causing radiation pressure and radiation stress (cf. Section 1.8), and that a control volume stores radiative energy [cf. equation (10.20) and Section 10.7]. However, these effects are generally negligible except at extremely high temperatures (> 50,000 K at 1 atm pressure) [146, 147] and will not be included here.

To improve the clarity of development, we will make the additional assumptions of constant fluid properties (ρ, c_p, μ, k, κ = const), slow flow (negligible dissipation term), a black plate [$\epsilon_w = 1$, or $J_w = E_b(T_w) = E_{bw}$], and constant free stream values (u_∞, T_∞ = const). Then equations (22.42) through (22.44) and (22.47) reduce to

$$\frac{\partial u}{\partial x} + \frac{\partial v}{\partial y} = 0, \tag{22.48}$$

$$u\frac{\partial u}{\partial x} + v\frac{\partial u}{\partial y} = \nu\frac{\partial^2 u}{\partial y^2}, \tag{22.49}$$

$$u\frac{\partial T}{\partial x} + v\frac{\partial T}{\partial y} = \alpha\frac{\partial^2 T}{\partial y^2} - \frac{1}{\rho c_p}\frac{\partial q_R}{\partial y}, \tag{22.50}$$

$$\frac{\partial q_R}{\partial y} = 2\kappa\Big[2E_b(x,\tau) - E_{bw}E_2(\tau) - \int_0^\infty E_b(x,\tau')E_1(|\tau-\tau'|)\,d\tau'\Big], \tag{22.51}$$

subject to boundary conditions (22.45). Here $\nu = \mu/\rho$ is the kinematic viscosity, and $\alpha = k/\rho c_p$ is the thermal diffusivity. Introducing the stream function ψ as

$$u = \frac{\partial \psi}{\partial y}, \quad v = -\frac{\partial \psi}{\partial x}, \tag{22.52}$$

eliminates the continuity equation and transforms the momentum and energy equations to

$$\frac{\partial \psi}{\partial y}\frac{\partial^2 \psi}{\partial x \partial y} - \frac{\partial \psi}{\partial x}\frac{\partial^2 \psi}{\partial y^2} = \nu\frac{\partial^3 \psi}{\partial y^3}, \tag{22.53}$$

$$\frac{\partial \psi}{\partial y}\frac{\partial T}{\partial x} - \frac{\partial \psi}{\partial x}\frac{\partial T}{\partial y} = \alpha\frac{\partial^2 T}{\partial y^2} - \frac{1}{\rho c_p}\frac{\partial q_R}{\partial y}. \tag{22.54}$$

Making the standard[4] coordinate transformation from x and y to the nondimensional ξ and η, where

$$\xi = \frac{4n^2\sigma T_\infty^3 \kappa x}{\rho c_p u_\infty}, \quad \eta = \left(\frac{u_\infty}{\nu x}\right)^{1/2} y, \tag{22.55}$$

and introducing new nondimensional dependent variables

$$f = \frac{\psi}{(\nu u_\infty x)^{1/2}}, \quad \theta = \frac{T}{T_\infty}, \quad \Psi_R = \frac{q_R}{n^2\sigma T_\infty^4} \tag{22.56}$$

reduces the momentum and energy equations to

$$\frac{d^3 f}{d\eta^3} + \frac{1}{2} f\frac{d^2 f}{d\eta^2} = 0, \tag{22.57}$$

$$\frac{1}{\Pr}\frac{\partial^2 \theta}{\partial \eta^2} + \frac{1}{2} f\frac{\partial \theta}{\partial \eta} = \frac{df}{d\eta}\xi\frac{\partial \theta}{\partial \xi} + \frac{1}{4}\left(\frac{\xi}{N\Pr}\right)^{1/2}\frac{\partial \Psi_R}{\partial \eta}. \tag{22.58}$$

[4]Except for the nondimensionalization factor for ξ.

In this equation $\mathrm{Pr} = \nu/\alpha = \mu c_p/k$ is the *Prandtl number* of the fluid, and N is the conduction-to-radiation parameter previously introduced as

$$N \equiv \frac{k\kappa}{4n^2\sigma T_\infty^3}. \tag{22.59}$$

Sometimes, a convection-to-radiation parameter, or *Boltzmann number*, is also introduced, which is defined as

$$\mathrm{Bo} \equiv \frac{\rho c_p u_\infty}{n^2\sigma T_\infty^3} = 4\left(\frac{N\mathrm{Re}_x\,\mathrm{Pr}}{\xi}\right)^{1/2}, \tag{22.60}$$

where $\mathrm{Re}_x = u_\infty x/\nu$ is the local *Reynolds number*. Very similar to the conduction-to-radiation parameter N, the Boltzmann number gives a qualitative measure of the relative magnitudes of convective and radiative heat fluxes.

Equation (22.57) contains no ξ-derivative since η turns out to be a similarity variable, i.e., no term in the equation (except the ξ-derivative) contains ξ, and the boundary conditions for f do not depend on ξ, collapsing to

$$\eta = 0: \quad f = \frac{df}{d\eta} = 0, \qquad \eta \to \infty: \quad \frac{df}{d\eta} = 1. \tag{22.61}$$

Thus, equation (22.57) is an ordinary differential equation for the unknown f, which is a function of the similarity variable η alone. Equation (22.57) and its solution was first given by Blasius and is well documented in fluid mechanics texts, such as [148]. The energy equation (22.58) is a partial differential equation for the unknown θ, subject to the boundary conditions

$$\eta = 0: \qquad \theta = \frac{T_w}{T_\infty} = \theta_w, \qquad \eta \to \infty: \quad \theta = 1, \tag{22.62a}$$

$$\xi = 0: \qquad \theta = 1. \tag{22.62b}$$

Since the boundary conditions at $x = 0$ correspond to both $\xi = 0$ and $\eta \to \infty$, equation (22.58) can also reduce to a similarity solution, but only if $\Psi_R \propto \xi^{-1/2}$. This is *not* the case if Ψ_R is evaluated from equation (22.51) or most approximate methods discussed in Chapter 15. However, if the thermal boundary layer is optically very thick, so that the diffusion approximation becomes applicable, one finds from equation (15.20)

$$\Psi_R = -\frac{4}{3\kappa}\frac{\partial\theta^4}{\partial y} = -\frac{4}{3(N\,\mathrm{Pr}\,\xi)^{1/2}}\frac{\partial\theta^4}{\partial\eta}. \tag{22.63}$$

This expression is substituted into equation (22.58), resulting in the ordinary differential equation

$$\frac{1}{\mathrm{Pr}}\frac{d^2\theta}{d\eta^2} + \frac{1}{2}f\frac{d\theta}{d\eta} = -\frac{1}{3N\,\mathrm{Pr}}\frac{d^2\theta^4}{d\eta^2}, \tag{22.64}$$

since then θ is a function of the similarity variable η only.

The interaction of radiation and convection in an optically thick laminar boundary layer of a gray gas was first investigated by Viskanta and Grosh [149] and others [150–153]. Figure 22-9 shows the similarity profile for the nondimensional temperature, as obtained using the diffusion approximation [149], for a number of different values for the conduction-to-radiation parameter N. For $N = 10$ the temperature profile was found to be within 2% of the pure convection case (which numerically corresponds to $N \to \infty$). When radiation is present, the thermal boundary layer was always found to thicken, which may be explained by the fact that radiation provides an *additional* means to diffuse energy. Even for strong radiation (large T_∞) the thickening of the thermal boundary layer may be limited if the fluid is optically thick (large κ). However, if the

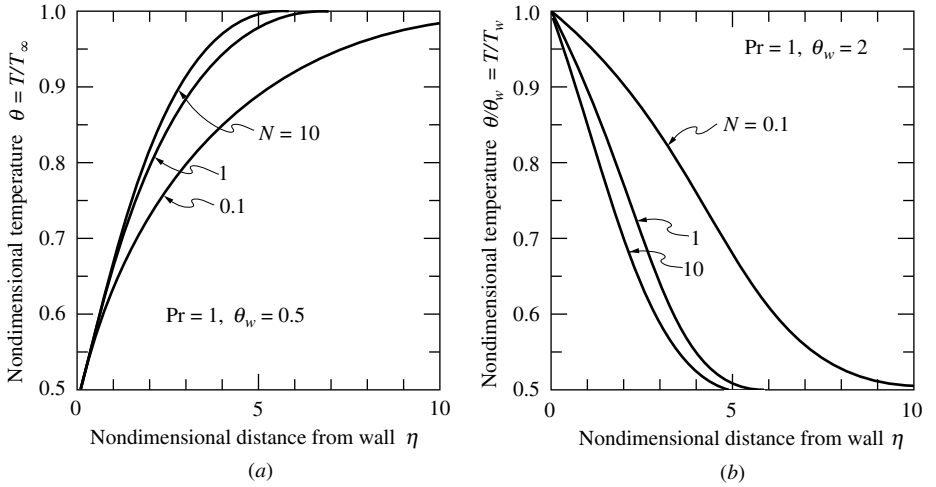

FIGURE 22-9
Similarity profiles for nondimensional temperature profiles across an optically thick laminar boundary over a flat plate; Pr = 1: (*a*) $\theta_w = T_w/T_\infty = 0.5$, (*b*) $\theta_w = 2$.

absorption coefficient is small (optically thin fluid), the thickening of the thermal boundary may become so large as to invalidate the basic boundary assumptions (i.e., the neglect of conduction and radiation in the x-direction).

Figure 22-10 shows nondimensional radiative, conductive, and total surface heat fluxes along the plate for a representative case as evaluated by three different methods. The radiative heat flux is evaluated according to the definition in equation (22.56), and the conductive heat flux is defined as

$$\Psi_C = -k \left.\frac{\partial T}{\partial y}\right|_{y=0} \Big/ n^2 \sigma T_\infty^4 = -4 \left(\frac{N}{\Pr \xi}\right)^{1/2} \left.\frac{\partial \theta}{\partial \eta}\right|_{\eta=0}, \tag{22.65}$$

and

$$\Psi = \Psi_C + \Psi_R. \tag{22.66}$$

The "exact" results are a numerical solution of equation (22.58) with the radiation term evaluated from equation (22.51), as obtained by Zamuraev [154] (and reported by Viskanta [155]). In the optically thick solution Ψ_R is evaluated from equation (22.63) as

$$\Psi_R = -\frac{4}{3(N \Pr \xi)^{1/2}} \left.\frac{\partial \theta^4}{\partial \eta}\right|_{\eta=0}, \tag{22.67}$$

and displays a simple $\xi^{-1/2}$ dependence. The optically thin solution has been taken from Cess [19, 156], who postulated a two-region temperature field consisting of a very thin conventional thermal boundary layer (in which radiation is neglected in favor of conduction) and an outer region with slowly changing temperature (in which conduction is neglected). As seen from Fig. 22-10, the diffusion approximation predicts the wall heat flux accurately over the entire length of the plate, while the optically thin approximation fails a short distance away from the leading edge (apparently since downstream the boundary layer grows too thick to neglect radiation and/or the outer layer becomes too nonisothermal to neglect conduction). Other early optically thin models have been reported by Smith and Hassan [157] and Tabaczynski and Kennedy [158]; Pai and Tsao [159] used the exponential kernel approach, and Oliver and McFadden [160] solved the "exact" relations, equation (22.51), by the method of successive approximations, stopping after three iterations. Dissipation effects [156, 161–163] as well as hypersonic conditions [162, 164–166] have been considered by a number of investigators. The influences of scattering [167, 168], nongray radiation properties [169–171], external irradiation

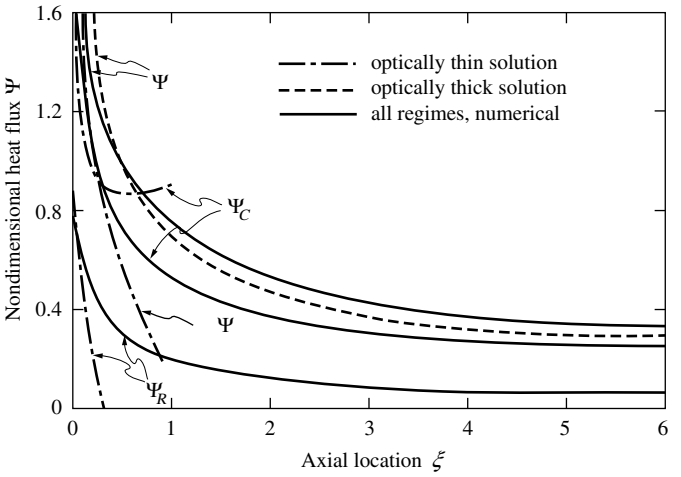

FIGURE 22-10
Comparison of conductive, radiative, and total heat fluxes for a laminar boundary layer over a flat plate: optically thin solution from [19], optically thick solution from [149], and exact solution from [154]; $N = 0.1$, $\Pr = 1.0$, $\theta_w = 0.1$.

[172, 173], turbulent boundary layers [174–176], as well as laminar flow across cylinders [171] and spheres [177] have also been addressed.

22.5 COMBINED RADIATION AND FREE CONVECTION

The effects of radiation are often even more important when combined with free convection rather than forced convection. The radiation effects on a vertical free-convection boundary layer have been modeled by Cess [178] for the optically thin case and by Arpaci [179] for the optically thin and thick cases, while Cheng and Özişik [180] and Desrayaud and Lauriat [181] looked at isotropic scattering effects, and Krishnaprakas *et al.* [182] considered linear anisotropic scattering. Hossain *et al.* [183] used the diffusion approximation to deal with an optically thick gas next to a porous vertical plate with suction. Webb and Viskanta [184] investigated the effects of external irradiation, verifying their model with experiment [185], and a vertical square duct was studied by Yan and Li [186, 187]. Careful experimental work by Lacona and Taine [188] verified standard (no-radiation) prediction models, and showed that radiation can strongly modify free convection temperature profiles. They used holographic interferometry and laser deflection techniques to measure temperatures in nitrogen (suppression of radiation) and pure carbon dioxide (strong radiation effects).

Thermal stability of horizontal layers with radiation has also found some attention [189–192] as has combined radiation and free convection within enclosed, particularly square cavities [193–199] and parallel vertical plates [200, 201]. In addition, horizontal [202] and vertical annuli [203] and cubical cavities [204] have been studied. The interaction between free convection and radiation in liquids was studied by Derby and coworkers [205], investigating a cylindrical container with molten glass, and by Tsukuda and colleagues [206], who considered internal radiation during Czochralski crystal growth.

Most of the above studies have been limited to the simple case of constant, gray radiation properties. Exceptions are the studies of Mesyngier and Farouk [198], who considered a H_2O–CO_2 mixture in a square enclosure, using the discrete ordinates method and the weighted-sum-of-gray-gases approach, and of Bdéoui and coworkers [207], who studied water vapor radiation effects on Rayleigh–Bénard convection, using an exact formulation together with the ADF method. In addition, Colomer *et al.* [199] studied square cavities filled with H_2O–CO_2 mixtures using the SLW method, and showed that nongray gas properties have very strong impact on temperature distributions in such flows.

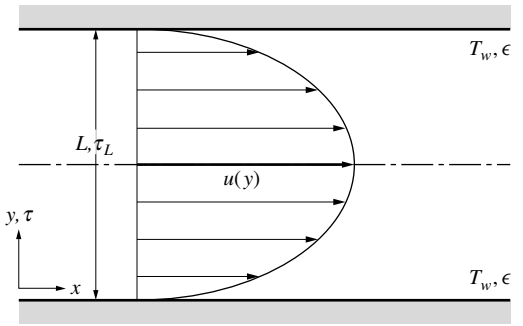

FIGURE 22-11
Thermally developing Poiseuille flow of a gray, absorbing and emitting fluid between gray-diffuse plates.

22.6 COMBINED RADIATION AND CONVECTION IN INTERNAL FLOW

Forced convective heat transfer in circular and noncircular ducts, for laminar and turbulent flow, has been thoroughly studied for situations in which radiative heat transfer may be neglected. The case of a transparent medium with radiating boundaries has been briefly discussed in Section 9.3. In this section we will examine the interaction of radiation and convection for a radiatively participating medium flowing through a duct. In the spirit of the previous sections we will again limit our theoretical development to one particularly simple case, namely hydrodynamically developed laminar flow of an incompressible, constant-property fluid through a parallel-plate channel. This is commonly referred to as *Poiseuille flow*. This will be followed by a brief discussion of trends in more involved situations together with a review of the state-of-the-art.

Poiseuille Flow

We will assume that the fluid is gray, absorbing, and emitting (but not scattering), and that the plates are gray and diffuse, a distance L apart, and isothermal, as indicated in Fig. 22-11. The fully developed velocity distribution for Poiseuille flow follows readily from equations (22.48) and (22.49), setting $u = u(y)$, as

$$u = 6u_m \frac{y}{L}\left(1 - \frac{y}{L}\right), \quad v = 0, \tag{22.68}$$

where u_m is the mean velocity across the duct. Thus, the energy equation (22.50) reduces to

$$u(y)\frac{\partial T}{\partial x} = \alpha \frac{\partial^2 T}{\partial y^2} - \frac{1}{\rho c_p}\frac{\partial q_R}{\partial y}, \tag{22.69}$$

if again we limit ourselves to the case in which conduction and radiation in the flow direction (along x) are negligible as compared to their transverse values (along y). This is generally a good assumption for channel locations that are a few plate spacings L removed from the inlet [208]. Equation (22.69) is subject to the boundary conditions

$$x = 0: \qquad T = T_i, \tag{22.70a}$$

$$y = 0, L: \qquad T = T_w, \tag{22.70b}$$

and the radiative heat flux may be obtained from equation (14.54) as[5]

$$q_R(x,y) = 2J_w(x)\left[E_3(\tau) - E_3(\tau_L - \tau)\right] + 2\int_0^\tau E_b(x,\tau')E_2(\tau - \tau')\,d\tau' - 2\int_\tau^{\tau_L} E_b(x,\tau')E_2(\tau' - \tau)\,d\tau'. \tag{22.71}$$

[5]Again using an approximate, i.e., one-dimensional, solution by neglecting the x-wise variation of emissive power in the evaluation of q_R.

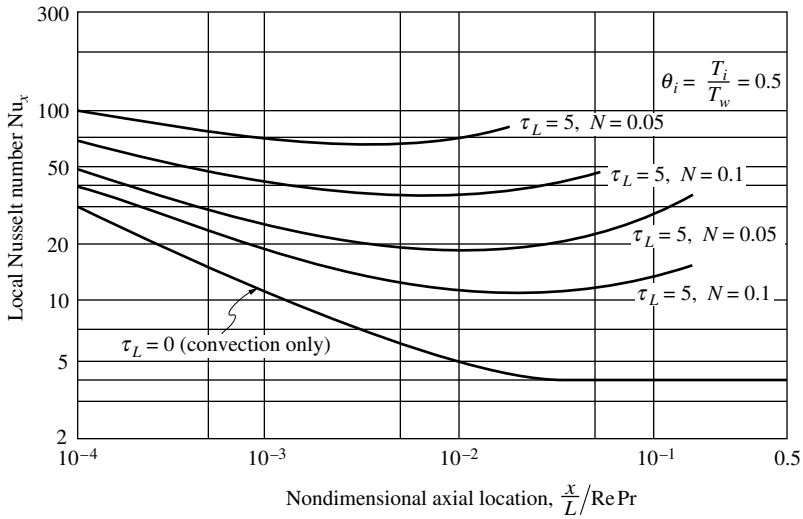

FIGURE 22-12
Influence of optical thickness and conduction–radiation parameter on Nusselt number development in Poiseuille flow—heated wall.

The radiative heat flux could, of course, instead be evaluated by any of the approximate methods discussed in Chapter 15.

Introducing similar nondimensional variables and parameters as in the previous section,

$$\theta = \frac{T}{T_w}, \quad \Psi_R = \frac{q_R}{n^2\sigma T_w^4}, \tag{22.72a}$$

$$\xi = \frac{x}{L\,\mathrm{Re}_m\,\mathrm{Pr}} = \frac{x}{L}\Big/\frac{u_m L}{\nu}\frac{\nu}{\alpha}, \quad \eta = \frac{y}{L}, \quad \tau = \kappa y, \tag{22.72b}$$

$$N = \frac{k\kappa}{4n^2\sigma T_w^3}, \quad \tau_L = \kappa L, \tag{22.72c}$$

transforms equations (22.68) through (22.71) to

$$6\eta(1-\eta)\frac{\partial\theta}{\partial\xi} = \frac{\partial^2\theta}{\partial\eta^2} - \frac{\tau_L}{4N}\frac{d\Psi_R}{d\eta}, \tag{22.73}$$

$$\xi = 0: \quad \theta = T_i/T_w = \theta_i, \quad \eta = 0, 1: \quad \theta = 1, \tag{22.74}$$

$$\Psi_R = 2\left[E_3(\tau) - E_3(\tau_L - \tau) + \int_0^\tau \theta^4(\xi,\tau')E_2(\tau-\tau')\,d\tau' - \int_\tau^{\tau_L} \theta^4(\xi,\tau')E_2(\tau'-\tau)\,d\tau'\right], \tag{22.75}$$

where, for simplicity, we have limited ourselves to black channel walls.

Equation (22.73) and its boundary conditions must be solved simultaneously with equation (22.75), making it a nonlinear integro-differential system. Equation (22.73) is a parabolic differential equation allowing a straightforward numerical solution technique, marching forward from $\xi = 0$. While, in principle, an explicit numerical solution is possible if small enough steps in ξ are taken, in practice implicit methods are employed. Because of the nonlinearity, this requires guessing the temperature field for the next ξ-location (as a function of η), followed by an iterative procedure until convergence criteria are met. This scheme is then repeated for all downstream locations. The Poiseuille flow problem described here was first solved by Kurosaki [209] and, a little later, with results reported for higher temperatures (smaller N), by Echigo and coworkers [210]. Figure 22-12 shows the axial development of the local Nusselt

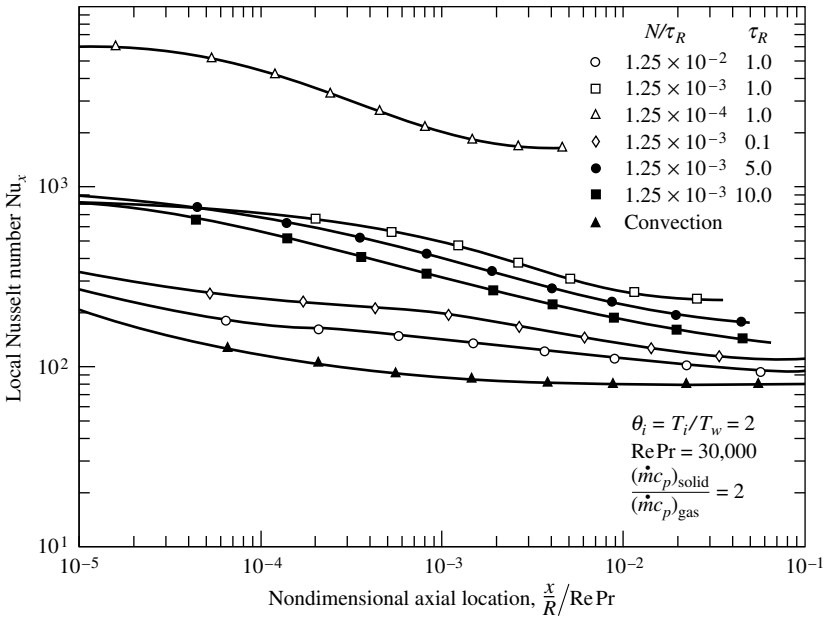

FIGURE 22-13
Influence of optical thickness and conduction–radiation parameter on Nusselt number development for gas–particulate flow through a tube—cooled wall.

number for the case of $\theta_i = 0.5$ (cold fluid, hot wall), with the Nusselt number defined as

$$\text{Nu}_x(\xi) = \frac{q_w L}{k\,[T_w - T_m(\xi)]}, \tag{22.76}$$

where $q_w = q_C + q_R$ is total heat flux per unit area at the wall, by radiation and conduction. In terms of nondimensional quantities, the local Nusselt number becomes

$$\text{Nu}_x(\xi) = \frac{4}{1 - \theta_m(\xi)} \left[-\frac{\partial \theta}{\partial \eta} + \frac{\tau_L}{4N} \Psi_R \right]_{\eta=0}. \tag{22.77}$$

It is apparent from Fig. 22-12 that—due to the nonlinear radiative contribution—no fully developed temperature profile, and consequently no asymptotic Nusselt number, develops. Rather, for the heated wall case ($T_w > T_i$), the Nusselt number goes through a minimum at a certain downstream location, behind which it tends to increase again. The location of the maximum moves toward the inlet with increasing importance of radiation. This phenomenon may be explained as follows: Downstream from the inlet the convective heat flux always decreases more rapidly than the temperature difference, $T_w - T_m(\xi)$, causing a steady decrease in the convective contribution to the Nusselt number; the fractional radiative heat flux, on the other hand, increases monotonically with x, leading to the observed behavior.

Laminar and Turbulent Channel Flow

Qualitatively, the Nusselt number development for other channel flows with heated walls is the same as for Poiseuille flow (regardless of geometry, turbulent flow, presence of scattering, nongrayness, etc.). The heat transfer behavior is somewhat different if a hot fluid enters a cold-walled duct ($T_w < T_i$). This is shown in Fig. 22-13 for turbulent tube flow of a gas seeded with small particles, from Azad and Modest [211]. The Nusselt number always decreases monotonically, somewhat similar to the pure convection case, and eventually appears to reach

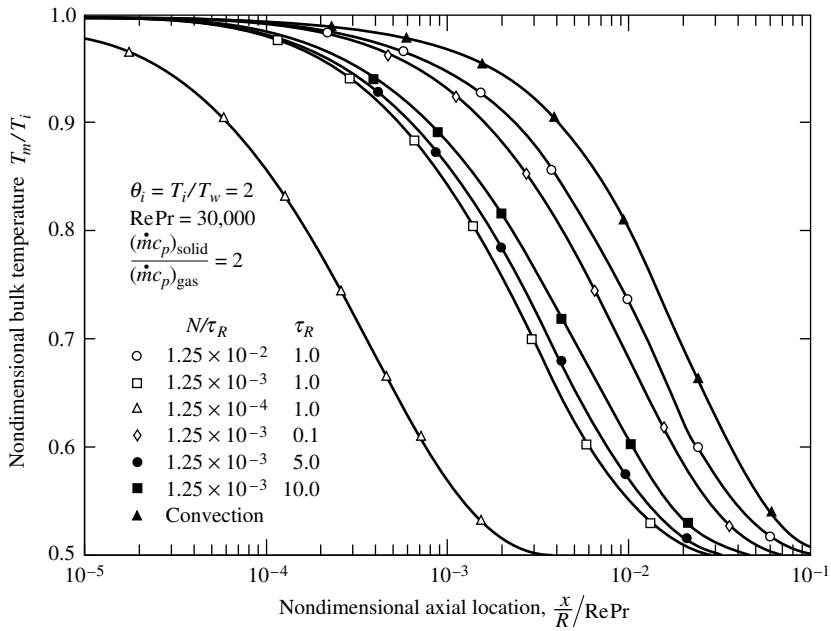

FIGURE 22-14
Influence of optical thickness and conduction–radiation parameter on bulk temperature development for gas-particulate flow through a tube—cooled wall.

an asymptotic value. However, as seen from Fig. 22-14, in the presence of thermal radiation this "fully developed" case is never reached until the bulk temperature is essentially equal to the wall temperature (note that, for pure convection, the bulk temperature has changed only by $\approx 20\%$ of maximum when fully developed conditions have been reached). Therefore, it may be concluded that *no thermally fully developed conditions can exist* for forced convection in duct flow combined with appreciable thermal radiation (i.e., radiative heat fluxes too large to be approximated by a linear expression in temperature). This fact was not realized by a number of early investigations on the subject, which employed "thermally developed" conditions to obtain relatively simple results [212–219]. Figures 22-13 and 22-14 also demonstrate how temperature level and optical thickness influence the variation of Nusselt number and bulk temperature. Reducing N/τ_R (which does not depend on absorption coefficient and, for a given medium and tube radius, implies raising temperatures) for a constant optical thickness results in increased heat transfer rates due entirely to an increase in radiative heat flux. The radiative heat flux goes through a maximum at an intermediate optical thickness, $\tau_R \simeq 1$ (for constant N/τ_R). This is readily explained by examining the optical limits. In the optically thin limit the medium does not emit or absorb any radiation, resulting in purely convective heat transfer. On the other hand, in the optically thick limit any emitted radiation is promptly absorbed again in the immediate vicinity of the emission point, again reducing radiative heat flux to zero.

A simple one-dimensional temperature profile does exist in the case of *Couette flow* (two infinite parallel plates moving at different velocities), since the entire problem becomes one-dimensional. The analysis for this case reduces to the same equations arrived at in the previous section for combined conduction and radiation, which have been solved numerically by Goulard and Goulard [220] and Viskanta and Grosh [221].

As indicated earlier, the Poiseuille flow problem was originally investigated by Kurosaki [209], using the exact integral relations for the radiative heat flux. The problem had been addressed a little earlier by Timofeyev and coworkers [222], using the two-flux method. The case of slug flow between parallel plates, with rigorous modeling of the radiative heat flux, has been treated by Lii and Özişik [223]. The influence of scattering on Poiseuille flow has been

discussed by a number of investigators [224–227]. Yener and coworkers [228, 229] examined the same problem for turbulent flow conditions, while Echigo and Hasegawa [230] addressed a laminar, scattering gas–particulate mixture. All of these publications neglected axial radiation. Two-dimensional radiation for Poiseuille flow has been studied by Einstein [18] (nonscattering fluid) and Kassemi and Chung [231] (isotropically scattering fluid), using the zonal method, and by Kim and Lee [232] (anisotropically scattering fluid), using the discrete ordinates method. Other investigations on turbulent tube flows with gray media, also using the discrete ordinates method, include those of Kim and Baek [233,234] (two-dimensional radiation without scattering) and Krishnaprakas and coworkers [235] (one-dimensional radiation with linear-anisotropic scattering).

Combined convection and radiation in thermally developing tube flow appears to have been investigated first by Einstein [236], deSoto [208], and Echigo and coworkers [237], considering two-dimensional (axial and radial) radiation, while Bergero and colleagues [238] considered developing flow and three-dimensional, gray radiation in a laminar rectangular duct, using the finite volume method (for radiation).

The effects of nongray molecular gas radiation on laminar tube and channel flows, employing the exponential wide band model, have been studied by a number of investigators [239–242]. Similar calculations for turbulent flows have also been carried out using fully developed flow and simple algebraic expressions for the eddy diffusivity for heat [219,240,243–245], while Smith and coworkers [246] used the two-dimensional zonal method and weighted-sum-of-gray-gases approach. More accurate analyses, using the statistical narrow band model, narrow band k-distributions, and the global ADF model for radiation calculations, have been carried out by the group around Soufiani and Taine for laminar [170, 247, 248] and turbulent [249, 250] tube and channel flows, the latter using the k–ϵ turbulence model. The general trends are similar to flows of gray media, i.e., strong radiation effects are evidenced by the much faster development of the temperature profiles (resulting in larger Nusselt numbers), regardless of whether the gas is heated or cooled. However, comparison with wide band model results showed that the latter can produce significant errors in predicting temperature fields and radiative fluxes. Comparison with experiment [247], on the other hand, showed excellent agreement with temperature fields predicted from the narrow band model.

Gas–particulate suspension flows were first addressed by Echigo and colleagues [251, 252] for laminar and turbulent flow of nonscattering media, respectively. Anisotropic scattering in tube suspension flows has been treated by Modest and coworkers for gray [211, 253] and nongray [245] carrier gases. Nongray effects in suspension flows have also been studied by Al-Turki and Smith [254], using the zonal method, while two-dimensional, gray particle radiation was considered by Park and Kim [255], using the P_1-approximation. Radiation effects in liquid glass jets were investigated by Yin and Jaluria [256, 257] and by Song *et al.* [258], both using a two-dimensional stepwise gray approach together with the zonal [256,257] or discrete ordinates method [258]. Finally, there have been several attempts at modeling radiation interactions with flow through porous media [259, 260] and packed beds [261–263]. A general overview of the literature has been given by Viskanta [264]

22.7 COMBINED RADIATION AND COMBUSTION

Thermal radiation from gases and particulates is an important, and often the dominant heat transfer mechanism during the burning of fuel. Therefore, inclusion of an adequate radiation model is essential to the success of a mathematical model of the combustion process, particularly in large systems (with larger optical thickness). The description of the burning process is an extremely difficult task even in the absence of radiation: "complete" chemical reaction mechanisms can involve hundreds of chemical species and thousands of elementary reactions [265], modeled by a nonlinear, stiff set of simultaneous differential equations. Furthermore,

the combustion process is generally accompanied by multidimensional (perhaps two-phase) convection involving all species, as well as by turbulent mixing. Comprehensive reviews of the pertinent literature up to 1986 [266] and 2004 [267] have been given by Viskanta and Mengüç. Here we will briefly discuss the particularly simple case of a laminar free convection diffusion flame, using a simple fuel (methane, CH_4), a simple global reaction mechanism,

$$CH_4 + 2O_2 \rightarrow CO_2 + 2H_2O \tag{22.78}$$

(neglecting multistep chemistry and intermediate species generation), and a simple reaction rate model (assuming an infinitely fast reaction wherever methane and oxygen come into contact). Such analyses were carried out in early work by Negrelli and coworkers [268] for the lower stagnation region of a horizontal cylinder, and by Liu and colleagues [269] for a vertical flat plate burner.

Results for combustion–radiation interaction in a simple, laminar diffusion flame are very characteristic for all reacting flows and can, qualitatively, be applied to fairly general combustion systems. For such a flame equations (22.42) through (22.45) are changed to

$$\frac{\partial}{\partial x}(\rho u) + \frac{\partial}{\partial y}(\rho v) = 0, \tag{22.79}$$

$$\rho\left(u\frac{\partial u}{\partial x} + v\frac{\partial u}{\partial y}\right) = \frac{\partial}{\partial y}\left(\mu\frac{\partial u}{\partial y}\right) - g(\rho_\infty - \rho), \tag{22.80}$$

$$\rho c_p\left(u\frac{\partial T}{\partial x} + v\frac{\partial T}{\partial y}\right) = \frac{\partial}{\partial y}\left(k\frac{\partial T}{\partial y}\right) - \frac{\partial q_R}{\partial y} + \dot{Q}'''_{\text{ch}}, \tag{22.81}$$

$$\rho\left(u\frac{\partial Y_i}{\partial x} + v\frac{\partial Y_i}{\partial y}\right) = \frac{\partial}{\partial y}\left(\rho D\frac{\partial Y_i}{\partial y}\right) + \dot{m}'''_i,\ i = \text{species}, \tag{22.82}$$

subject to the boundary conditions where, for free convection, the pressure term in the momentum equation has been replaced in favor of a buoyancy term, and the dissipation function has been dropped. The energy equation now has a heat source term (due to the release of chemical energy), and diffusion equations must be added for the mass fractions Y_i of all species. In early work it was common practice to further simplify the problem by assuming a single mass diffusivity, D, for all species and to only consider fuel (methane, F), oxidizer (oxygen, O), and products (H_2O and CO_2, P) as independent "species." The system of equations is closed with the ideal gas law, or ρT = const (assuming constant pressure), while the sources $\dot{Q}'''_{\text{ch}}$ and $\dot{m}'''_i$ are calculated from the reaction kinetics. Finally, the boundary conditions are replaced by

$$x = 0: \qquad u(0,y) = 0, T(0,y) = T_\infty, Y_F = Y_P = 0, Y_O = Y_{O\infty}; \tag{22.83a}$$

$$y = 0: \qquad u(x,0) = 0, v(x,0) = v_w, T(x,0) = T_w, Y_F = 1, Y_P = Y_O = 0; \tag{22.83b}$$

$$y \rightarrow \infty: \qquad u(x,\infty) = 0, T(x,\infty) = T_\infty, Y_F = Y_P = 0, Y_O = Y_{O\infty}. \tag{22.83c}$$

For the radiation term, both Negrelli [268] and Liu [269] used an exact 1D-solution of the RTE together with the wide band model to simulate the nongray radiation from the absorbing/emitting combustion gases (CH_4, CO_2, and H_2O). The above set of equations was solved by, both, Negrelli and coworkers [268] and Liu and colleagues [269] in a semianalytical way and compared with experiment. Both teams found rather good agreement between theory and experiment, especially in light of the rather primitive models. Figure 22-15 shows an example of the results of Negrelli *et al.* [268], who performed their calculations also for the cases of a transparent gas (no radiation) and a gray gas (using a Planck-mean absorption coefficient based on local partial pressures). Comparison with the no-radiation solution makes it evident that radiation lowers the temperatures in the high-temperature region of the boundary layer (by more than 100°C), and raises them in the cooler region near the outer edge of the boundary layer. Obviously, radiation's "action at a distance" allows energy to travel directly from the hot zone to the colder

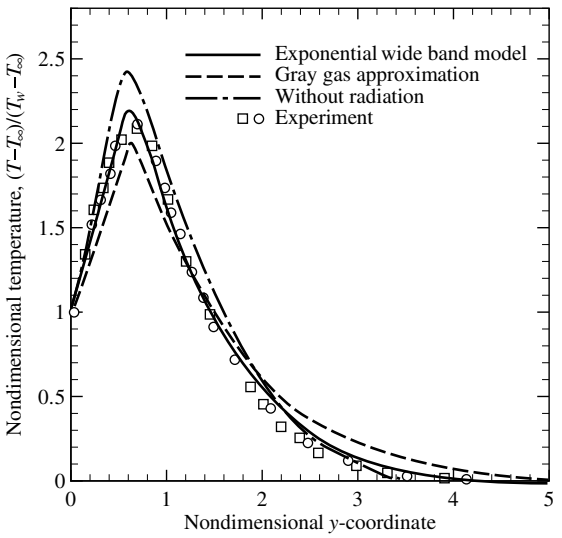

FIGURE 22-15
Experimental and theoretical temperature profiles for a laminar methane diffusion flame; from [268].

parts. It is also observed that radiation increases the thermal boundary layer thickness, for the same reasons. On the other hand, using a gray gas approximation severely overpredicts the effect of radiation on flame temperature and heat loss from the flame. The nongray gas emits and absorbs radiation across spectral lines that may be optically very thick, i.e., the emitted energy is reabsorbed in the immediate vicinity of the emission point; little emission occurs over vast parts of the spectrum ("spectral windows" with near-zero absorption coefficient). The gray approximation replaces the nongray absorption coefficient by a single, intermediate value, which predicts the correct overall emission, but (for large enough flames) strongly underpredicts reabsorption of this emission.

More recent investigations of laminar, methane diffusion flames have used more sophisticated reaction kinetics together with the CHEMKIN software [270, 271], and employed the statistical narrow band model for radiation [272, 273]. The influence of soot radiation on laminar diffusion flames has been studied for ethylene [274–277] and acetylene flames [278]. The older investigations used simple one-step kinetics and assumed the absorption coefficient to be gray (assuming radiation to be dominated by the near-gray soot), but used different soot nucleation, growth, coagulation and oxidation models as well as different RTE solvers. The more recent ones used full chemistry and the statistical narrow band model together with nongray soot for radiation. Kaplan and coworkers [274] also assessed the importance of radiation by comparing with calculations, in which radiation was ignored. Figure 22-16 is an example of their work, which clearly indicates that ignoring radiation, with its overprediction of temperature levels, leads to grossly overpredicted soot levels. Similar conclusions about the importance of radiative heat transfer can be drawn with respect to high-temperature production of trace pollutants, such as NO_x [279, 280]. Liu and coworkers [277] noted that radiation effects become much stronger under microgravity conditions.

Today, the literature on the interaction of radiative heat transfer in combustion applications is growing at a rapid pace, including investigations on turbulent jet diffusion flames [281–289], flame spread along vertical plates [290–293], droplet [294–296] and packed bed [297] combustion, simulations of fires [298] and of entire furnaces [299–305] and, very recently, of future oxy-fuel combustors [306] (designed for carbon capture). The results from all these studies are consistent with the qualitative behavior described in this section. Also notable is the finding that nongray soot modeling is of greater importance than nongray gas modeling in sooty flame simulations, with gray soot models producing large errors [289].

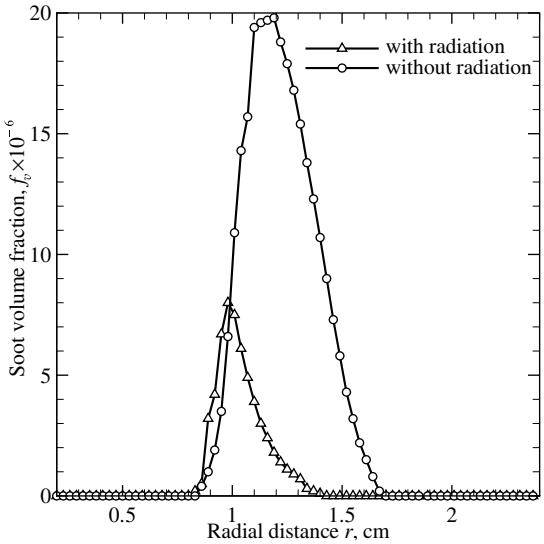

FIGURE 22-16
Experimental and theoretical soot level profiles for a laminar acetylene diffusion flame; from [274].

22.8 INTERFACING BETWEEN TURBULENT FLOW FIELDS AND RADIATION

The past years have seen tremendous advances in the modeling of turbulent flows and chemical reactions, as well as in the field of multidimensional, nongray radiation, each requiring their own sophisticated and time-consuming algorithms to produce accurate results. While the development of modern *large eddy simulations* (LES) and *direct numerical simulations* (DNS) is progressing at a rapid pace, most *computational fluid dynamics* (CFD) calculations will rely on *Reynolds-averaged Navier-Stokes* (RANS) solution methods during the foreseeable future. In RANS calculations the Navier-Stokes equations are solved in terms of time-averaged means, with all turbulence effects being modeled. While turbulence–convection interaction is always accounted for in these schemes (with eddy diffusivities or more advanced models), the interaction between the turbulent flow field and fluctuating intensities has generally been neglected. In this section we describe how time-averaged flow fields are interfaced with radiative heat transfer calculations in the absence of such turbulence–radiation interactions (TRI). Details on Reynolds averaging and on TRI will be given in the following section.

Forced convection problems tend to be parabolic in nature (i.e., downstream conditions are irrelevant), but have enormous gradients near surfaces (as well as near combustion fronts), necessitating a very fine grid system in their vicinity. Radiation problems, on the other hand, tend to be elliptic (i.e., the entire volume needs to be considered simultaneously), and are further complicated by directional and spectral dependence of the radiative intensity. Combining high-level models for turbulence and radiation requires great care to avoid instabilities, lack of convergence, and/or exorbitant computer memory and CPU requirements. The overall algorithm generally consists of the following steps:

1. A first estimate for the local radiative heat source $\dot{Q}_R''' = -\nabla \cdot \mathbf{q}_R$ is made.
2. The flow field is calculated, including velocity, temperature (or enthalpy), and species concentrations (if chemical reactions are present). This may include several iterations for complicated flow fields that are not strictly parabolic.
3. The absorption coefficient is calculated from the flow field as a function of pressure, temperature, and species concentrations.

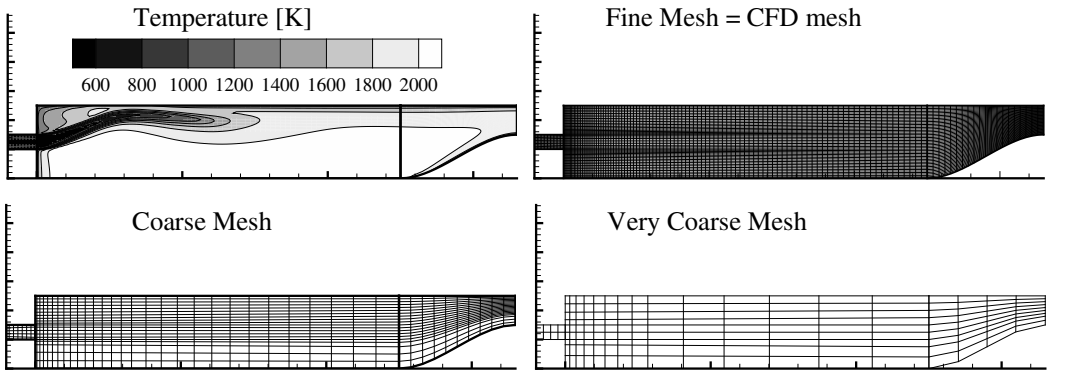

FIGURE 22-17
Combustor temperature distribution in the absence of radiation, and the three radiation meshes; from [307].

4. For the given temperature and absorption coefficient field the RTE is solved to obtain the radiative source term. Simple or sophisticated RTE solvers may be employed (P_1-approximation, different levels of the discrete ordinates or finite volume methods, etc.), and primitive or advanced spectral models may be used (gray gas, wide band models, narrow band models, k-distributions, etc.). It is also possible to start out with relatively crude RTE solutions, moving toward more accurate models as the overall solution progresses.
5. The radiative source is updated and the calculation returns to step 2 above until some overall convergence criteria are met.

Most combined convection–radiation calculations to date have used a common spatial grid for, both, the flow field and the thermal radiation calculations. This tends to be rather inefficient in turbulent flows since the flow field solver requires many mesh points near interfaces, while the RTE solver does not. RTE solvers, on the other hand, tend to require limits on the optical thickness of its computational cells, which may also be incompatible with the flow field solver. Having two separate meshes, however, has its own drawbacks. First, interpolation back and forth between the two meshes may be computationally expensive as well as inaccurate, commonly accumulating errors that lead to instability. Also, defining a second mesh requires additional work to define its topology, as well as additional computer memory.

An efficient solution to these problems is to establish a radiation grid whose cells are combinations of several flow field cells, similar to the multigrid algorithm often used in numerical analysis (provided no flow field cell violates optical thickness restrictions of the RTE solver). This was investigated in detail by Badinand and Fransson [307] looking at the plume flow of hot combustion gases behind a jet engine. During the iteration variables relevant to radiation (pressure, temperature, species concentrations) must be transferred from the CFD grid to the radiation grid, while updated values of the radiation source must be transferred from the radiation grid to the CFD grid. Badinand and Fransson used the simplest possible passing scheme, i.e., volumetric averages from all included CFD cells to the radiation cell, and placing the radiative source evaluated for a radiation cell into each of its included CFD cells. A slightly more involved passing scheme has been described by Omori and coworkers [305]. Figure 22-17 shows a set of meshes used by Badinand and Fransson [307] for an axisymmetric premixed combustor, and the resulting temperature field if radiation effects are neglected. Turbulence was modeled with the k–ϵ model, while for combustion the simple eddy dissipation model with one-step kinetics was used. Only the fine mesh was used for the flow field calculations (32,625 cells), while the fine, coarse (2,727 cells) and very coarse (625 cells) meshes were used for the radiation calculations. These were carried out using a gray gas with a spatially varying Planck-mean absorption coefficient and the finite volume method of Section 17.6 with 8×8 directions. Figure 22-18 shows the strong effects of radiation on temperature levels inside the combustor: Hot combustion gases

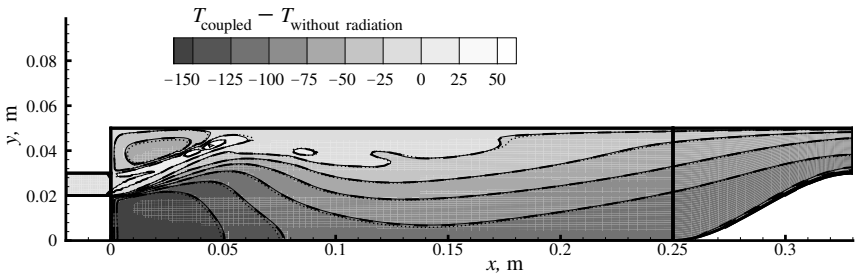

FIGURE 22-18
Combustor temperature differences due to radiation using the fine mesh (flood and solid line), the coarse mesh (dashed line), and the very coarse mesh (dotted line); from [307].

lose a lot of energy due to radiative emission, lowering local temperature levels by up to 150 K. Much of this emission travels to the walls, and some is absorbed by colder parts, raising the cold fuel–air jet temperature by 50 K. It is also seen from Fig. 22-18 that the choice of radiation mesh has virtually no effect on the results: As compared to the fine mesh, the temperature differences shown in the figure have errors of less than ±0.2% for the coarse mesh, and less than ±0.4% for the very coarse mesh. However, radiation computations are speeded up by a factor of 20 using the coarse mesh, and by a factor of 100 for the very coarse mesh.

The same scheme was employed by Soufiani and coworkers [248], while a somewhat more sophisticated approach was taken by Howell and coworkers [308] with what they term adaptive-mesh refinement (AMR). In effect, they use a multigrid algorithm for each flow field solution, and a similar but separate multigrid scheme for their discrete ordinates RTE solver. They achieved a respectable maximum CPU savings of a factor of 4, but this is considerably less than Badinand and Fransson because the RTE is, at its highest level, solved for the finest CFD grid.

22.9 INTERACTION OF RADIATION WITH TURBULENCE

During the development of the radiative transfer equation (RTE) in Chapter 10, we noted that heat transfer due to thermal radiation is essentially instantaneous, depending on the temporal temperature distribution as well as the temporal concentration field of the absorbing, emitting, and/or scattering medium. During turbulent flow the temperature field and, for mixtures, the concentration fields undergo rapid and irregular local oscillations (but slow compared with the response time of thermal radiation). The governing equations, such as equations (22.42) through (22.44) or equations (22.79) through (22.82), are then rewritten in terms of time-averaged quantities (denoted by an overbar), e.g.,

$$\overline{\rho}(x, y) = \frac{1}{\delta t} \int_{\delta t} \rho(x, y, t)\, dt, \tag{22.84}$$

where δt is the (small) time interval used for averaging. Commonly, the so-called Favre averaging (or mass-weighted averaging), denoted by a tilde, is also employed for compressible flows, that is,

$$\widetilde{\phi} = \overline{\rho\phi} \big/ \overline{\rho}, \tag{22.85}$$

where ϕ is the quantity to be averaged. For 2D forced convection with chemical reactions this leads to

$$\frac{\partial}{\partial x} (\overline{\rho}\, \widetilde{u}) + \frac{\partial}{\partial y} (\overline{\rho}\, \widetilde{v}) = 0, \tag{22.86}$$

$$\overline{\rho}\left(\widetilde{u}\frac{\partial\widetilde{u}}{\partial x}+\widetilde{v}\frac{\partial\widetilde{u}}{\partial y}\right)=\frac{\partial}{\partial y}\left[\overline{\rho}(\overline{\nu}+\nu_t)\frac{\partial\widetilde{u}}{\partial y}\right]-\frac{d\overline{p}}{dx}, \tag{22.87}$$

$$\overline{\rho}\left(\widetilde{u}\frac{\partial\widetilde{h}}{\partial x}+\widetilde{v}\frac{\partial\widetilde{h}}{\partial y}\right)=\frac{\partial}{\partial y}\left[\overline{\rho}(\overline{\alpha}+\alpha_t)\frac{\partial\widetilde{h}}{\partial y}\right]+\overline{\dot{Q}'''_{\text{ch}}}+\overline{\dot{Q}'''_R}, \tag{22.88}$$

$$\overline{\rho}\left(\widetilde{u}\frac{\partial\widetilde{Y}_i}{\partial x}+\widetilde{v}\frac{\partial\widetilde{Y}_i}{\partial y}\right)=\frac{\partial}{\partial y}\left[\overline{\rho}(\overline{D}_i+D_t)\frac{\partial\widetilde{Y}_i}{\partial y}\right]+\overline{\dot{m}'''_i}, \quad i=1,\ldots,s-1, \tag{22.89}$$

where temperature has been replaced in favor of enthalpy $h=\int c_p\,dT$. In these relations ν_t, α_t, and D_t are turbulent viscosity and heat and mass diffusivity, respectively. The source terms, $\dot{Q}'''_{\text{ch}}$, $\dot{Q}'''_R$, and $\dot{m}'''_i$ are strongly nonlinear functions of the *s composition variables*, collected into a vector $\boldsymbol{\phi}$ ($\phi_i=Y_i, i=1,\ldots,s-1; \phi_s=h$), and must be determined in time-averaged form. Turbulence modeling is a field of great complexity and research interest that has seen dramatic progress during recent years. Reynolds-averaged Navier–Stokes (RANS)-based turbulence models are the most popular today, in particular the ubiquitous k–ε model [309], and a number of more accurate models are also available. Another level of difficulty arises if the interaction between turbulence and a nonlinear source term is to be considered. The interaction between turbulence and chemistry has received considerable attention, resulting in flamelet models [310–312] and PDF (probability density function) methods [313]. While very relevant for the modeling of turbulence–radiation interactions, these models go much beyond the scope of this book, and the reader is referred to the relevant literature [314–319].

To account for the interaction between turbulence and radiation (TRI), the time-averaged radiative source must be evaluated, or

$$\overline{\dot{Q}'''_R}=-\overline{\nabla\cdot\mathbf{q}_R}=-\overline{\int_0^\infty\kappa_\eta\left[4\pi I_{b\eta}-\int_{4\pi}I_\eta\,d\Omega\right]d\eta}=-\int_0^\infty\left[4\pi\overline{\kappa_\eta I_{b\eta}}-\int_{4\pi}\overline{\kappa_\eta I_\eta}\,d\Omega\right]d\eta. \tag{22.90}$$

Because of their nonlinear dependence on composition variables these terms cannot be determined based on mean values. Thus, two *turbulence moments* or *correlations* are required: the correlations between absorption coefficient and Planck function, $\overline{\kappa_\eta I_{b\eta}}$, and between absorption coefficient and radiative intensity, $\overline{\kappa_\eta I_\eta}$. The former correlation is termed

$$\textit{Emission TRI}: \qquad \overline{\kappa_\eta I_{b\eta}}\neq\kappa_\eta(\widetilde{\boldsymbol{\phi}})I_{b\eta}(\widetilde{T}), \tag{22.91}$$

while the latter is known as

$$\textit{Absorption TRI}: \qquad \overline{\kappa_\eta I_\eta}\neq\kappa_\eta(\widetilde{\boldsymbol{\phi}})I_\eta(\widetilde{\boldsymbol{\phi}}). \tag{22.92}$$

Absorption TRI is particularly difficult to evaluate because the fluctuations of the local intensity may be influenced by property fluctuations from everywhere in the medium. On the other hand, in some early work Kabashnikov and coworkers [320–322] have suggested that, if the mean free path of radiation is much larger than the turbulence eddy length scale l_t, then the local radiative intensity is only weakly correlated with the local absorption coefficient, i.e.,

$$\textit{Absorption TRI}: \qquad \overline{\kappa_\eta I_\eta}\simeq\overline{\kappa_\eta}\,\overline{I_\eta}. \tag{22.93}$$

This expression, valid if $\kappa_\eta l_t\ll 1$, and commonly known as the (*optically*) *thin eddy approximation*, or *optically thin fluctuation approximation* (OTFA), simplifies the evaluation of $\overline{\dot{Q}'''_R}$ considerably, since the remaining correlations $\overline{\kappa_\eta}$ and $\overline{\kappa_\eta I_{b\eta}}$ can be constructed from single-point statistics of the composition variables. Note that, in order to invoke this approximation, one must have $\kappa_\eta l_t\ll 1$ for *all* wavenumbers. While this condition is generally violated by combustion gases

for very small parts of the spectrum (see, e.g., Fig. 11-6), and also for extremely sooty flames, it is justifiable in the vast majority of applications. To date most predictions of TRI (turbulence–radiation interactions) have employed the OTFA.

Very similar to the time-averaged chemical source term, evaluation of the remaining correlations, $\overline{\kappa_\eta}$ and $\overline{\kappa_\eta I_{b\eta}}$, requires equations or models for the correlations between any two composition variables, for a total of s^2 moments [323]; this task is clearly not feasible with traditional RANS-based models.

Because of these difficulties radiation and turbulence have traditionally been treated as independent phenomena, i.e., the influence of turbulent fluctuations on the composition variables (that determine the local values of radiative properties, blackbody intensity and, therefore, the local radiative intensity) have been neglected. If effects of radiation are considered at all, the calculations are generally based on mean (time-averaged) composition variables. Experimental data, obtained by the groups around Faeth and Gore [324–333] have indicated that, depending on fuel and other conditions, radiative emission from a flame may be as much as 50% to 300% higher than would be expected based on mean values of temperature and absorption coefficient. Cox [334] has shown that emission from a hot medium increases dramatically due to turbulence, simply by expanding the emissive power into a Taylor series. For example, for a simple, gray medium with constant absorption coefficient, the TRI reduce to $\overline{\kappa I_b} = \kappa \overline{I_b} = \kappa \overline{E_b}/\pi$, where

$$\overline{E_b(x,y,t)} = \frac{1}{\delta t} \int_{\delta t} n^2 \sigma T^4(x,y,t)\, dt. \tag{22.94}$$

If one writes temperature and its fluctuations in terms of a time average,

$$T(x,y,t) = \overline{T}(x,y,t) + T'(x,y,t), \quad \overline{T'} = 0, \tag{22.95}$$

then $E_b(x,y,t)$ can be approximated by a truncated Taylor series as

$$E_b(T) \simeq E_b(\overline{T}) + T' \frac{dE_b}{d\overline{T}} + \frac{1}{2}(T')^2 \frac{d^2 E_b}{d\overline{T}^2} + \ldots, \tag{22.96a}$$

and

$$\overline{E_b(T)} \simeq E_b(\overline{T}) + \frac{1}{2} \frac{d^2 E_b}{d\overline{T}^2} \overline{(T')^2} = \sigma \overline{T}^4 \left[1 + 6 \frac{\overline{(T')^2}}{\overline{T}^2} \right]. \tag{22.96b}$$

Equation (22.96*b*) shows that the so-called *temperature self-correlation* (time-averaged emissive power) is always positive, resulting in enhanced emission due to turbulence–radiation interactions. In the present case (gray, constant-property medium) temperature fluctuations of ± 30% would increase emission by more than 50%!

In most early works on turbulence–radiation interactions the radiation calculations were not coupled with the flow field model; rather, the fluctuation fields were *assumed* [249, 250, 335–340]. It was generally concluded that TRI are of importance only in the presence of chemical reactions (combustion of fuel), and there were some suggestions of temperature fluctuations to dominate turbulence radiation interactions. While it is now widely recognized that turbulent fluctuations affect the radiative transfer rates, the reverse is also true, i.e., radiation has an effect on temperature fluctuations in a turbulent flow. This was first recognized by Townsend [341], and has been further studied in the atmospheric sciences [342, 343] and for high-temperature gases [344, 345].

It was observed in Sections 22.4 and 22.6 that, in boundary layers and in internal flows, radiation is often dominated by its transverse component and can, thus, be approximated as one-dimensional, greatly facilitating the solution because of the parabolic nature of forced convection. Turbulent fluctuations are always transient and three-dimensional, although problems may be statistically steady and one- or two-dimensional [i.e., in a time-averaged sense, equation (22.84)]. Similarly, time-mean radiative transfer in boundary layers and in internal flows

tends to again be dominantly in the transverse direction. Sakurai and colleagues [346] have shown that, if radiation is statistically one-dimensional, TRI may be adequately evaluated with a one-dimensional RTE solver (i.e., neglecting the three-dimensionality of turbulence), greatly reducing the necessary effort.

The first study modeling TRI from basic principles was done by Mazumder and Modest [347, 348], who considered a methane–air diffusion flame and a nonreacting combustion gas mixture, respectively. Using a Monte Carlo solution to the velocity-composition PDF approach invoking the thin eddy approximation and using the box model of Section 20.4 for radiation, they were able to evaluate turbulence–radiation interactions without further approximation. Studying nonreacting flows [348], it was confirmed that, indeed, TRI are never of great importance in nonreacting flows, never changing radiative sources and fluxes by more than 10%. On the other hand, in the methane–air flame heat loss rate increases due to TRI of up to 75% *beyond* the temperature self-correlation were observed [347].

A systematic analysis of turbulence–radiation interactions in two-dimensional, axisymmetric, nonluminous jet diffusion flames was first carried out by Li and Modest [349–351]. They employed a hybrid approach, using a commercial finite volume code (Fluent [352]) together with the composition PDF method [313, 319], and also invoked the thin eddy approximation (OTFA). The philosophy of the probability density function (PDF) approach is to consider the thermo-fluid variables ($\mathbf{u}$, h, $\mathbf{Y}$, etc.) as random variables and consider the transport of their PDFs rather than their moments. The composition PDF is the simplest form of the PDF methods since it carries information for the composition variables only, collected in the vector $\boldsymbol{\phi}$, which contains the $s-1$ mass fractions $\mathbf{Y}$ and the enthalpy h. The great advantage of PDF methods is that the mean for any quantity, say a source $\overline{\dot{Q}'''}$, can be evaluated directly from the PDF, provided $\dot{Q}'''$ is a function of local composition variables $\boldsymbol{\phi}$ only. This leads to

$$\overline{\dot{Q}'''} = \int_0^\infty f(\boldsymbol{\psi})\dot{Q}'''(\boldsymbol{\psi})\,d\boldsymbol{\psi}, \tag{22.97}$$

where $\boldsymbol{\psi}$ represents the *sample space* for the composition variables $\boldsymbol{\phi}$ (for example, $0 \le \psi_s < \infty$ is the range of values that the last composition variable, $\phi_s = h$, can attain); $f(\boldsymbol{\psi})$ is the probability density of the compound event of $\boldsymbol{\phi} = \boldsymbol{\psi}$ (i.e., $\phi_1 = \psi_1, \phi_2 = \psi_2, \ldots, \phi_s = \psi_s$), so that

$$f(\boldsymbol{\psi})\,d\boldsymbol{\psi} = \text{probability}(\boldsymbol{\psi} \le \boldsymbol{\phi} \le \boldsymbol{\psi} + d\boldsymbol{\psi}). \tag{22.98}$$

The transport equation for the composition PDF for radiating reactive flow has been developed by Li and Modest [349] based on the extensive work of Pope [313]. This resulted in a partial differential equation in $s + 4$ independent variables (time, space, and composition variable space), which—because of its high dimensionality—must be solved through stochastic particle tracing [313, 319, 353, 354]. The composition PDF carries no information on the velocity field and, therefore, must be combined with another solver to provide the solutions to the mean momentum equations as well as a turbulence model (such as k–ε).

Li and Modest employed a simple single-step mechanism for chemistry, and the FSK method of Section 20.8 together with the P_1-approximation for the evaluation of thermal radiation from the combustion gases (CO_2, H_2O, and CH_4). Flames were characterized through nondimensional parameters, namely Reynolds number Re (describing jet velocity, flame size, turbulence level), optical thickness τ_L (flame size), Damköhler number Da (flow time scale *vs.* chemical reaction time scale) and Froude number Fr (buoyancy effects), and their impact on turbulence–radiation interactions was assessed. Their base configuration was Sandia Flame D [355], for which an abundance of experimental measurements is available (including radiation data). However, Sandia D is a small laboratory flame (as are most experimentally documented flames) with, therefore, relatively little radiation. Thus, Li and Modest also studied flames scaled up

by factors of 2 and 4 to determine radiation and TRI effects in larger flames. It was found that TRI affect the flame in two ways: (1) emission from and self-absorption by the flame are both strongly, and about equally, increased, and (2) the additional net heat loss causes the flame to cool (and this, in turn, can substantially lower emission as well as chemical reaction rates to the point of flame extinction). Not surprisingly, the strength of TRI is most strongly sensitive to the flame's optical thickness. Optically thin flames lose relatively little heat by radiation; TRI cause this loss to increase by a substantial 50%, but decrease flame temperature only by a small amount (maybe 20°C). This additional heat loss causes optically thick flames to cool down substantially (by 100°C and more), resulting in a sharp drop in emissive power, and overall heat loss rates are only increased by a few percent.

To isolate the importance of the various turbulence interactions that combine for the total TRI effect, Li and Modest [350] looked at "frozen" composition variable fields for several flames (using the converged temperature and species mass fraction fields for the flame with fully considered TRI). They determined the various radiative contributions to flame emission and self-absorption under a number of different scenarios. It was found that, on a percentage basis, the increase in radiative heat losses due to TRI is essentially independent of optical thickness: for all three flames, both, emission and self-absorption are consistently increased by about 60%. However, in optically thin flames this translates into a *net additional loss* of 50%, since temperature levels (in an "unfrozen" field) decrease by only 20°C or so. In optically thick flames TRI bring down temperature levels by more than 100°C, and the *net* heat loss is hardly increased at all. The different underlying TRI mechanisms display similarly consistent trends: if only the Planck function self-correlation is considered, emission and absorption increase by roughly 35% for a gray medium. However, if the nongrayness of the combustion gases is accounted for, this increase is less than 10%, again regardless of optical thickness (absorption lagging behind emission, since it is a response to the raised emission level). The reason is that the gas radiates only over the fairly narrow absorption–emission bands, across which the nonlinearity of the Planck function is much less severe. Even for a gray medium, for which the Planck function self-correlation *is* the most important driving force of the TRI, it by no means *dominates* the interaction. The strongest contributions to TRI always come from the correlation between absorption coefficient and Planck function fluctuations.

Several other investigators have investigated Sandia Flame D in the context of TRI [345,356–359], most of them at a lesser level of sophistication than the work of Li and Modest [349,350], but all providing consistent answers for the quantitative importance of radiation and turbulence–radiation interactions. The most advanced and accurate model to date of Flame D is the one by Wang and coworkers [345], using models similar to those of Li and Modest, but employing a more advanced composition PDF code, a more realistic chemical reaction mechanism, and the line-by-line accurate photon Monte Carlo scheme described in Section 21.6, which was specifically developed for the stochastic media employed in transported PDF methods. As can be seen from Fig. 22-19, their model predicts centerline temperatures very well, but also that radiation (with or without TRI) has little influence in a small, optically thin flame. Wang and coworkers also scaled up the flame by factors of 2 ($kL2$) and 4 ($kL3$) (but in a different way from Li and Modest to preserve realistic chemistry). Consistent with Li and Modest's observation they noted that increasing flame size, and thus its optical thickness, increases radiative heat loss while also reducing temperature levels. The relative importance of TRI was found to be independent of optical thickness (roughly 30% for all flames).

While temperature levels in optically thin flames are only weakly dependent on radiation, pollutant levels tend to be a strong function of temperature. Pal *et al.* [359] used Wang and coworkers' code to investigate NO levels in Sandia D, as shown in Fig. 22-20. Radiation is seen to decrease NO levels appreciably (due to the slightly lower temperatures). The agreement between experiment and theory is rather encouraging, and Fig. 22-20 clearly demonstrates the importance of radiation and TRI on mean pollutant levels and their turbulent fluctuations: Radiation lowers temperatures in the center of the flame (lowering NO levels), but heats colder

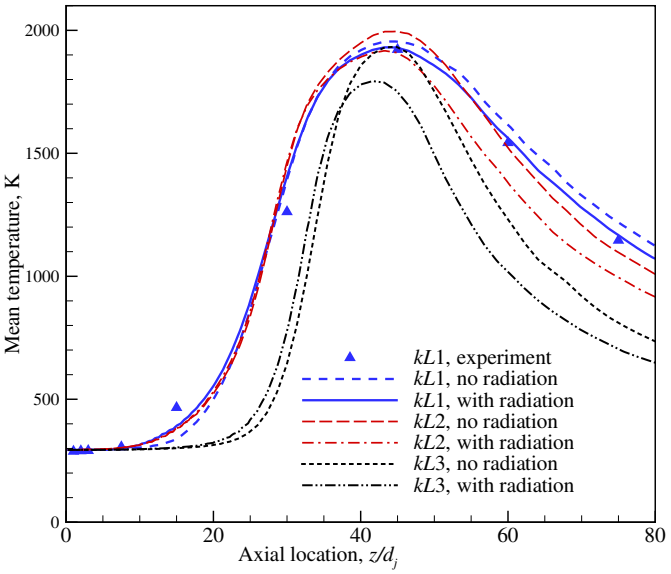

FIGURE 22-19
Comparison of centerline temperatures in an axisymmetric methane–air jet diffusion flame, with and without turbulence–radiation interaction; from Wang and coworkers [345].

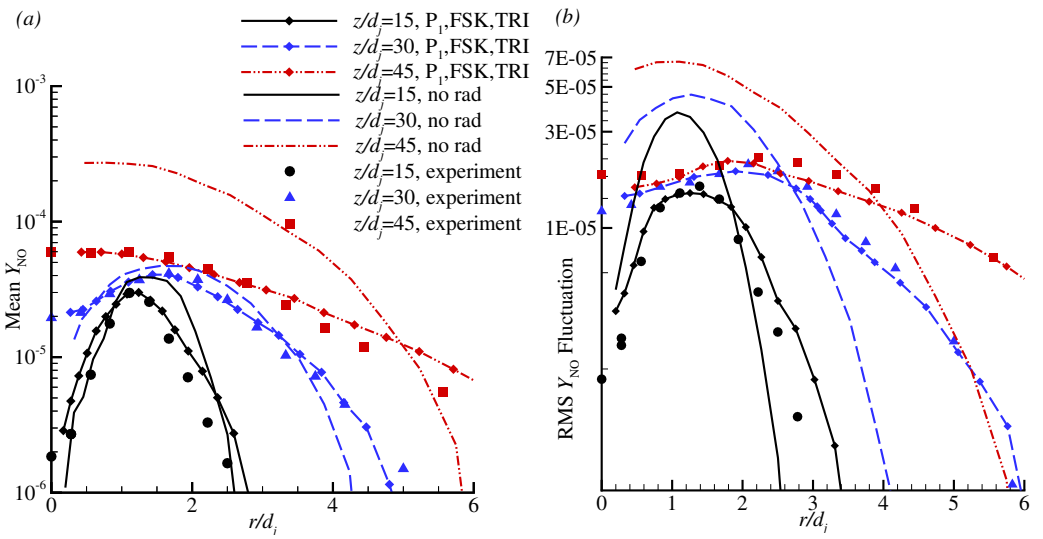

FIGURE 22-20
Radial profiles of NO mass fraction at various axial locations of Flame D: *(a)* mean values, *(b)* RMS fluctuations; from Pal *et al.* [359].

regions further away (increasing NO). Radiation's "action at a distance" decreases RMS fluctuations everywhere, except for colder regions that have no NO at all without radiation. These effects are multiplied in larger flames, with greater influence of radiation and TRI on temperatures: predicted NO levels decrease by orders of magnitude when radiation and TRI are taken into account.

The first attempt to quantify absorption TRI was made by Tessé and coworkers [360], who investigated a small sooting (luminous) ethylene flame, using detailed chemistry and a sophisticated soot model [361], together with a Lagrangian solver to obtain the composition PDF. They then constructed many homogeneous turbulence structures from this PDF and determined the thermal radiation with a photon Monte Carlo scheme together with the narrow band

k-distribution model of Soufiani and Taine [362]. They found emission to increase by 30%, and also found absorption TRI to be appreciable (5% of total emission) for this luminous flame, indicating eddies of appreciable optical thickness. The first ones to assess absorption TRI from basic principles (i.e., without the assumptions for turbulence structures made by Tessé) were Wang and coworkers [345], who used a transported composition PDF to determine composition variables and their turbulence moments, together with Wang's [363, 364] LBL-accurate photon Monte Carlo scheme for stochastic particles. This radiation solver was specifically developed to determine a PDF for photons, providing full compatibility with the stochastic turbulence model. With their model Wang and coworkers [345] provided proof that absorption TRI is negligible for Sandia D and, indeed, also for large nonluminous flames. The method was further employed to investigate the influence of TRI in sooting flames: Mehta *et al.* [365–367] modeled six sooting flames [368–370] using Wang and coworkers' [345] schemes together with a sophisticated soot model [371], to assess the importance of both emission and absorption TRI in such systems. They found emission TRI (30% to 60%) and heat losses from the flame (increases of 45% to 90%) to be stronger than in nonluminous flames. However, in contrast to Tessé's [360] observations, absorption TRI was found to be negligible for all six laboratory-scale flames, despite the soot. Only when scaling up the sootiest flame [369] by a factor of 32 did absorption TRI become appreciable (6% of total emission).

Turbulence–radiation interactions may also be assessed using more sophisticated CFD methods, such as *large eddy simulations* (LES) and *direct numerical simulations* (DNS). Chandy and coworkers [372] were the first to study TRI using LES together with a *filtered density function* (FDF) for composition variables (the LES equivalent of the transported PDF used with RANS simulations), looking at an idealized luminous flame with a primitive soot model. They concluded that, while emission TRI is always important at the subgrid scale (SGS) level, absorption TRI at the SGS level can always be neglected. Similar conclusions were drawn by Gupta *et al.* [373], who used a similar LES/FDF approach, but coupled with Wang's [363, 364] LBL-accurate photon Monte Carlo scheme. Finally, Roger [374, 375] also showed SGS absorption TRI to be negligible by using DNS of stationary isotropic turbulence. Turbulence–radiation interactions in the context of DNS have been investigated by the group around Haworth and Modest [376–380] for a number of artificial scenarios. However, to date DNS simulations are limited to system sizes in the mm range, i.e., ranges over which combustion media are optically extremely thin.

Today the study of turbulence–radiation interactions remains an extremely active field of research. For further reading the reader is directed toward several review articles by Modest [381–383] and the very exhaustive monograph by Coelho [384].

22.10 RADIATION IN CONCENTRATING SOLAR ENERGY SYSTEMS

Radiative heat transfer plays an important role in the harnessing of concentrated solar radiation. Applications include solar thermal power [385, 386], solar thermochemistry [387–389], and concentrating photovoltaics [390–392], in which solar radiation is converted to thermal, chemical, and electrical energy, respectively.

Radiative fluxes that can be obtained with optical concentrators vary between few kW/m^2 and several MW/m^2. Concentrating solar systems are characterized by the solar concentration ratio, defined as the ratio of the concentrated solar flux to solar irradiation of 1 kW/m^2. High temperatures can be achieved by increasing the concentration ratio to limit the reradiation losses from a receiver [393]. While high temperatures are targeted in solar thermal power and thermochemical systems to increase their efficiency, they are unwanted in photovoltaic cells due to cell efficiency decreasing with temperature. Thus, concentrating photovoltaics systems typically utilize lower fluxes and research efforts are focused on cell thermal management [390].

High-temperature solar thermal systems often include solid-gas heterogeneous media at

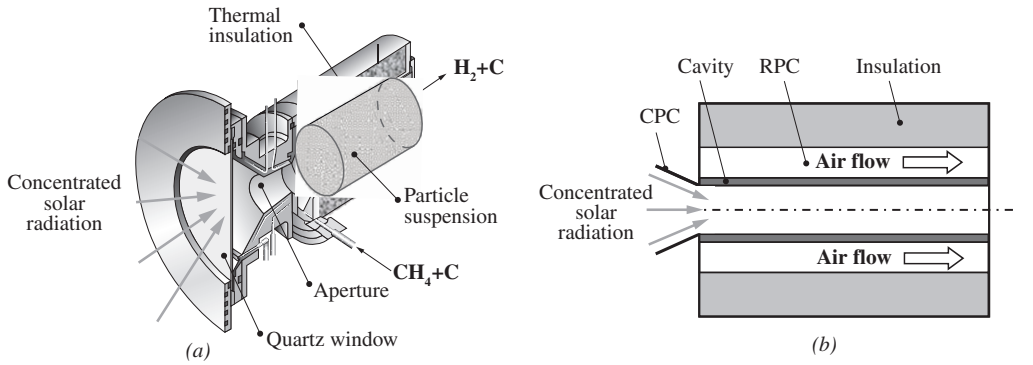

FIGURE 22-21
Examples of high-temperature devices utilizing concentrated solar radiation: *(a)* a directly irradiated solar thermochemical test reactor for thermal decomposition of methane, featuring a flow of methane laden with carbon particles exposed to concentrated solar radiation [394]; and *(b)* an indirectly irradiated solar receiver prototype featuring an annular layer of reticulated porous ceramics (RPC) bounded by two concentric cylinders: concentrated solar radiation passes through a compound parabolic concentrator (CPC), and is absorbed by the inner cylindrical cavity, and converted into heat, which is further transferred by conduction, radiation, and convection to the pressurized air flowing across the layer of RPC [395].

temperatures exceeding several hundred degrees Celsius, and in some applications reaching more than 2000°C. Such media serve multiple purposes. They absorb high-flux irradiation (absorption is predominantly by the solid phase as direct gas absorption is ineffective for length scales of a solar device) and transfer the heat to a working gas in a *solar thermal receiver* driving a thermodynamic power cycle, and/or to a chemical reaction in a *solar thermochemical reactor*. In *directly irradiated receivers/reactors* radiation is absorbed by a solid that is in direct contact with the working gas or provides surface to a chemical reaction, respectively (Fig. 22-21*a*). In *indirectly irradiated receivers/reactors* radiation is absorbed by a solid, and then transferred to a gas or to a chemical reaction by conduction, convection, and/or radiation through an intermediate heat transfer medium (solid, fluid, or multiphase medium, Fig. 22-21*b*).

Radiation in Solar Thermal Receivers

The design of a receiver depends on the type of concentrator, the working fluid, and the operating ranges of temperature, pressure, and radiative flux. A comprehensive review of solar receivers up to 1998 was given by Karni *et al.* [396], and a more recent review of volumetric receivers for solar thermal power plants with a central receiver by Ávila-Marín [397].

An early radiative heat transfer analysis in a volumetric solar absorber was presented by Flamant [398] for solar fluidized beds of silicon carbide, chamotte, zirconia, and silica particles. Temperature profiles, total emissivity, heat flux distribution, and effective mean penetration distance were determined and compared to experimental data. Combined radiative, conductive, and forced convective heat transfer in a volumetric selective solar absorber containing a packed bed of two spectrally dissimilar slabs of particles was analyzed by Flamant *et al.* [399] using the two-flux approximation. The model accounted for the variation of absorption and scattering of the layers in the visible and infrared spectral ranges, and its predictions were validated experimentally using a bed of glass and silicon carbide particles that were heating the gas phase. An array of irradiated fin-pins exposed to a gas flow was studied experimentally in a solar furnace by Karni *et al.* [396].

A two-dimensional steady-state heat transfer model coupling radiation, conduction, and convection was developed for a novel design of a high-temperature pressurized-air receiver for power generation via combined Brayton–Rankine cycles (see Fig. 22-21) [395]. The model employs separate energy equations for solid and gas phases in the annular layer of reticulated

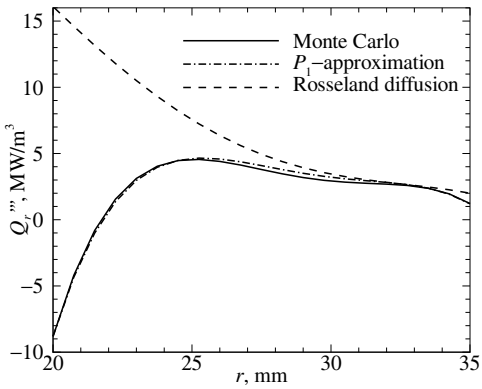

FIGURE 22-22
Radial distribution of radiative source term within the RPC of the receiver shown in Fig. 22-21*b*, at a selected axial location $z/L = 0.12$ (for receiver length of 65 mm, outer radius of SiC tube of 20 mm, and a total solar power input of 1 kW) [395].

porous ceramics saturated with pressurized air:

$$\text{solid :} \qquad \frac{1}{r}\frac{\partial}{\partial r}\left(rk_s\frac{\partial T_s}{\partial r}\right)+\frac{\partial}{\partial z}\left(k_s\frac{\partial T_s}{\partial z}\right)+\dot{Q}_R'''=sh\left(T_s-T_f\right), \tag{22.99a}$$

$$\text{air :} \qquad \rho c_p v\frac{\partial T_f}{\partial z}=sh\left(T_s-T_f\right), \tag{22.99b}$$

where s is the specific surface area of the solid–fluid interface and h is the heat transfer coefficient between particles and air. Radiative transfer in the receiver cavity was modeled using enclosure theory. The Rosseland diffusion approximation, the P_1-approximation and the Monte Carlo method were employed as alternative methods to study radiative transfer in the porous layer, which was assumed to be gray and isotropically scattering:

$$\text{diffusion, equation (15.16) :} \qquad \dot{Q}_R'''=\frac{1}{r}\frac{\partial}{\partial r}\left(r\frac{16\sigma T_s^3}{3\beta}\frac{\partial T_s}{\partial r}\right), \tag{22.100a}$$

$$P_1\text{, equation (16.50}a\text{) :} \qquad \dot{Q}_R'''=\kappa(G-4\sigma T_s^4), \tag{22.100b}$$

$$\text{Monte Carlo, equation (21.45) :} \qquad \dot{Q}_R'''=\frac{\delta Q_a}{\delta V}-4\kappa\sigma T_s^4, \tag{22.100c}$$

where the radiative power δQ_a absorbed by the volume δV is directly computed by the Monte Carlo method. Figure 22-22 shows the radial distributions of the radiative source term for the three solution methods at a selected location $z/L = 0.12$. The P_1 results were found to agree reasonably well with those obtained by the Monte Carlo method, while the Rosseland approximation led to inaccurate results due to the relatively small optical thickness of the porous layer made of reticulated porous ceramics ($\tau_{RPC} = 3$). P_1 was found to be the most appropriate method as it simultaneously led to good accuracy and short computational times. A combined heat transfer numerical study using the discrete ordinate method for a solid-particle receiver was presented in [400].

Cavity-receivers are often enclosed by semitransparent windows to separate the hot gas inside the receiver from a cold ambient atmosphere. Radiative heat transfer in a cavity-receiver containing a windowed aperture was analyzed by Maag *et al.* [401] for quartz and sapphire windows using the band approximation of Chapter 7. Radiative heat transfer in a solar cavity receiver with a plano-convex window was studied by Yong *et al.* [402] with the Monte Carlo method.

Radiation in Solar Thermochemical Reactors

The use of concentrated solar radiation in chemistry dates back to the 18th century, when Antoine Lavoisier conducted combustion experiments in a solar furnace consisting of two

concentric lenses [403]. Pioneering work on solar processes and reactors was done by Trombe and Foex [404], Nakamura [405], Fletcher and Moen [393], and others. In a solar thermochemical reactor the incident solar radiation enters a reactor cavity through an aperture, which may be windowed, and is absorbed by reactants and cavity walls. Reactor design and optimization is typically guided by thermochemical models coupling radiation, conduction, and convection to the chemical kinetics [406]. Radiation analyses range from models with surface radiative exchange to more sophisticated models, in which medium composition and phases vary with time as chemical reactions progress.

Solar-driven redox thermochemical cycles have been investigated to produce H_2 and CO from H_2O and CO_2, respectively. A two-step cycle for a generic metal oxide M_xO_y can be written as [407]:

$$\text{solar, endothermic step:} \qquad \frac{1}{\Delta\delta}M_xO_{y-\delta_{ox}} \rightarrow \frac{1}{\Delta\delta}M_xO_{y-\delta_{red}} + 0.5O_2, \tag{22.101}$$

$$\text{nonsolar, exothermic step:} \qquad \frac{1}{\Delta\delta}M_xO_{y-\delta_{red}} + H_2O \rightarrow \frac{1}{\Delta\delta}M_xO_{y-\delta_{ox}} + H_2, \tag{22.102}$$

$$\text{or} \qquad \frac{1}{\Delta\delta}M_xO_{y-\delta_{red}} + CO_2 \rightarrow \frac{1}{\Delta\delta}M_xO_{y-\delta_{ox}} + CO, \tag{22.103}$$

where δ_{ox} and δ_{red} are the nonstoichiometric coefficients of the reduced and oxidized forms of the metal oxide, and $\Delta\delta = \delta_{red} - \delta_{ox}$. Lipiński *et al.* [408] studied the decomposition of micrometer-sized zinc oxide particles in a stationary particle suspension under direct high-flux irradiation. A numerical model coupling transient radiative heat transfer to chemical kinetics accounted for time-dependent radiative properties due to decreasing particle sizes, computed from Mie theory at each time step of the transient solution. Abanades *et al.* [409] developed a multiphase model coupling fluid flow, heat and mass transfer, and chemical kinetics of the zinc oxide decomposition reaction, treating the particles as opaque spheres. Transient radiative heat transfer in directly irradiated solar reactors containing packed beds of zinc oxide particles was numerically analyzed using the Rosseland diffusion approximation by Müller *et al.* [410] and Schunk and coworkers [411]. A diffusion-based model of internal radiative transport in the packed bed of zinc oxide was also proposed by Dombrovsky *et al.* [412]. The numerically determined temperature profiles reported in [411, 412] were found to be in good agreement with those measured in a solar-driven thermogravimeter. Radiative heat transfer in a solar thermochemical reactor for the reduction of cerium dioxide was analyzed using the Monte Carlo method by Villafán-Vidales *et al.* [413]. The participating medium was a nonisothermal, nongray, absorbing, emitting, and anisotropically scattering suspension of particles with properties obtained from Mie theory. Radiative characteristics of novel cerium dioxide-based materials for applications in nonstoichiometric redox cycles were studied by Liang *et al.* [414], Ganesan *et al.* [415, 416], and Haussener and Steinfeld [417].

Directly irradiated particles of carbonaceous materials are encountered in several solar thermochemical processes including steam gasification of coal and methane decomposition,

$$CH_xO_{1-y} + yH_2O = (x/2 + y)H_2 + CO, \tag{22.104}$$

$$CH_4 \rightarrow C + 2H_2. \tag{22.105}$$

Transient radiative heat transfer in directly irradiated stationary suspensions of coal particles undergoing steam gasification was studied numerically using the Monte Carlo method and Mie theory by Lipiński and Steinfeld [418] and geometric optics by Lipiński *et al.* [419]. The Monte Carlo method and geometric optics were also applied in a simulation of a solid–gas fluidized bed reactor for coal gasification. Maag and coworkers [394] developed a transient combined convective–radiative heat transfer model of directly irradiated CH_4 flow laden with carbon particles. Mie theory was applied to obtain radiative properties of particles growing due to deposition of carbon from the decomposition reaction. A combined radiative–conductive–convective heat transfer model of an entrained-flow reactor for methane decomposition was

developed by Maag *et al.* [420]. The net radiation method was applied to a cavity with opaque walls and a semi-transparent aperture.

Thermal decomposition of calcium carbonate has been studied for the solar production of lime and cement, as well as solar thermochemical CO_2 capture. In these models for reacting packed beds $CaCO_3$ particles were assumed to be in the size range of geometric optics. The Rosseland diffusion approximation was applied in a transient combined radiation–conduction model [421], while spectral characteristics of the refracting and absorbing semitransparent particles were accounted for in another study [422].

References

1. Wylie, C. R.: *Advanced Engineering Mathematics*, 5th ed., McGraw-Hill, New York, 1982.
2. Viskanta, R., and R. J. Grosh: "Effect of surface emissivity on heat transfer by simultaneous conduction and radiation," *International Journal of Heat and Mass Transfer*, vol. 5, pp. 729–734, 1962.
3. Viskanta, R., and R. J. Grosh: "Heat transfer by simultaneous conduction and radiation in an absorbing medium," *ASME Journal of Heat Transfer*, vol. 84, pp. 63–72, 1963.
4. Lick, W.: "Energy transfer by radiation and conduction," in *Proceedings of the Heat Transfer and Fluid Mechanics Institute*, Stanford University Press, Palo Alto, California, pp. 14–26, 1963.
5. André, S., and A. Degiovanni: "A theoretical study of the transient coupled conduction and radiation heat transfer in glass: Phonic diffusivity measurements by the flash technique," *International Journal of Heat and Mass Transfer*, vol. 38, pp. 3401–3412, 1995.
6. Heinemann, U., R. Caps, and J. Fricke: "Radiation–conduction interaction: an investigation on silica aerogels," *International Journal of Heat and Mass Transfer*, vol. 39, pp. 2115–2130, 1996.
7. Manohar, S. S., A. K. Kulkarni, and S. T. Thynell: "In-depth absorption of externally incident radiation in nongray media," *ASME Journal of Heat Transfer*, vol. 117, no. 1, pp. 146–151, 1995.
8. Soufiani, A., J.-M. Hartmann, and J. Taine: "Validity of band-model calculations for CO_2 and H_2O applied to radiative properties and conductive–radiative transfer," *Journal of Quantitative Spectroscopy and Radiative Transfer*, vol. 33, pp. 243–257, 1985.
9. Yao, C., and B. T. F. Chung: "Transient heat transfer in a scattering–radiating–conducting layer," *Journal of Thermophysics and Heat Transfer*, vol. 13, no. 1, pp. 18–24, 1999.
10. Abulwafa, E. M.: "Conductive–radiative heat transfer in an inhomogeneous slab with directional reflecting boundaries," *Journal of Physics D: Applied Physics*, vol. 32, pp. 1626–1632, 1999.
11. Tan, H. P., L. Ruan, X. L. Xia, and T. W. Tong: "Transient coupled radiative and conductive heat transfer in an absorbing, emitting and scattering medium," *International Journal of Heat and Mass Transfer*, vol. 42, pp. 2967–2980, 1999.
12. Ruperti, N., Jr, M. Raynaud, and J.-F. Sacadura: "A method for the solution of the coupled inverse heat conduction–radiation problem," *ASME Journal of Heat Transfer*, vol. 118, pp. 10–17, 1996.
13. Wu, C. Y., and N. R. Ou: "Transient two-dimensional radiative and conductive heat transfer in a scattering medium," *International Journal of Heat and Mass Transfer*, vol. 37, no. 17, pp. 2675–2686, 1994.
14. Tuntomo, A., and C. L. Tien: "Transient heat transfer in a conducting particle with internal radiant absorption," *ASME Journal of Heat Transfer*, vol. 114, pp. 304–309, 1992.
15. Siegel, R.: "Transient thermal effects of radiant energy in translucent materials," *ASME Journal of Heat Transfer*, vol. 120, no. 1, pp. 5–23, 1998.
16. Ferziger, J. H.: *Numerical Methods for Engineering Application*, John Wiley & Sons, New York, 1981.
17. Wang, L. S., and C. L. Tien: "Study of the interaction between radiation and conduction by a differential method," in *Proceedings of the Third International Heat Transfer Conference*, vol. 5, Hemisphere, Washington, D.C., pp. 190–199, 1966.
18. Einstein, T. H.: "Radiant heat transfer to absorbing gases enclosed between parallel flat plates with flow and conduction," *NASA TR R-154*, 1963.
19. Cess, R. D.: "The interaction of thermal radiation with conduction and convection heat transfer," in *Advances in Heat Transfer*, vol. 1, Academic Press, New York, pp. 1–50, 1964.
20. Zeng, S. Q., A. J. Hunt, R. Greif, and W. Cao: "Approximate formulation for coupled conduction and radiation through a medium with arbitrary optical thickness," *ASME Journal of Heat Transfer*, vol. 117, pp. 797–799, 1995.
21. Howell, J. R.: "Determination of combined conduction and radiation of heat through absorbing media by the exchange factor approximation," *Chemical Engineering Progress Symposium Series*, vol. 61, no. 59, pp. 162–171, 1965.
22. Wang, L. S., and C. L. Tien: "A study of various limits in radiation heat-transfer problems," *International Journal of Heat and Mass Transfer*, vol. 10, pp. 1327–1338, 1967.
23. Chang, Y. P.: "A potential treatment of energy transfer by conduction, radiation, and convection," *AIAA Journal*, vol. 5, pp. 1024–1026, 1967.
24. Timmons, D. H., and J. O. Mingle: "Simultaneous radiation and conduction with specular reflection," *AIAA Paper No. 68-28*, January 1968.

25. Tien, C. L., P. S. Jagannathan, and B. F. Armaly: "Analysis of lateral conduction and radiation along two parallel long plates," *AIAA Journal*, vol. 7, pp. 1806–1808, 1969.
26. Tarshis, L. A., S. O'Hara, and R. Viskanta: "Heat transfer by simultaneous conduction and radiation for two absorbing media in intimate contact," *International Journal of Heat and Mass Transfer*, vol. 12, pp. 333–347, 1969.
27. Anderson, E. E., R. Viskanta, and W. H. Stevenson: "Heat transfer through semitransparent solids," *ASME Journal of Heat Transfer*, vol. 95, no. 2, pp. 179–186, 1973.
28. Viskanta, R.: "Heat transfer by conduction and radiation in absorbing and scattering materials," *ASME Journal of Heat Transfer*, vol. 87, pp. 143–150, 1965.
29. Bergquam, J. B., and R. A. Seban: "Heat transfer by conduction and radiation in absorbing and scattering materials," *ASME Journal of Heat Transfer*, vol. 93, pp. 236–238, 1971.
30. Dayan, A., and C. L. Tien: "Heat transfer in a gray planar medium with linear anisotropic scattering," *ASME Journal of Heat Transfer*, vol. 97, pp. 391–396, 1975.
31. Roux, J. A., and A. M. Smith: "Combined conductive and radiative heat transfer in an absorbing scattering infinite slab," *ASME Journal of Heat Transfer*, vol. 100, no. 1, pp. 98–104, 1978.
32. Yuen, W. W., and L. W. Wang: "Heat transfer by conduction and radiation in a one-dimensional absorbing, emitting and anisotropically scattering medium," *ASME Journal of Heat Transfer*, vol. 102, pp. 303–307, 1980.
33. Wu, S. T., R. E. Ferguson, and L. L. Altigilbers: "Application of finite-element techniques to the interaction of conduction and radiation in a participating medium," in *Heat Transfer and Thermal Control, Progress in Aeronautics and Astronautics*, vol. 78, AIAA, New York, pp. 61–69, 1981.
34. Fernandes, R., J. Francis, and J. N. Reddy: "A finite-element approach to combined conductive and radiative heat transfer in a planar medium," in *Heat Transfer and Thermal Control, Progress in Aeronautics and Astronautics*, vol. 78, AIAA, New York, pp. 92–109, 1981.
35. Ratzel, A. C., and J. R. Howell: "Heat transfer by conduction and radiation in one-dimensional planar medium using differential approximation," *ASME Journal of Heat Transfer*, vol. 104, pp. 388–391, 1982.
36. Houston, R. L., and S. A. Korpela: "Heat transfer through fiberglass insulation," in *Proceedings of the Seventh International Heat Transfer Conference, Munich*, vol. 2, Hemisphere, Washington, D.C., pp. 499–504, 1982.
37. Mishkin, M., and G. J. Kowalski: "Application of Monte Carlo techniques to the steady state radiative and conductive heat transfer through a participating medium," *ASME Paper No. 83-WA/HT-27*, 1983.
38. Kamiuto, K., and M. Iwamoto: "Combined conductive and radiative heat transfer through a glass particle layer," in *Proceedings of the Second ASME/JSME Conference*, vol. 4, pp. 77–84, 1987.
39. Ho, C. H., and M. N. Özişik: "Simultaneous conduction and radiation in a two-layer planar medium," *Journal of Thermophysics and Heat Transfer*, vol. 1, no. 2, pp. 154–161, 1987.
40. Ho, C. H., and M. N. Özişik: "Combined conduction and radiation in a two-layer planar medium with flux boundary condition," *Numerical Heat Transfer*, vol. 11, no. 3, p. 321, 1987.
41. Tsai, J. H., and J. D. Lin: "Transient combined conduction and radiation with anisotropic scattering," *Journal of Thermophysics and Heat Transfer*, vol. 4, no. 1, pp. 92–97, 1990.
42. Tseng, C. J., and H. S. Chu: "Transient combined conduction and radiation in an absorbing, emitting and anisotropically-scattering medium with variable thermal conductivity," *International Journal of Heat and Mass Transfer*, vol. 35, pp. 1844–1847, 1992.
43. Kamiuto, K., M. Iwamoto, and Y. Nagumo: "Combined conduction and correlated–radiation heat transfer in packed beds," *Journal of Thermophysics and Heat Transfer*, vol. 7, no. 3, pp. 496–501, 1993.
44. Siegel, R., and C. M. Spuckler: "Approximate solution methods for spectral radiative transfer in high refractive index layers," *International Journal of Heat and Mass Transfer*, vol. 37, pp. 403–413, 1994.
45. Doermann, D., and J.-F. Sacadura: "Heat transfer in open cell foam insulation," *ASME Journal of Heat Transfer*, vol. 118, pp. 88–93, 1996.
46. Jones, P. D., D. G. McLeod, and D. E. Dorai-Raj: "Correlation of measured and computed radiation intensity exiting a packed bed," *ASME Journal of Heat Transfer*, vol. 118, pp. 94–102, 1996.
47. Siegel, R.: "Radiative exchange in a parallel-plate enclosure with translucent protective coatings on its walls," *International Journal of Heat and Mass Transfer*, vol. 42, no. 1, pp. 73–84, 1999.
48. Li, H. Y.: "Estimation of thermal properties in combined conduction and radiation," *International Journal of Heat and Mass Transfer*, vol. 42, no. 3, pp. 565–572, 1999.
49. Wu, J. W., and H. S. Chu: "Combined conduction and radiation heat transfer in plane-parallel packed beds with variable porosity," *Journal of Quantitative Spectroscopy and Radiative Transfer*, vol. 61, no. 4, pp. 443–452, 1999.
50. Lazard, M., S. André, and A. D. Maillet: "Transient coupled radiative–conductive heat transfer in a gray planar medium with anisotropic scattering," *Journal of Quantitative Spectroscopy and Radiative Transfer*, vol. 69, pp. 23–33, 2001.
51. Liu, L. H., and H. P. Tan: "Non-Fourier effects on transient coupled radiative–conductive heat transfer in one-dimensional semitransparent medium subjected to periodic irradiation," *Journal of Quantitative Spectroscopy and Radiative Transfer*, vol. 71, pp. 11–24, 2001.
52. Greif, R.: "Energy transfer by radiation and conduction with variable gas properties," *International Journal of Heat and Mass Transfer*, vol. 7, pp. 891–900, 1964.
53. Lick, W.: "Transient energy transfer by radiation and conduction," *International Journal of Heat and Mass Transfer*, vol. 8, pp. 119–127, 1965.

54. Echigo, R., S. Hasegawa, and Y. Miyazaki: "Composite heat transfer with thermal radiation in nongray medium: Part I: Interaction of radiation with conduction," *International Journal of Heat and Mass Transfer*, vol. 14, pp. 2001–2015, 1971.
55. Crosbie, A. L., and R. Viskanta: "Interaction of heat transfer by conduction and radiation in a nongray planar medium," *Wärme- und Stoffübertragung*, vol. 4, pp. 205–212, 1971.
56. Anderson, E. E., and R. Viskanta: "Spectral and boundary effects on coupled conduction–radiation heat transfer through semitransparent solids," *Wärme- und Stoffübertragung*, vol. 1, pp. 14–24, 1973.
57. Viskanta, R., and D. M. Kim: "Heat transfer through irradiated semi-transparent layer at high temperature," *ASME Journal of Heat Transfer*, vol. 102, pp. 388–390, 1980.
58. Vasilev, M. G., and V. S. Yuferev: "Radiative–conductive heat transfer in a thin semitransparent plate in the guide-wave approximation for a temperature and frequency-dependent absorption coefficient," *J. Appl. Mech. Techn. Phys.*, vol. 22, pp. 80–85, 1981.
59. Ramerth, D., and R. Viskanta: "Heat transfer through coal-ash deposits," *ASME Paper No. 82-HT-11*, 1982.
60. Smith, T. F., A. M. Al-Turki, K. H. Byun, and T. K. Kim: "Radiative and conductive transfer for a gas/soot mixture between diffuse parallel plates," *Journal of Thermophysics and Heat Transfer*, vol. 1, no. 1, pp. 50–55, 1987.
61. Kamiuto, K.: "Combined conduction and nongray radiation heat transfer in carbon dioxide," *Journal of Thermophysics and Heat Transfer*, vol. 10, no. 4, pp. 701–704, 1996.
62. Hahn, O., F. Raether, and M. C. Arduini-Schuster: "Transient coupled conductive/radiative heat transfer in absorbing, emitting and scattering media: Application to laser-flash measurements on ceramic materials," *International Journal of Heat and Mass Transfer*, vol. 40, pp. 689–698, 1997.
63. Lentes, F. T., and N. Siedow: "Three-dimensional radiative heat transfer in glass cooling processes," *Glass Science and Technology: Glastechnische Berichte*, vol. 72, no. 6, pp. 188–196, 1999.
64. Hutchison, J. R., and R. F. Richards: "Effect of nongray gas radiation on thermal stability in carbon dioxide," *Journal of Thermophysics and Heat Transfer*, vol. 13, no. 1, pp. 25–32, 1999.
65. Lee, K. H., and R. Viskanta: "Comparison of the diffusion approximation and the discrete ordinates method for the investigation of heat transfer in glass," *Glass Science and Technology*, vol. 72, pp. 254–265, 1999.
66. Wendlandt, B. C. H.: "Temperature in an irradiated thermally conducting medium," *Journal of Physics D: Applied Physics*, vol. 6, pp. 657–660, 1973.
67. Gilpin, R. R., R. B. Roberton, and B. Singh: "Radiative heating in ice," *ASME Journal of Heat Transfer*, vol. 99, pp. 227–232, 1977.
68. Viskanta, R., and E. D. Hirleman: "Combined conduction–radiation heat transfer through an irradiated semi-transparent plate," *ASME Journal of Heat Transfer*, vol. 100, pp. 169–172, 1978.
69. Zakhidov, R. A., S. Y. Bogomolov, D. A. Kirgizbaev, and S. I. Klychev: "Determination of the temperature field of semitransparent materials when they are heated with optical radiant," *Applied Solar Energy*, vol. 23, no. 6, p. 36, 1987.
70. Kowalski, G. J.: "Transient response of an optically thick medium exposed to short pulses of laser radiation," in *Fundamentals and Applications in Radiation Heat Transfer*, vol. HTD-72, ASME, pp. 67–74, 1987.
71. Heping, T., B. Maestre, and M. Lallemand: "Transient and steady-state combined heat transfer in semi-transparent materials subjected to a pulse or a step irradiation," *ASME Journal of Heat Transfer*, vol. 113, no. 1, pp. 166–173, 1991.
72. André, S., and A. Degiovanni: "A new way of solving transient radiative–conductive heat transfer problems," *ASME Journal of Heat Transfer*, vol. 120, no. 4, pp. 943–955, 1998.
73. Liu, L. H., H. P. Tan, and T. W. Tong: "Non-Fourier effects on transient temperature response in semitransparent medium caused by laser pulse," *International Journal of Heat and Mass Transfer*, vol. 44, pp. 3335–3344, 2001.
74. Hazzak, A. S., and J. V. Beck: "Unsteady combined conduction–radiation energy transfer using a rigorous differential method," *International Journal of Heat and Mass Transfer*, vol. 13, pp. 517–522, 1970.
75. Lii, C. C., and M. N. Özişik: "Transient radiation and conduction in an absorbing, emitting, scattering slab with reflective boundaries," *International Journal of Heat and Mass Transfer*, vol. 15, pp. 1175–1179, 1972.
76. Weston, K. C., and J. L. Hauth: "Unsteady, combined radiation and conduction in an absorbing, scattering, and emitting medium," *ASME Journal of Heat Transfer*, vol. 95, pp. 357–364, 1973.
77. Matthews, L. K., R. Viskanta, and F. P. Incropera: "Combined conduction and radiation heat transfer in porous materials heated by intense solar radiation," *Solar Energy*, vol. 107, no. 1, p. 29, 1985.
78. Tong, T. W., D. L. McElroy, and D. W. Yarbrough: "Transient conduction and radiation heat transfer in porous thermal insulations," *Journal of Thermal Insulation*, vol. 9, pp. 13–29, July 1985.
79. Barker, C., and W. H. Sutton: "The transient radiation and conduction heat transfer in a gray participating medium with semi-transparent boundaries," in *Radiation Heat Transfer*, vol. HTD-49, ASME, pp. 25–36, 1985.
80. Sutton, W. H.: "A short time solution for coupled conduction and radiation in a participating slab geometry," *ASME Journal of Heat Transfer*, vol. 108, no. 2, pp. 465–466, 1986.
81. Burka, A. L.: "Nonsteady combined heat transfer, taking account of scattering anisotropy," *High Temperature*, vol. 25, no. 1, p. 99, 1987.
82. Crosbie, A. L., and M. Pattabongse: "Radiative ignition in a planar medium," *Journal of Quantitative Spectroscopy and Radiative Transfer*, vol. 37, no. 2, p. 193, 1987.
83. Glass, D. E., M. N. Özişik, and D. S. McRae: "Hyperbolic heat conduction with radiation in an absorbing and emitting medium," *Numerical Heat Transfer*, vol. 12, no. 3, p. 321, 1987.

84. Rish III, J. W., and J. A. Roux: "Heat transfer analysis of fiberglass insulations with and without foil radiant barriers," *Journal of Thermophysics and Heat Transfer*, vol. 1, no. 1, pp. 43–49, 1987.
85. Rubtsov, N. A., and E. P. Golova: "Taking into account scattering in the study of nonstationary radiative conductive heat transfer in multilayered media," *High Temperature*, vol. 25, no. 4, p. 559, 1987.
86. Webb, B. W., and R. Viskanta: "Crystallographic effects during radiative melting of semitransparent materials," *Journal of Thermophysics and Heat Transfer*, vol. 1, no. 4, pp. 313–320, 1987.
87. Park, H. M., and T. Y. Yoon: "Solution of the inverse radiation problem using a conjugate gradient method," *International Journal of Heat and Mass Transfer*, vol. 43, no. 10, pp. 1767–1776, 2000.
88. Chawla, T. C., and S. H. Chan: "Solution of radiation–conduction problems with collocation method using B-splines as approximating functions," *International Journal of Heat and Mass Transfer*, vol. 22, no. 12, pp. 1657–1667, 1979.
89. Petrov, V. A.: "Combined radiation and conduction heat transfer in high temperature fiber thermal insulation," *International Journal of Heat and Mass Transfer*, vol. 40, pp. 2241–2247, 1997.
90. Campo, A., and A. Tremante: "Two-flux model applied to combined conduction–radiation in a gray planar medium," *Wärme- und Stoffübertragung*, vol. 21, no. 4, p. 221, 1987.
91. Tremante, A., and F. Malpica: "Analysis of the temperature profile of ceramic composite materials exposed to combined conduction–radiation between concentric cylinders," *Journal of Engineering for Gas Turbines and Power*, vol. 120, no. 2, pp. 271–275, 1998.
92. Baek, S. W., and T. Y. Kim: "The conductive and radiative heat transfer in rectangular enclosure using the discrete ordinates method," in *Proceedings of the Ninth International Heat Transfer Conference*, Hemisphere, Washington, D.C., pp. 433–438, 1990.
93. Baek, S. W., T. Y. Kim, and J. S. Lee: "Transient cooling of a finite cylindrical medium in the rarefied cold environment," *International Journal of Heat and Mass Transfer*, vol. 36, pp. 3949–3956, 1993.
94. Sakami, M., A. Charette, and V. Le Dez: "Application of the discrete ordinates method to combined conductive and radiative heat transfer in a two-dimensional complex geometry," *Journal of Quantitative Spectroscopy and Radiative Transfer*, vol. 56, no. 4, pp. 517–533, 1996.
95. Lee, K. H., and R. Viskanta: "Transient conductive–radiative cooling of an optical quality glass disk," *International Journal of Heat and Mass Transfer*, vol. 41, pp. 2083–2096, 1998.
96. Park, H. M., T. H. Kim, and J. H. Lee: "Dynamic simulation of thermal radiation in participating media by means of mode reduction," *Journal of Quantitative Spectroscopy and Radiative Transfer*, vol. 62, pp. 141–161, 1999.
97. Kholodov, N. M., Z. H. Flom, and P. S. Koltun: "Calculation of radiative conductive transfer in a semitransparent plate by the Monte Carlo method," *Journal of Engineering Physics*, vol. 42, pp. 333–338, 1982.
98. Abed, A. A., and J.-F. Sacadura: "A Monte Carlo–finite difference method for coupled radiation–conduction heat transfer in semi-transparent media," *ASME Journal of Heat Transfer*, vol. 105, no. 4, p. 931, 1983.
99. Götz, T.: "Coupling heat conduction and radiative transfer," *Journal of Quantitative Spectroscopy and Radiative Transfer*, vol. 72, pp. 57–73, 2002.
100. Nishimura, M., M. Hasatani, and S. Sugiyama: "Simultaneous heat transfer by radiation and conduction: High-temperature one-dimensional heat transfer in molten glass," *Intern. Chem. Eng.*, vol. 8, pp. 739–745, 1968.
101. Eryou, N. D., and L. R. Glicksman: "An experimental and analytical study of radiative and conductive heat transfer in molten glass," *ASME Journal of Heat Transfer*, vol. 94, no. 2, pp. 224–230, 1972.
102. Scheuerpflug, P., R. Caps, D. Buettner, and J. Fricke: "Apparent thermal conductivity of evacuated, SiO_2 aerogel tiles under variation of radiative boundary conditions," *International Journal of Heat and Mass Transfer*, vol. 28, no. 12, pp. 2299–2306, 1985.
103. Kamiuto, K., Y. Miyoshi, I. Kinoshita, and S. Hasegawa: "Combined conductive and radiative heat transfer in an optically thick porous body (case of cordierite porous bodies)," *Bulletin of Japan Society of Mechanical Engineers*, vol. 27, p. 1136, 1984.
104. Schimmel, W. P., J. L. Novotny, and F. A. Olsofka: "Interferometric study of radiation–conduction interaction," in *Proceedings of the Fourth International Heat Transfer Conference*, Elsevier, New York, September 1970.
105. Viskanta, R., and R. L. Merriam: "Heat transfer by combined conduction and radiation between concentric spheres separated by radiating medium," *ASME Journal of Heat Transfer*, vol. 90, pp. 248–256, 1968.
106. Tsai, J. R., and M. N. Özişik: "Transient combined conduction and radiation in an absorbing, emitting, and isotropically scattering solid sphere," *Journal of Quantitative Spectroscopy and Radiative Transfer*, vol. 38, no. 4, pp. 243–251, 1987.
107. Jones, P. D., and Y. Bayazitoğlu: "Combined radiation and conduction from a sphere in a participating medium," in *Proceedings of the Ninth International Heat Transfer Conference*, Hemisphere, Washington, D.C., pp. 397–402, 1990.
108. Thynell, S. T.: "Interaction of conduction and radiation in anisotropically scattering, spherical media," *Journal of Thermophysics and Heat Transfer*, vol. 4, no. 3, pp. 299–304, 1990.
109. Miliauskas, G.: "Regularities of unsteady radiative–conductive heat transfer in evaporating semitransparent liquid droplets," *International Journal of Heat and Mass Transfer*, vol. 44, pp. 785–798, 2001.
110. Liu, L. H., H. P. Tan, and T. W. Tong: "Transient coupled radiation–conduction in semitransparent spherical particle," *Journal of Thermophysics and Heat Transfer*, vol. 16, no. 1, pp. 43–49, 2002.
111. Gordoninejad, F., and J. Francis: "A finite difference solution to transient combined conductive and radiative heat transfer in an annular medium," *ASME Journal of Heat Transfer*, vol. 106, no. 4, pp. 888–891, 1984.

112. Kim, T. K., and T. F. Smith: "Radiative and conductive transfer for a real gas cylinder enclosure with gray walls," *International Journal of Heat and Mass Transfer*, vol. 28, no. 12, pp. 2269–2277, 1985.
113. Youssef, A. M., and J. A. Harris: "The P-1 solution to the conduction/radiation problem in a cylindrical medium with a constant heat source," in *Proceedings of the 1988 National Heat Transfer Conference*, vol. HTD-96, ASME, pp. 187–192, 1988.
114. Tsai, J. R., and M. N. Özişik: "Transient combined conduction and radiation in an absorbing, emitting, and isotropically scattering solid cylinder," *Journal of Applied Physics*, vol. 64, no. 8, p. 3820, 1988.
115. Harris, J. A.: "Solution of the conduction/radiation problem with linear-anisotropic scattering in an annular medium by the spherical harmonics method," *ASME Journal of Heat Transfer*, vol. 111, no. 1, pp. 194–196, 1989.
116. Pandey, D. K.: "Combined conduction and radiation heat transfer in concentric cylindrical media," *Journal of Thermophysics and Heat Transfer*, vol. 3, no. 1, pp. 75–82, 1989.
117. Amlin, D. W., and S. A. Korpela: "Influence of thermal radiation on the temperature distribution in semi-transparent solid," *ASME Journal of Heat Transfer*, vol. 102, pp. 76–80, 1980.
118. Ratzel, A. C., and J. R. Howell: "Two-dimensional energy transfer in radiatively participating media with conduction by the P-N approximation," in *Proceedings of the Seventh International Heat Transfer Conference, Munich*, vol. 2, Hemisphere, Washington, D.C., pp. 535–540, 1982.
119. Shih, T. M., and Y. N. Chen: "A discretized-intensity method proposed for two-dimensional systems enclosing radiative and conductive media," *Numerical Heat Transfer*, vol. 6, pp. 117–134, 1983.
120. Razzaque, M. M., J. R. Howell, and D. E. Klein: "Coupled radiative and conductive heat transfer in a two-dimensional enclosure with gray participating media using finite elements," in *Proceedings of the First JSME/ASME Joint Thermal Conference, Honolulu*, vol. 4, pp. 41–48, 1983.
121. Yücel, A., and M. L. Williams: "Heat transfer by combined conduction and radiation in axisymmetric enclosures," *Journal of Thermophysics and Heat Transfer*, vol. 1, no. 4, pp. 301–306, 1987.
122. Yücel, A., and M. L. Williams: "Interaction of conduction and radiation in cylindrical geometry without azimuthal symmetry," in *Proceedings of the 1988 National Heat Transfer Conference*, vol. HTD-96, ASME, pp. 281–288, 1988.
123. Ho, C. H., and M. N. Özişik: "Combined conduction and radiation in a two-dimensional rectangular enclosure," *Numerical Heat Transfer*, vol. 13, no. 2, p. 229, 1988.
124. Yuen, W. W., and E. E. Takara: "Analysis of combined conductive–radiative heat transfer in a two-dimensional rectangular enclosure with a gray medium," *ASME Journal of Heat Transfer*, vol. 110, no. 2, pp. 468–474, 1988.
125. Hsu, P.-F., and Z. M. Tan: "Radiative and combined-mode heat transfer within L-shaped nonhomogeneous and nongray participating media," *Numerical Heat Transfer – Part A: Applications*, vol. 31, no. 8, pp. 819–835, 1997.
126. Habib, I. S.: "Solidification of semi-transparent materials by conduction and radiation," *International Journal of Heat and Mass Transfer*, vol. 14, pp. 2161–2164, 1971.
127. Habib, I. S.: "Solidification of a semi-transparent cylindrical medium by conduction and radiation," *ASME Journal of Heat Transfer*, vol. 95, pp. 37–41, 1973.
128. Abrams, M., and R. Viskanta: "The effects of radiative heat transfer upon the melting and solidification of semi-transparent crystals," *ASME Journal of Heat Transfer*, vol. 96, pp. 184–190, 1974.
129. Viskanta, R., and E. E. Anderson: "Heat transfer in semi-transparent solids," in *Advances in Heat Transfer*, vol. 11, Academic Press, New York, pp. 317–441, 1975.
130. Cho, C., and M. N. Özişik: "Effects of radiation on melting of a semi-transparent, semi-infinite medium," in *Proceedings of the Sixth International Heat Transfer Conference*, vol. 3, Hemisphere, Washington, D.C., pp. 373–378, 1978.
131. Seki, N., M. Sugawara, and S. Fukusako: "Radiative melting of horizontal clear ice layer," *Wärme- und Stoffübertragung*, vol. 11, pp. 207–216, 1978.
132. Seki, N., M. Sugawara, and S. Fukusako: "Radiative melting of ice layer adhering to a vertical surface," *Wärme- und Stoffübertragung*, vol. 12, pp. 137–144, 1979.
133. Seki, N., M. Sugawara, and S. Fukusako: "Back melting of a horizontal cloudy ice layer with radiative heating," *ASME Journal of Heat Transfer*, vol. 101, pp. 90–95, 1979.
134. Diaz, L. A., and R. Viskanta: "Melting of a semitransparent material by irradiation from an external radiation source," in *Spacecraft Radiative Heat Transfer and Temperature Control*, vol. 83, AIAA, New York, pp. 38–60, 1982.
135. Diaz, L. A., and R. Viskanta: "Radiation induced melting of a semitransparent phase change material," *AIAA Paper No. 82-0848*, 1982.
136. Viskanta, R., and X. Wu: "Effect of radiation on the melting of glass batch," *Glastechnische Berichte*, vol. 56, pp. 138–147, 1983.
137. Dorsey, N. E.: *Properties of Ordinary Water Substance*, Hafner, New York, p. 404, 1963.
138. Knight, C. A.: *The Freezing of Supercooled Liquids*, Van Nostrand, Princeton, p. 125, 1967.
139. Chan, S. H., D. H. Cho, and G. Kocamustafaogullari: "Melting and solidification with internal radiative transfer – a generalized phase change model," *International Journal of Heat and Mass Transfer*, vol. 26, no. 4, pp. 621–633, 1983.
140. Carslaw, H. S., and J. C. Jaeger: *Conduction of Heat in Solids*, 2nd ed., Oxford University Press, 1959.
141. Oruma, F. O., M. N. Özişik, and M. A. Boles: "Effects of anisotropic scattering on melting and solidification of a semi-infinite, semi-transparent medium," *International Journal of Heat and Mass Transfer*, vol. 28, no. 2, pp. 441–449, 1985.

142. Burka, A. L., N. A. Rubtsov, and N. A. Savvinova: "Nonsteady-state radiant–conductive heat exchange in a semitransparent medium with phase transition," *Journal of Applied Mechanics and Technical Physics*, vol. 28, no. 1, p. 91, 1987.
143. Chan, S. H., and K. Y. Hsu: "The mushy zone in a phase change model of a semitransparent material with internal radiative transfer," *ASME Journal of Heat Transfer*, vol. 110, pp. 260–264, February 1988.
144. Yao, C., B. T. F. Chung, and G. X. Wang: "Mushy zone equilibrium solidification of a semitransparent layer subject to radiative and convective cooling," *International Journal of Heat and Mass Transfer*, vol. 45, pp. 2397–2405, 2002.
145. Kays, W. M., and M. E. Crawford: *Convective Heat and Mass Transfer*, McGraw-Hill, 1980.
146. Pai, S. I.: "Inviscid flow of radiation gas dynamics," *J. Math Phys. Sci.*, vol. 39, pp. 361–370, 1969.
147. Özişik, M. N.: *Radiative Transfer and Interactions With Conduction and Convection*, John Wiley & Sons, New York, 1973.
148. Schlichting, H.: *Boundary Layer Theory*, 7th ed., McGraw-Hill, New York, 1979.
149. Viskanta, R., and R. J. Grosh: "Boundary layer in thermal radiation absorbing and emitting media," *International Journal of Heat and Mass Transfer*, vol. 5, pp. 795–806, 1962.
150. Rumynskii, A. N.: "Boundary layers in radiating and absorbing media," *American Rocket Society Journal*, vol. 32, pp. 1135–1138, 1962.
151. Goulard, R.: "The transition from black body to Rosseland formulations in optically thick flows," *International Journal of Heat and Mass Transfer*, vol. 7, pp. 1145–1146, 1964.
152. Novotny, J. L., and K. T. Yang: "The interaction of thermal radiation in optically thick boundary layers," *ASME Paper No. 67-HT-9*, 1967.
153. Pai, S. I., and A. P. Scaglione: "Unsteady laminar boundary layers of an infinite plate in an optically thick radiating gas," *Applied Scientific Research*, vol. 22, pp. 97–112, 1970.
154. Zamuraev, V. P.: *Zh. Prikl. Mekhan. i Tekhn. Fiz.*, vol. 3, p. 73, 1964.
155. Viskanta, R.: "Radiation transfer and interaction of convection with radiation heat transfer," in *Advances in Heat Transfer*, vol. 3, Academic Press, New York, pp. 175–251, 1966.
156. Cess, R. D.: "Radiation effects upon boundary layer flow of an absorbing gas," *ASME Journal of Heat Transfer*, vol. 86C, pp. 469–475, 1964.
157. Smith, A. M., and H. A. Hassan: "Nongray radiation effects on the boundary layer at low Eckert numbers," *ASME Paper No. 66-WA/HT-35*, 1966.
158. Tabaczynski, R. J., and L. A. Kennedy: "Thermal radiation effects in laminar boundary-layer flow," *AIAA Journal*, vol. 5, pp. 1893–1894, 1967.
159. Pai, S. I., and C. K. Tsao: "A uniform flow of a radiating gas over a flat plate," *Proceedings of the Third International Heat Transfer Conference*, vol. 5, pp. 129–137, 1966.
160. Oliver, C. C., and P. W. McFadden: "The interaction of radiation and convection in the laminar boundary layer," *ASME Journal of Heat Transfer*, vol. C88, pp. 205–213, 1966.
161. Rumynskii, A. N.: "Boundary layer with an opaque underlayer," *American Rocket Society Journal*, vol. 32, pp. 1139–1140, 1962.
162. Koh, J. C. Y., and C. N. DeSilva: "Interaction between radiation and convection in the hypersonic boundary layer on a flat plate," *American Rocket Society Journal*, vol. 32, pp. 739–743, 1962.
163. Taitel, Y., and J. P. Hartnett: "Equilibrium temperature in a boundary layer flow over a flat plate of absorbing–emitting gas," *ASME Paper No. 66-WA/HT-48*, 1966.
164. Robin, M. N., R. I. Souloukhin, and I. B. Yutevich: "Influence of reflection of radiation on radiative–convective heat exchange during hypersonic flow over a blunt body," *J. Appl. Mech. Tech. Phys.*, vol. 21, pp. 239–245, 1980.
165. Golubkin, V. N.: "On the asymptotic theory of the three-dimensional flow of a hypersonic stream of radiating gas around a body," *Appl. Math. Mech.*, vol. 47, p. 493, 1983.
166. Tiwari, S. N., K. Y. Szema, J. N. Moss, and S. V. Subramanian: "Convective and radiative heating of a Saturn entry probe," *International Journal of Heat and Mass Transfer*, vol. 27, pp. 191–206, 1984.
167. Dombrovsky, L. A.: "Radiation–convection heat transfer by an optically thick boundary layer on a plate," *High Temperature*, vol. 19, pp. 100–109, 1981.
168. Yücel, A., and Y. Bayazitoğlu: "Radiative heat transfer in absorbing, emitting and anisotropically scattering boundary layer," *AIAA Paper No. 83-1504*, 1983.
169. Yücel, A., R. H. Kehtarenavaz, and Y. Bayazitoğlu: "Interaction of radiation with the boundary layer: Nongray media," *ASME Paper No. 83-HT-33*, 1983.
170. Soufiani, A., and J. Taine: "Application of statistical narrow-band model to coupled radiation and convection at high temperature," *International Journal of Heat and Mass Transfer*, vol. 30, no. 3, pp. 437–448, 1987.
171. Kaminski, D. A., X. D. Fu, and M. K. Jensen: "Numerical and experimental analysis of combined convective and radiative heat transfer in laminar flow over a circular cylinder," *International Journal of Heat and Mass Transfer*, vol. 38, no. 17, pp. 3161–3169, 1995.
172. Fritsch, C. A., R. J. Grosh, and M. W. Wild: "Radiative heat transfer through an absorbing boundary layer," *ASME Journal of Heat Transfer*, vol. 86, no. 4, pp. 296–304, 1966.
173. Houf, W. G., F. P. Incropera, and R. Viskanta: "Thermal conditions in irradiated, slowly moving liquid layers," *ASME Journal of Heat Transfer*, vol. 107, no. 1, pp. 92–98, 1985.

174. Elliott, J. M., R. I. Vachon, D. F. Dyer, and J. R. Dunn: "Application of the Patankar–Spalding finite difference procedure to turbulent radiating boundary layer flow," *International Journal of Heat and Mass Transfer*, vol. 14, pp. 667–672, 1971.
175. Goswami, D. Y., and R. I. Vachon: "Turbulent boundary layer flow of absorbing, emitting and axisymmetrically scattering gaseous medium," *AIAA Paper No. 80-1518*, 1980.
176. Naidenov, V. I., and S. A. Shindini: "Interaction of radiation with turbulent fluctuations in a boundary layer," *High Temperature*, vol. 19, pp. 106–109, 1981.
177. Jones, P. D., and Y. Bayazitoğlu: "Radiation, conduction and convection from a sphere in an absorbing, emitting, gray medium," *ASME Journal of Heat Transfer*, vol. 114, no. 1, pp. 250–254, 1992.
178. Cess, R. D.: "The interaction of thermal radiation with free convection heat transfer," *International Journal of Heat and Mass Transfer*, vol. 9, pp. 1269–1277, 1966.
179. Arpaci, V. S.: "Effect of thermal radiation on the laminar free convection from a heated vertical plate," *International Journal of Heat and Mass Transfer*, vol. 11, pp. 871–881, 1968.
180. Cheng, E. H., and M. N. Özişik: "Radiation with free convection in an absorbing, emitting and scattering medium," *International Journal of Heat and Mass Transfer*, vol. 15, pp. 1243–1252, 1972.
181. Desrayaud, G., and G. Lauriat: "Natural convection of a radiating fluid in a vertical layer," *ASME Journal of Heat Transfer*, vol. 107, no. 3, pp. 710–712, 1985.
182. Krishnaprakas, C. K., K. B. Narayana, and P. Dutta: "Interaction of radiation with natural convection," *Journal of Thermophysics and Heat Transfer*, vol. 13, no. 3, pp. 387–390, 1999.
183. Hossain, M. A., M. A. Alim, and D. A. S. Rees: "The effect of radiation on free convection from a porous vertical plate," *International Journal of Heat and Mass Transfer*, vol. 42, no. 1, pp. 181–191, 1999.
184. Webb, B. W., and R. Viskanta: "Analysis of radiation-induced natural convection in rectangular enclosures," *Journal of Thermophysics and Heat Transfer*, vol. 1, no. 2, pp. 146–153, 1987.
185. Webb, B. W.: "Interaction of radiation and free convection on a heated vertical plate: Experiment and analysis," *Journal of Thermophysics and Heat Transfer*, vol. 4, no. 1, pp. 117–120, 1990.
186. Yan, W. M., and H. Y. Li: "Radiation effects on laminar mixed convection in an inclined square duct," *ASME Journal of Heat Transfer*, vol. 121, no. 1, pp. 194–200, 1999.
187. Yan, W. M., and H. Y. Li: "Radiation effects on mixed convection heat transfer in a vertical square duct," *International Journal of Heat and Mass Transfer*, vol. 44, pp. 1401–1410, 2001.
188. Lacona, E., and J. Taine: "Holographic interferometry applied to coupled free convection and radiative transfer in a cavity containing a vertical plate between 290 and 650K," *International Journal of Heat and Mass Transfer*, vol. 44, pp. 3755–3764, 2001.
189. Arpaci, V. S., K. Kabiri-Bamoradian, and E. Cesmebasi: "Finite amplitude Benard convection of purely radiating fluids," *ASME Paper No. 78-HT-40*, 1978.
190. Epstein, M., F. B. Cheung, T. C. Chawla, and G. M. Hauser: "Effective thermal conductivity for combined radiation and free convection in an optically thick heated fluid layer," *ASME Journal of Heat Transfer*, vol. 103, pp. 114–120, 1981.
191. Bakan, S.: "Thermal stability of radiating fluids: The scattering problem," *Physics of Fluids*, vol. 27, no. 12, p. 2969, 1984.
192. Yang, W. M.: "Thermal instability of a fluid layer induced by radiation," *Numerical Heat Transfer – Part A: Applications*, vol. 17, pp. 365–376, 1990.
193. Chang, L. C., K. T. Yang, and J. R. Lloyd: "Radiation–natural convection interactions in two-dimensional enclosures," *ASME Journal of Heat Transfer*, vol. 105, no. 1, pp. 89–95, 1983.
194. Webb, B. W., and R. Viskanta: "Analysis of radiation-induced melting with natural convection in the melt," in *Fundamentals and Applications of Radiation Heat Transfer*, vol. HTD-72, ASME, pp. 75–82, 1987.
195. Yücel, A., S. Acharya, and M. L. Williams: "Combined natural convection and radiation in a square enclosure," in *Proceedings of the 1988 National Heat Transfer Conference*, vol. HTD-96, ASME, pp. 209–218, 1988.
196. Fusegi, T., and B. Farouk: "A computational and experimental study of natural convection and surface/gas radiation interactions in a square cavity," *ASME Journal of Heat Transfer*, vol. 112, pp. 802–804, 1990.
197. Tan, Z. M., and J. R. Howell: "Combined radiation and natural convection in a two-dimensional participating square medium," *International Journal of Heat and Mass Transfer*, vol. 34, no. 3, pp. 785–794, 1991.
198. Mesyngier, C., and B. Farouk: "Turbulent natural convection–nongray gas radiation analysis in a square enclosure," *Numerical Heat Transfer – Part A: Applications*, vol. 29, no. 7, pp. 671–687, 1996.
199. Colomer, G., R. Cònsul, and A. Oliva: "Coupled radiation and natural convection: Different approaches of the SLW model for a non-gray gas mixture," *Journal of Quantitative Spectroscopy and Radiative Transfer*, vol. 107, no. 1, pp. 30–46, 2007.
200. Carpenter, J. R., D. G. Briggs, and V. Sernas: "Combined radiation and developing laminar free convection between vertical flat plates with asymmetric heating," *ASME Paper No. 75-HT-19*, 1975.
201. Yamada, Y.: "Combined radiation and free convection heat transfer in a vertical channel with arbitrary wall emissivities," *International Journal of Heat and Mass Transfer*, vol. 31, no. 2, pp. 429–440, 1988.
202. Kuo, D. C., J. C. Morales, and K. S. Ball: "Combined natural convection and volumetric radiation in a horizontal annulus: Spectral and finite volume predictions," *ASME Journal of Heat Transfer*, vol. 121, pp. 610–615, 1999.
203. Campo, A., and U. Lacoa: "Influence of thermal radiation on natural convection inside vertical annular enclosures," in *Proceedings of the 1988 National Heat Transfer Conference*, vol. HTD-96, ASME, pp. 219–226, 1988.

204. Fusegi, T., K. Ishii, B. Farouk, and K. Kuwahara: "Three-dimensional study of convection–radiation interactions in a cubical enclosure field with a non-gray gas," in *Proceedings of the Ninth International Heat Transfer Conference*, Hemisphere, Washington, D.C., pp. 421–426, 1990.
205. Derby, J. J., S. Brandon, and A. G. Salinger: "The diffusion and P1 approximations for modeling buoyant flow of an optically thick fluid," *International Journal of Heat and Mass Transfer*, vol. 41, no. 11, pp. 1405–1415, 1998.
206. Tsukada, T., K. Kakinoki, M. Hozawa, and N. Imaishi: "Effect of internal radiation within crystal and melt on Czochralski crystal growth of oxide," *International Journal of Heat and Mass Transfer*, vol. 38, pp. 2707–2714, 1995.
207. Bdéoui, F., A. Soufiani, and P. L. Quéré: "A numerical study of Rayleigh–Benard convection in radiating gases," in *Proceedings of the 11th International Heat Transfer Conference*, vol. 7, Kyongju, Korea, pp. 261–266, 1998.
208. DeSoto, S.: "Coupled radiation, conduction and convection in entrance region flow," *International Journal of Heat and Mass Transfer*, vol. 11, pp. 39–53, 1968.
209. Kurosaki, Y.: "Heat transfer by simultaneous radiation and convection in an absorbing and emitting medium in a flow between parallel plates," in *Proceedings of the Fourth International Heat Transfer Conference*, vol. 3, No. R2.5, Elsevier, New York, 1970.
210. Echigo, R., K. Kamiuto, and S. Hasegawa: "Analytical method on composite heat transfer with predominant radiation—analysis by integral equation and examination on radiation slip," in *Proceedings of the Fifth International Heat Transfer Conference*, vol. 1, JSME, Japan, pp. 103–107, 1974.
211. Azad, F. H., and M. F. Modest: "Combined radiation and convection in absorbing, emitting and anistropically scattering gas–particulate tube flow," *International Journal of Heat and Mass Transfer*, vol. 24, pp. 1681–1698, 1981.
212. Viskanta, R.: "Interaction of heat transfer by conduction, convection, and radiation in a radiating fluid," *ASME Journal of Heat Transfer*, vol. 85, pp. 318–328, 1963.
213. Viskanta, R.: "Heat transfer in a radiating fluid with slug flow in a parallel plate channel," *Applied Scientific Research Part A*, vol. 13, pp. 291–311, 1964.
214. Chen, J. C.: "Simultaneous radiative and convective heat transfer in an absorbing, emitting, and scattering medium in slug flow between parallel plates," *AIChE Journal*, vol. 10, no. 2, pp. 253–259, 1964.
215. DeSoto, S., and D. K. Edwards: *Radiative Emission and Absorption in Nonisothermal Nongray Gases in Tubes*, Stanford University Press, Stanford, CA, pp. 358–372, 1965.
216. Edwards, D. K., and A. Balakrishnan: "Nongray radiative transfer in a turbulent gas layer," *International Journal of Heat and Mass Transfer*, vol. 16, pp. 1003–1015, 1973.
217. Edwards, D. K., and A. Balakrishnan: "Self absorption of radiation in turbulent molecular gases," *Combustion and Flame*, vol. 20, pp. 401–417, 1973.
218. Balakrishnan, A., and D. K. Edwards: "Established laminar and turbulent channel flow of a radiating molecular gas," in *Proceedings of the Fifth International Heat Transfer Conference*, vol. 1, JSME, Japan, pp. 93–97, 1974.
219. Wassel, A. T., and D. K. Edwards: "Molecular radiation in a laminar or turbulent pipe flow," *ASME Journal of Heat Transfer*, vol. 98, pp. 101–107, 1976.
220. Goulard, R., and M. Goulard: *Energy Transfer in the Couette Flow of a Radiant and Chemically Reacting Gas*, Stanford University Press, Stanford, CA, pp. 126–139, 1959.
221. Viskanta, R., and R. J. Grosh: "Temperature distribution in Couette flow with radiation," *American Rocket Society Journal*, vol. 31, pp. 839–840, 1961.
222. Timofeyev, V. N., F. R. Shklyar, V. M. Malkin, and K. H. Berland: "Combined heat transfer in an absorbing stream moving in a flat channel. Parts I, II, and III," *Heat Transfer, Soviet Research*, vol. 1, no. 6, pp. 57–93, November 1969.
223. Lii, C. C., and M. N. Özişik: "Heat transfer in an absorbing, emitting and scattering slug flow between parallel plates," *ASME Journal of Heat Transfer*, vol. 95C, pp. 538–540, 1973.
224. Bergquam, J. B., and N. S. Wang: "Heat transfer by convection and radiation in an absorbing, scattering medium flowing between parallel plates," *ASME Paper No. 76-HT-50*, 1976.
225. Chawla, T. C., and S. H. Chan: "Spline collocation solution of combined radiation–convection in thermally developing flows with scattering," *Numerical Heat Transfer*, vol. 3, pp. 47–76, 1980.
226. Chawla, T. C., and S. H. Chan: "Combined radiation and convection in thermally developing Poiseuille flow with scattering," *ASME Journal of Heat Transfer*, vol. 102, pp. 297–302, 1980.
227. Mengüç, M. P., Y. Yener, and M. N. Özişik: "Interaction of radiation in thermally developing laminar flow in a parallel plate channel," *ASME Paper No. 83-HT-35*, 1983.
228. Yener, Y., B. Shahidi-Zandi, and M. N. Özişik: "Simultaneous radiation and forced convection in thermally developing turbulent flow through a parallel plate channel," *ASME Paper No. 84-WA/HT-15*, 1984.
229. Yener, Y., and M. N. Özişik: "Simultaneous radiation and forced convection in thermally developing turbulent flow through a parallel plate channel," *ASME Journal of Heat Transfer*, vol. 108, no. 4, pp. 985–987, 1986.
230. Echigo, R., and S. Hasegawa: "Radiative heat transfer by flowing multiphase medium—Part I: An analysis on heat transfer of laminar flow between parallel flat plates," *International Journal of Heat and Mass Transfer*, vol. 15, pp. 2519–2534, 1972.
231. Kassemi, M., and B. T. F. Chung: "Two-dimensional convection and radiation with scattering from a Poiseuille flow," *Journal of Thermophysics and Heat Transfer*, vol. 4, no. 1, pp. 98–105, 1990.
232. Kim, T. K., and H. S. Lee: "Two-dimensional anisotropic scattering radiation in a thermally developing Poiseuille flow," *Journal of Thermophysics and Heat Transfer*, vol. 4, no. 3, pp. 292–298, 1990.

233. Kim, T. Y., and S. W. Baek: "Thermal development of radiatively active pipe flow with nonaxisymmetric circumferential convective heat loss," *International Journal of Heat and Mass Transfer*, vol. 39, no. 14, pp. 2969–2976, 1996.
234. Kim, S. S., and S. W. Baek: "Radiation affected compressible turbulent flow over a backward facing step," *International Journal of Heat and Mass Transfer*, vol. 39, no. 16, pp. 3325–3332, 1996.
235. Krishnaprakas, C. K., K. B. Narayana, and P. Dutta: "Combined convective and radiative heat transfer in turbulent tube flow," *Journal of Thermophysics and Heat Transfer*, vol. 13, no. 3, pp. 390–394, 1999.
236. Einstein, T. H.: "Radiant heat transfer to absorbing gases enclosed in a circular pipe with conduction, gas flow, and internal heat generation," *NASA TR R-156*, 1963.
237. Echigo, R., S. Hasegawa, and K. Kamiuto: "Composite heat transfer in a pipe with thermal radiation of two-dimensional propagation," *International Journal of Heat and Mass Transfer*, vol. 18, pp. 1149–1159, 1975.
238. Bergero, S., E. Nannei, and R. Sala: "Combined radiative and convective heat transfer in a three-dimensional rectangular channel at different wall temperatures," *Wärme- und Stoffübertragung*, vol. 36, no. 6, pp. 443–450, 1999.
239. Kim, D. M., and R. Viskanta: "Interaction of convection and radiation heat transfer in high pressure and temperature steam," *International Journal of Heat and Mass Transfer*, vol. 27, pp. 939–941, 1984.
240. Gau, C., and D. C. Chi: "A simple numerical study of combined radiation and convection heat transfer in the entry region of a circular pipe flow," in *Proceedings of the Second ASME/JSME Conference*, vol. 3, pp. 635–643, 1987.
241. Kamiuto, K.: "Combined laminar forced convection and nongray-radiation heat transfer to carbon dioxide flowing in a nonblack plane-parallel duct," *Numerical Heat Transfer – Part A: Applications*, vol. 28 Part A, pp. 575–587, 1995.
242. Mesyngier, C., and B. Farouk: "Convection–nongray gas radiation interactions in a channel flow," in *Proceedings of the 1996 Heat Transfer Conference*, vol. HTD-325 No. 3, ASME, pp. 103–113, 1996.
243. Habib, I. S., and R. Greif: "Heat transfer to a flowing non-gray radiating gas: An experimental and theoretical study," *International Journal of Heat and Mass Transfer*, vol. 13, pp. 1571–1582, 1970.
244. Chiba, Z., and R. Greif: "Heat transfer to steam flowing turbulently in a pipe," *International Journal of Heat and Mass Transfer*, vol. 16, pp. 1645–1648, 1973.
245. Tabanfar, S., and M. F. Modest: "Combined radiation and convection in tube flow with non-gray gases and particulates," *ASME Journal of Heat Transfer*, vol. 109, pp. 478–484, 1987.
246. Smith, T. F., Z. F. Shen, and A. M. Al-Turki: "Radiative and convective transfer in a cylindrical enclosure for a real gas," *ASME Journal of Heat Transfer*, vol. 107, no. 2, pp. 482–485, 1985.
247. Soufiani, A., and J. Taine: "Experimental and theoretical studies of combined radiative and convective transfer in CO_2 and H_2O laminar flows," *International Journal of Heat and Mass Transfer*, vol. 32, no. 3, pp. 477–486, 1989.
248. Sediki, E., A. Soufiani, and M. S. Sifaoui: "Spectrally correlated radiation and laminar forced convection in the entrance region of a circular duct," *International Journal of Heat and Mass Transfer*, vol. 45, pp. 5069–5081, 2002.
249. Soufiani, A., P. Mignon, and J. Taine: "Radiation–turbulence interaction in channel flows of infrared active gases," in *Proceedings of the Ninth International Heat Transfer Conference*, vol. 6, Hemisphere, Washington, D.C., pp. 403–408, 1990.
250. Soufiani, A., P. Mignon, and J. Taine: "Radiation effects on turbulent heat transfer in channel flows of infrared active gases," in *Proceedings of the 1990 AIAA/ASME Thermophysics and Heat Transfer Conference*, vol. HTD-137, ASME, pp. 141–148, 1990.
251. Echigo, R., S. Hasegawa, and H. Tamehiro: "Radiative heat transfer by flowing multiphase medium—Part II: An analysis on heat transfer of laminar flow in an entrance region of circular tube," *International Journal of Heat and Mass Transfer*, vol. 15, pp. 2595–2610, 1972.
252. Tamehiro, H., R. Echigo, and S. Hasegawa: "Radiative heat transfer by flowing multiphase medium—Part III: An analysis on heat transfer of turbulent flow in a circular tube," *International Journal of Heat and Mass Transfer*, vol. 16, pp. 1199–1213, 1973.
253. Modest, M. F., B. R. Meyer, and F. H. Azad: "Combined convection and radiation in tube flow of an absorbing, emitting and anisotropically scattering gas–particulate suspension," *ASME Paper No. 80-HT-27*, 1980.
254. Al-Turki, A. M., and T. F. Smith: "Radiative and convective transfer in a cylindrical enclosure for a gas/soot mixture," *ASME Journal of Heat Transfer*, vol. 109, no. 1, p. 259, 1987.
255. Park, S. H., and S. S. Kim: "Thermophoretic deposition of absorbing, emitting and isotropically scattering particles in laminar tube flow with high particle mass loading," *International Journal of Heat and Mass Transfer*, vol. 36, no. 14, pp. 3477–3485, 1993.
256. Yin, Z., and Y. Jaluria: "Zonal method to model radiative transport in an optical fiber drawing furnace," *ASME Journal of Heat Transfer*, vol. 119, pp. 597–603, 1997.
257. Yin, Z., and Y. Jaluria: "Thermal transport and flow in high-speed optical fiber drawing," *ASME Journal of Heat Transfer*, vol. 120, no. 4, pp. 916–930, 1998.
258. Song, M., K. S. Ball, and T. L. Bergman: "A model for radiative cooling of a semitransparent molten glass jet," *ASME Journal of Heat Transfer*, vol. 120, no. 4, pp. 931–938, 1998.
259. Tong, T. W., S. B. Sathe, and R. E. Peck: "Improving the performance of porous radiant burners through use of sub-micron size fibers," *International Journal of Heat and Mass Transfer*, vol. 33, no. 6, pp. 1339–1346, 1990.
260. Martin, A. R., C. Saltiel, J. C. Chai, and W. Shyy: "Convective and radiative internal heat transfer augmentation with fiber arrays," *International Journal of Heat and Mass Transfer*, vol. 41, pp. 3431–3440, 1998.

261. Singh, B. P., and M. Kaviany: "Modelling radiative heat transfer in packed beds," *International Journal of Heat and Mass Transfer*, vol. 35, pp. 1397–1405, 1992.
262. Lu, J. D., G. Flamant, and B. Variot: "Theoretical study of combined conductive, convective and radiative heat transfer between plates and packed beds," *International Journal of Heat and Mass Transfer*, vol. 37, no. 5, pp. 727–736, 1994.
263. Kamiuto, K., and S. Saitoh: "Combined forced-convection and correlated–radiation heat transfer in cylindrical packed beds," *Journal of Thermophysics and Heat Transfer*, vol. 8, no. 1, pp. 119–124, 1994.
264. Viskanta, R.: "Overview of convection and radiation in high temperature gas flows," *International Journal of Engineering Science*, vol. 36, pp. 1677–1699, 1998.
265. Curran, H. J., P. Gaffuri, W. J. Pitz, and C. K. Westbrook: "Comprehensive modeling study of iso-octane oxidation," Lawrence Livermore National Laboratories, Livermore, CA, 2000.
266. Viskanta, R., and M. P. Mengüç: "Radiation heat transfer in combustion systems," *Progress in Energy and Combustion Science*, vol. 13, pp. 97–160, 1987.
267. Viskanta, R.: *Radiative Transfer in Combustion Systems: Fundamentals and Applications*, Begell House, New York, 2005.
268. Negrelli, D. E., J. R. Lloyd, and J. L. Novotny: "A theoretical and experimental study of radiation–convection interaction in a diffusion flame," *ASME Journal of Heat Transfer*, vol. 99, pp. 212–220, 1977.
269. Liu, K. V., J. R. Lloyd, and K. T. Yang: "An investigation of a laminar diffusion flame adjacent to a vertical flat plate burner," *International Journal of Heat and Mass Transfer*, vol. 24, no. 12, pp. 1959–1970, 1981.
270. Kee, R. J., F. M. Rupley, and J. A. Miller: "CHEMKIN-II: A Fortran chemical kinetics package for the analysis of gas-phase chemical kinetics," Technical Report SAND89-8009B, Sandia National Laboratories, 1989.
271. Kee, R. J., G. Dixon-Lewis, J. Warnatx, M. E. Coltrin, and J. A. Miller: "A Fortran computer code package for the evaluation of gas-phase, multicomponent transport properties," Technical Report SAND86-8246, Sandia National Laboratory, 1986.
272. Daguse, T., T. Croonenbroek, J. C. Rolon, N. Darabiha, and A. Soufiani: "Study of radiative effects on laminar counterflow $H_2/O_2/N_2$ diffusion flames," *Combustion and Flame*, vol. 106, pp. 271–287, 1996.
273. Ruan, J., H. Kobayashi, T. Niioka, and Y. Ju: "Combined effects of nongray radiation and pressure on premixed $CH_4/O_2/CO_2$ flames," *Combustion and Flame*, vol. 124, pp. 225–230, 2001.
274. Kaplan, C. R., S. W. Baek, E. S. Oran, and J. L. Ellzey: "Dynamics of a strongly radiating unsteady ethylene jet diffusion flame," *Combustion and Flame*, vol. 96, pp. 1–21, 1994.
275. Liu, F., H. Guo, G. J. Smallwood, and O. L. Gülder: "Effects of gas and soot radiation on soot formation in a coflow laminar ethylene diffusion flame," *Journal of Quantitative Spectroscopy and Radiative Transfer*, vol. 73, pp. 409–421, 2002.
276. Liu, F., H. Guo, G. J. Smallwood, and M. El Hafi: "Effects of gas and soot radiation on soot formation in counterflow ethylene diffusion flames," *Journal of Quantitative Spectroscopy and Radiative Transfer*, vol. 84, pp. 501–511, 2004.
277. Liu, F., G. J. Smallwood, and W. Kong: "The importance of thermal radiation transfer in laminar diffusion flames at normal and microgravity," *Journal of Quantitative Spectroscopy and Radiative Transfer*, vol. 112, no. 7, pp. 1241–1249, 2011.
278. Ezekoye, O. A., and Z. Zhang: "Convective and radiative coupling in a burner-supported diffusion flame," *Journal of Thermophysics and Heat Transfer*, vol. 11, no. 2, pp. 239–245, 1997.
279. Turns, S. R.: "Understanding NO_x formation in nonpremixed flames: experiments and modeling," *Progress in Energy and Combustion Science*, vol. 21, pp. 361–385, 1995.
280. Barlow, R. S., N. S. A. Smith, J. Y. Chen, and R. W. Bilger: "Comparison of CMC and PDF modeling predictions with experimental nitric oxide LIF/Raman measurements in a turbulent H_2 jet flame," *Combustion Science and Technology*, vol. 105, pp. 357–375, 1995.
281. Delichatsios, M. A., L. Orloff, and M. M. Delichatsios: "The effects of fuel sooting tendency and the flow on flame radiation in luminous turbulent jet flames," *Combustion Science and Technology*, vol. 84, no. 1/6, pp. 199–215, 1992.
282. Orloff, L., J. de Ris, and M. A. Delichatsios: "Radiation from buoyant turbulent diffusion flames," *Combustion Science and Technology*, vol. 84, no. 1/6, pp. 177–186, 1992.
283. Ramamurthy, H., S. Ramadhyani, and R. Viskanta: "A two-dimensional axisymmetric model for combusting, reacting and radiating flows in radiant tubes," *Journal of the Institute of Energy*, vol. 67, pp. 90–100, 1994.
284. Bressloff, N. W., J. B. Moss, and P. A. Rubini: "CFD prediction of coupled radiation heat transfer and soot production in turbulent flames," in *Proceedings of Twenty-Sixth Symposium (International) on Combustion*, vol. 2, The Combustion Institute, pp. 2379–2386, 1996.
285. Zimberg, M. J., S. H. Frankel, J. P. Gore, and Y. R. Sivathanu: "A study of coupled turbulent mixing, soot chemistry, and radiation effects using the linear eddy model," *Combustion and Flame*, vol. 113, pp. 454–469, 1998.
286. Brookes, S. J., and J. B. Moss: "Predictions of soot and thermal radiation properties in confined turbulent jet diffusion flames," *Combustion and Flame*, vol. 116, pp. 486–503, 1999.
287. Brookes, S. J., and J. B. Moss: "Measurements of soot production and thermal radiation from confined turbulent jet diffusion flames of methane," *Combustion and Flame*, vol. 116, pp. 49–61, 1999.
288. Wang, L., D. C. Haworth, S. R. Turns, and M. F. Modest: "Interactions among soot, thermal radiation, and NOx emissions in oxygen-enriched turbulent nonpremixed flames: a CFD modeling study," *Combustion and Flame*, vol. 141, no. 1-2, 2005, 170–179.

289. Wang, L., M. F. Modest, D. C. Haworth, and S. R. Turns: "Modeling nongray soot and gas-phase radiation in luminous turbulent nonpremixed jet flames," *Combustion Theory and Modelling*, vol. 9, no. 3, pp. 479–498, 2005.
290. Kim, J. S., S. W. Baek, and C. R. Kaplan: "Effect of radiation on diffusion flame behavior over a combustible solid," *Combustion Science and Technology*, vol. 88, no. 1/2, pp. 133–150, 1993.
291. Bhattacharjee, S., R. A. Altenkirch, and K. Sacksteder: "The effect of ambient pressure on flame spread over thin cellulosic fuel in a quiescent, microgravity environment," *ASME Journal of Heat Transfer*, vol. 118, pp. 181–190, 1996.
292. Wang, H. Y., P. Joulain, and J. M. Most: "Modeling on burning of large-scale vertical parallel surfaces with fire-induced flow," *Fire Safety Journal*, vol. 32, no. 3, pp. 241–247, 1999.
293. Lin, T. H., and C. H. Chen: "Influence of two-dimensional gas phase radiation on downward flame spread," *Combustion Science and Technology*, vol. 141, no. 1, pp. 83–106, 1999.
294. Baek, S. W., J. H. Park, and C. E. Choi: "Investigation of droplet combustion with nongray gas radiation effects," *Combustion Science and Technology*, vol. 142, no. 1, pp. 55–79, 1999.
295. Duval, R., A. Soufiani, and J. Taine: "Coupled radiation and turbulent multiphase flow in an aluminised solid propellant rocket engine," *Journal of Quantitative Spectroscopy and Radiative Transfer*, vol. 84, pp. 513–526, 2004.
296. Byun, D. Y., and S. W. Baek: "Numerical investigation of combustion with non-gray thermal radiation and soot formation effect in a liquid rocket engine," *International Journal of Heat and Mass Transfer*, vol. 50, pp. 412–422, 2007.
297. Mohamad, A. A., S. Ramadhyani, and R. Viskanta: "Modelling of combustion and heat transfer in a packed bed with embedded coolant tubes," *International Journal of Heat and Mass Transfer*, vol. 37, no. 8, pp. 1181–1191, 1994.
298. Sacadura, J.-F.: "Radiative heat transfer in fire safety science," *Journal of Quantitative Spectroscopy and Radiative Transfer*, vol. 93, pp. 5–24, 2005.
299. Chui, E. H., P. M. J. Hughes, and G. D. Raithby: "Implementation of the finite volume method for calculating radiative transfer in a pulverized fuel flame," *Combustion Science and Technology*, vol. 92, no. 4/6, pp. 225–242, 1993.
300. Visona, S. P., and B. R. Stanmore: "3-D modelling of NOx formation in a 275 MW utility boiler," *Journal of the Institute of Energy*, vol. 69, pp. 68–79, 1996.
301. Yuan, J., V. Semião, and M. G. Carvalho: "Predictions of particulate formation, oxidation and distribution in a three-dimensional oil-fired furnace," *Journal of the Institute of Energy*, vol. 70, pp. 57–70, 1997.
302. Song, G., T. Bjorge, J. Holen, and B. F. Magnussen: "Simulation of fluid flow and gaseous radiation heat transfer in a natural gas-fired furnace," *Int. J. Numerical Methods for Heat and Fluid Flow*, vol. 7, no. 2–3, pp. 169–180, 1997.
303. Liu, F., H. A. Becker, and Y. Bindar: "A comparative study of radiative heat transfer modelling in gas-fired furnaces using the simple grey gas and the weighted-sum-of-grey-gases models," *International Journal of Heat and Mass Transfer*, vol. 41, no. 22, pp. 3357–3371, 1998.
304. Keramida, E. P., H. H. Liakos, and M. A. Founti: "Radiative heat transfer in natural gas-fired furnaces," *International Journal of Heat and Mass Transfer*, vol. 43, no. 10, pp. 1801–1809, 2000.
305. Omori, T., S. Yamaguchi, and T. Fusegi: "Computational heat transfer analysis of a furnace using the WSGG model," in *Proceedings of 2000 IMECE*, vol. HTD-366-1, ASME, pp. 103–108, 2000.
306. Edge, P., M. Gharebaghi, R. Irons, R. Porter, R. T. J. Porter, M. Pourkashaniana, D. Smith, P. Stephenson, and A. Williams: "Combustion modelling opportunities and challenges for oxy-coal carbon capture technology," *Chemical Engineering Research and Design*, vol. 89, pp. 1470–1493, 2011.
307. Badinand, T., and T. Fransson: "Improvement of the finite volume method for coupled flow and radiation calculations by the use of two grids and rotational periodic interface," in *Radiative Transfer 2001 — The Third International Symposium on Radiative Transfer*, eds. M. P. Mengüç and N. Selçuk, Begell House, 2001.
308. Howell, L. H., R. B. Pember, P. Colella, J. P. Jessee, and W. A. Fiveland: "A conservative adaptive-mesh algorithm for unsteady, combined-mode heat transfer using the discrete ordinates method," *Numerical Heat Transfer – Part B: Fundamentals*, vol. 35, no. 4, pp. 407–430, 1999.
309. Jones, W. P., and B. E. Launder: "The prediction of laminarization with a two-equation model of turbulence," *International Journal of Heat and Mass Transfer*, vol. 15, pp. 301–304, 1972.
310. Carrier, G. F., F. E. Fendell, and F. E. Marble: "The effect of strain rate on diffusion flames," *SIAM Journal of Applied Mathematics*, vol. 28, p. 463, 1975.
311. Williams, F. A.: "Recent advances in theoretical descriptions of turbulent diffusion flames," in *Turbulent Mixing in Nonreactive and Reactive Flows*, ed. S. N. B. Murphy, Plenum Press, New York, pp. 189–208, 1975.
312. Peters, N.: "Laminar diffusion flamelet models in nonpremixed turbulent combustion," *Progress in Energy and Combustion Science*, vol. 10, p. 319, 1984.
313. Pope, S. B.: "PDF methods for turbulent reactive flows," *Progress in Energy and Combustion Science*, vol. 11, pp. 119–192, 1985.
314. Bilger, R. W.: "Turbulent flows with nonpremixed reactants," in *Turbulent Reacting Flows*, Springer Verlag, pp. 65–113, 1980.
315. Kuo, K. K.: *Principles of Combustion*, Wiley Interscience, New York, 1986.
316. Lesieur, M.: *Turbulence in Fluids*, 3rd ed., Kluwer Academic Publishers, 1996.
317. Peters, N.: *Turbulent Combustion*, Cambridge University Press, Cambridge, 2000.
318. Pope, S. B.: *Turbulent Flows*, Cambridge University Press, Cambridge, 2000.

319. Haworth, D. C.: "Progress in probability density function methods for turbulent reacting flows," *Progress in Energy and Combustion Science*, vol. 16, pp. 168–259, 2010.
320. Kabashnikov, V. P., and G. I. Kmit: "Influence of turbulent fluctuations of thermal radiation," *Journal of Applied Spectroscopy*, vol. 31, pp. 963–967, 1979.
321. Kabashnikov, V. P.: "Thermal radiation of turbulent flows in the case of large fluctuations of the absorption coefficient and the Planck function," *Journal of Engineering Physics*, vol. 49, no. 1, pp. 778–784, 1985.
322. Kabashnikov, V. P., and G. I. Myasnikova: "Thermal radiation in turbulent flows—temperature and concentration fluctuations," *Heat Transfer-Soviet Research*, vol. 17, no. 6, pp. 116–125, 1985.
323. Mazumder, S.: "Numerical study of chemically reactive turbulent flows with radiative heat transfer," Ph.D. thesis, The Pennsylvania State University, University Park, PA, 1997.
324. Jeng, S. M., M. C. Lai, and G. M. Faeth: "Nonluminous radiation in turbulent buoyant axisymmetric flames," *Combustion Science and Technology*, vol. 40, pp. 41–53, 1984.
325. Faeth, G. M.: "Heat and mass transfer in flames," in *Proceedings of the Eighth International Heat Transfer Conference*, Hemisphere, Washington, D.C., pp. 151–160, 1986.
326. Gore, J. P., and G. M. Faeth: "Structure and spectral radiation properties of turbulent ethylene/air diffusion flames," in *Proceedings of the Twenty-First Symposium (International) on Combustion*, pp. 1521–1531, 1986.
327. Gore, J. P., S. M. Jeng, and G. M. Faeth: "Spectral and total radiation properties of turbulent carbon monoxide/air diffusion flames," *AIAA Journal*, vol. 25, no. 2, pp. 339–345, 1987.
328. Gore, J. P., and G. M. Faeth: "Structure and spectral radiation properties of luminous acetylene/air diffusion flames," *ASME Journal of Heat Transfer*, vol. 110, pp. 173–181, 1988.
329. Kounalakis, M. E., J. P. Gore, and G. M. Faeth: "Turbulence/radiation interactions in nonpremixed hydrogen/air flames," in *Twenty-Second Symposium (International) on Combustion*, The Combustion Institute, pp. 1281–1290, 1988.
330. Kounalakis, M. E., J. P. Gore, and G. M. Faeth: "Mean and fluctuating radiation properties of nonpremixed turbulent carbon monoxide/air flames," *ASME Journal of Heat Transfer*, vol. 111, pp. 1021–1030, 1989.
331. Faeth, G. M., J. P. Gore, S. G. Chuech, and S. M. Jeng: "Radiation from turbulent diffusion flames," in *Annual Review of Numerical Fluid Mechanics and Heat Transfer*, vol. 2, Hemisphere, Washington, D.C., pp. 1–38, 1989.
332. Sivathanu, Y. R., M. E. Kounalakis, and G. M. Faeth: "Soot and continuous radiation statistics of luminous turbulent diffusion flames," in *Twenty-Third Symposium (International) on Combustion*, The Combustion Institute, pp. 1543–1550, 1990.
333. Kounalakis, M. E., Y. R. Sivathanu, and G. M. Faeth: "Infrared radiation statistics of nonluminous turbulent diffusion flames," *ASME Journal of Heat Transfer*, vol. 113, no. 2, pp. 437–445, 1991.
334. Cox, G.: "On radiant heat transfer from turbulent flames," *Combustion Science and Technology*, vol. 17, pp. 75–78, 1977.
335. Song, T.-H., and R. Viskanta: "Interaction of radiation with turbulence: Application to a combustion system," *Journal of Thermophysics and Heat Transfer*, vol. 1, no. 1, pp. 56–62, 1987.
336. Nelson, D. A.: "Band radiation from a fluctuating medium," *ASME Journal of Heat Transfer*, vol. 111, no. 1, pp. 131–134, 1989.
337. Kritzstein, F., and A. Soufiani: "Infrared gas radiation from a homogeneously turbulent medium," *International Journal of Heat and Mass Transfer*, vol. 36, no. 7, pp. 1749–1762, 1993.
338. Hall, R. J., and A. Vranos: "Efficient calculations of gas radiation from turbulent flames," *International Journal of Heat and Mass Transfer*, vol. 37, no. 17, pp. 2745–2750, 1994.
339. Hartick, J. W., M. Tacke, G. Fruchtel, E. P. Hassel, and J. Janicka: "Interaction of turbulence and radiation in confined diffusion flames," in *Twenty-Sixth Symposium (International) on Combustion*, The Combustion Institute, pp. 75–82, 1996.
340. Krebs, W., R. Koch, B. Ganz, L. Eigenmann, and S. Wittig: "Effect of temperature and concentration fluctuations on radiative heat transfer in turbulent flames," in *Twenty-Sixth Symposium (International) on Combustion*, The Combustion Institute, pp. 2763–2770, 1996.
341. Townsend, A. A.: "The effects of radiative transfer on turbulent flow of a stratified fluid," *Journal of Fluid Mechanics*, vol. 4, pp. 361–375, 1958.
342. Sheved, G. M., and R. A. Akmayev: "Influence of radiative heat transfer on turbulence in planetary atmospheres," *Atmospheric and Oceanic Physics*, vol. 10, pp. 547–559, 1974.
343. Coantic, M., and O. Simonin: "Radiative effects on turbulent temperature spectra and budgets in the planetary boundary layer," *Journal of the Atmospheric Sciences*, vol. 41, pp. 2629–2629, 1984.
344. Soufiani, A.: "Temperature turbulence spectrum for high-temperature radiating gases," *Journal of Thermophysics and Heat Transfer*, vol. 5, no. 4, pp. 489–494, 1991.
345. Wang, A., M. F. Modest, D. C. Haworth, and L. Wang: "Monte Carlo simulation of radiative heat transfer and turbulence interactions in methane/air jet flames," *Journal of Quantitative Spectroscopy and Radiative Transfer*, vol. 109, no. 2, pp. 269–279, 2008.
346. Sakurai, A., S. Maruyama, K. Matsubara, T. Miura, and M. Behnia: "An efficient method for radiative heat transfer applied to a turbulent channel flow," *ASME Journal of Heat Transfer*, vol. 132, no. 2, p. 023507, 2010.
347. Mazumder, S., and M. F. Modest: "A PDF approach to modeling turbulence–radiation interactions in nonluminous flames," *International Journal of Heat and Mass Transfer*, vol. 42, pp. 971–991, 1999.
348. Mazumder, S., and M. F. Modest: "Turbulence–radiation interactions in nonreactive flow of combustion gases," *ASME Journal of Heat Transfer*, vol. 121, pp. 726–729, 1999.

349. Li, G., and M. F. Modest: "Application of composition PDF methods in the investigation of turbulence–radiation interactions," *Journal of Quantitative Spectroscopy and Radiative Transfer*, vol. 73, no. 2–5, pp. 461–472, 2002.
350. Li, G., and M. F. Modest: "Importance of turbulence–radiation interactions in turbulent diffusion jet flames," *ASME Journal of Heat Transfer*, vol. 125, pp. 831–838, 2003.
351. Li, G.: "Investigation of turbulence–radiation interactions by a hybrid FV/PDF Monte Carlo method," Ph.D. thesis, The Pennsylvania State University, University Park, PA, 2002.
352. *FLUENT Computational Fluid Dynamics Software*, Version 5, Fluent Corp., New Hampshire, 1998.
353. Pope, S. B.: "On the relationship between stochastic Lagrangian models of turbulence and second-moment closures," *Physics of Fluids*, vol. 6, pp. 973–985, 1994.
354. Pope, S. B.: "Particle method for turbulent flows: Integration of stochastic model equations," *Journal of Computational Physics*, vol. 117, pp. 332–349, 1995.
355. Barlow, R. S.: *International Workshop on Measurement and Computation of Turbulent Nonpremixed Flames (TNF)* website: http://www.sandia.gov/TNF/abstract.html.
356. Coelho, P. J.: "Detailed numerical simulation of radiative transfer in a nonluminous turbulent jet diffusion flame," *Combustion and Flame*, vol. 136, pp. 481–492, 2004.
357. Xu, X., Y. Chen, and H. Wang: "Detailed numerical simulation of thermal radiation influence in Sandia flame D," *International Journal of Heat and Mass Transfer*, vol. 49, pp. 2347–2355, 2006.
358. Habibi, A., B. Merci, and D. Roekaerts: "Turbulence radiation interaction in Reynolds-averaged Navier-Stokes simulations of nonpremixed piloted turbulent laboratory-scale flames," *Combustion and Flame*, vol. 151, pp. 303–320, 2007.
359. Pal, G., A. Gupta, M. F. Modest, and D. C. Haworth: "Comparison of accuracy and computational expense of radiation models in simulation of nonpremixed turbulent jet flames," in *Proceedings of 2011 ASME/JSME Thermal Engineering Joint Conference*, 2011.
360. Tessé, L., F. Dupoirieux, and J. Taine: "Monte Carlo modeling of radiative transfer in a turbulent sooty flame," *International Journal of Heat and Mass Transfer*, vol. 47, pp. 555–572, 2004.
361. Zamuner, B., and F. Dupoirieux: "Numerical simulation of soot formation in a turbulent flame with a Monte-Carlo PDF approach and detailed chemistry," *Combustion Science and Technology*, vol. 158, pp. 407–438, 2000.
362. Soufiani, A., and J. Taine: "High temperature gas radiative property parameters of statistical narrow-band model for H_2O, CO_2 and CO, and correlated-k model for H_2O and CO_2," *International Journal of Heat and Mass Transfer*, vol. 40, no. 4, pp. 987–991, 1997.
363. Wang, A., and M. F. Modest: "An adaptive emission model for Monte Carlo ray-tracing in participating media represented by statistical particle fields," *Journal of Quantitative Spectroscopy and Radiative Transfer*, vol. 104, no. 2, pp. 288–296, 2007.
364. Wang, A., and M. F. Modest: "Spectral Monte Carlo models for nongray radiation analyses in inhomogeneous participating media," *International Journal of Heat and Mass Transfer*, vol. 50, pp. 3877–3889, 2007.
365. Mehta, R. S., A. Wang, M. F. Modest, and D. C. Haworth: "Modeling of a turbulent ethylene/air flame using hybrid finite volume/Monte Carlo methods," *Computational Thermal Sciences*, vol. 1, pp. 37–53, 2009.
366. Mehta, R. S., D. C. Haworth, and M. F. Modest: "Composition PDF/photon Monte Carlo modeling of moderately sooting turbulent jet flames," *Combustion and Flame*, vol. 157, pp. 982–994, 2010.
367. Mehta, R. S., M. F. Modest, and D. C. Haworth: "Radiation characteristics and turbulence–radiation interactions in sooting turbulent jet flames," *Combust. Theory and Modelling*, vol. 14, no. 1, pp. 105–124, 2010.
368. Coppalle, A., and D. Joyeux: "Temperature and soot volume fraction in turbulent diffusion flames: Measurements of mean and fluctuating values," *Combustion and Flame*, vol. 96, pp. 275–285, 1994.
369. Kent, J. H., and D. Honnery: "Modeling sooting turbulent jet flames using an extended flamelet technique," *Combustion Science and Technology*, vol. 54, pp. 383–397, 1987.
370. Endrud, N. E.: "Soot, radiation and pollutant emissions in oxygen-enhanced turbulent jet flames," M.S. thesis, The Pennsylvania State University, University Park, PA, 2000.
371. Mehta, R. S., D. C. Haworth, and M. F. Modest: "An assessment of gas-phase thermochemistry and soot models for laminar atmospheric-pressure ethylene–air flames," *Proceedings of the Combustion Institute*, vol. 32, pp. 1327–1334, 2009.
372. Chandy, A. J., D. J. Glaze, and S. H. Frankel: "A general semicausal stochastic model for turbulence/ radiation interactions in flames," *ASME Journal of Heat Transfer*, vol. 113, no. 3, pp. 509–516, 1997.
373. Gupta, A., D. C. Haworth, and M. F. Modest: "Turbulence-radiation interactions in large-eddy simulations of luminous and nonluminous nonpremixed flames," *Proceedings of the Combustion Institute*, vol. 34, 2013, accepted.
374. Roger, M., C. B. D. Silva, and P. J. Coelho: "Analysis of the turbulence–radiation interactions for large eddy simulations of turbulent flows," *International Journal of Heat and Mass Transfer*, vol. 52, pp. 2243–2254, 2009.
375. Roger, M., P. J. Coelho, and C. B. da Silva: "The influence of the non-resolved scales of thermal radiation in large eddy simulation of turbulent flows: A fundamental study," *International Journal of Heat and Mass Transfer*, vol. 53, pp. 2897–2907, 2010.
376. Wu, Y., D. C. Haworth, M. F. Modest, and B. Cuenot: "Direct numerical simulation of turbulence/radiation interaction in premixed combustion systems," *Proceedings of the Combustion Institute*, vol. 30, pp. 639–646, 2005.
377. Wu, Y., M. F. Modest, and D. C. Haworth: "A high-order photon Monte Carlo method for radiative transfer in direct numerical simulation of chemically reacting turbulent flows," *Journal of Computational Physics*, vol. 223 (2), pp. 898–922, 2007.

378. Deshmukh, K. V., D. C. Haworth, and M. F. Modest: "Direct numerical simulation of turbulence–radiation interactions in a statistically homogeneous nonpremixed combustion system," *Proceedings of the Combustion Institute*, vol. 31, pp. 1641–1648, 2007.
379. Deshmukh, K. V., M. F. Modest, and D. C. Haworth: "Direct numerical simulation of turbulence–radiation interactions in statistically one-dimensional nonpremixed combustion systems," *Journal of Quantitative Spectroscopy and Radiative Transfer*, vol. 109, no. 14, pp. 2391–2400, 2008.
380. Deshmukh, K. V., M. F. Modest, and D. C. Haworth: "Higher-order spherical harmonics to model radiation in direct numerical simulation of turbulent reacting flows," *Computational Thermal Sciences*, vol. 1, pp. 207–230, 2009.
381. Modest, M. F., and G. Li: "Turbulence radiation interactions," in *Modelling and Simulation of Turbulent Heat Transfer*, eds. B. Sundeń and M. Faghri, Developments in Heat Transfer, WIT Press, Southampton, England, 2004.
382. Modest, M. F.: "Multiscale modeling of turbulence, radiation, and combustion interactions in turbulent flames," *International Journal for Multiscale Computational Engineering*, vol. 3, no. 2, pp. 85–106, 2005.
383. Modest, M. F.: "Radiative heat transfer in fire modeling," in *Transport Phenomena in Fires*, eds. B. Sundeń and M. Faghri, Developments in Heat Transfer, WIT Press, Southampton, England, 2006.
384. Coelho, P. J.: "Numerical simulation of the interaction between turbulence and radiation in reactive flows," *Progress in Energy and Combustion Science*, vol. 33, pp. 311–383, 2007.
385. Lovegrove, K., and A. Luzzi: "Solar thermal power systems," in *Encyclopedia of Physical Science and Technology*, ed. R. A. Meiers, vol. 15, Academic Press, San Diego, pp. 223–235, 2001.
386. Barlev, D., R. Vidu, and P. Stroeve: "Innovation in concentrated solar power," *Solar Energy Materials and Solar Cells*, vol. 95, pp. 2703–2725, 2011.
387. Fletcher, E. A.: "Solarthermal processing: A review," *ASME Journal of Solar Energy Engineering*, vol. 123, pp. 63–74, 2001.
388. Steinfeld, A., and R. Palumbo: "Solar thermochemical process technology," in *Encyclopedia of Physical Science and Technology*, ed. R. Meiers, vol. 15, Academic Press, San Diego, pp. 237–256, 2001.
389. Kodama, T.: "High-temperature solar chemistry for converting solar heat to chemical fuels," *Progress in Energy and Combustion Science*, vol. 29, pp. 567–597, 2003.
390. Royne, A., C. J. Dey, and D. R. Mills: "Cooling of photovoltaic cells under concentrated illumination: A critical review," *Solar Energy Materials and Solar Cells*, vol. 86, pp. 451–483, 2005.
391. Vossier, A., D. Chemisana, G. Flamant, and A. Dollet: "Very high fluxes for concentrating photovoltaics: Considerations from simple experiments and modeling," *Renewable Energy*, vol. 16, pp. 31–39, 2012.
392. Cotal, H., C. Fetzer, J. Boisvert, G. Kinsey, R. King, P. Hebert, H. Yoon, and N. Karam: "III–V multijunction solar cells for concentrating photovoltaics," *Energy and Environmental Science*, vol. 5, pp. 174–192, 2003.
393. Fletcher, E. A., and R. L. Moen: "Hydrogen and oxygen from water," *Science*, vol. 197, pp. 1050–1056, 1977.
394. Maag, G., W. Lipiński, and A. Steinfeld: "Particle–gas reacting flow under concentrated solar irradiation," *International Journal of Heat and Mass Transfer*, vol. 52, pp. 4997–5004, 2009.
395. Hischier, I., D. Hess, W. Lipiński, M. F. Modest, and A. Steinfeld: "Heat transfer analysis of a novel pressurized air receiver for concentrated solar power via combined cycles," *Journal of Thermal Science and Engineering Applications*, vol. 1, p. 041002, 2009.
396. Karni, J., A. Kribus, R. Rubin, and P. Doron: "The "Porcupine": A novel high-flux absorber for volumetric solar receivers," *ASME Journal of Solar Energy Engineering*, vol. 120, pp. 85–95, 1998.
397. Ávila Marín, A. L.: "Volumetric receivers in solar thermal power plants with central receiver system technology: A review," *Solar Energy*, vol. 85, no. 5, pp. 891–910, 2011.
398. Flamant, G.: "Theoretical and experimental study of radiant heat transfer in a solar fluidized-bed receiver," *AIChE Journal*, vol. 18, pp. 529–535, 1982.
399. Flamant, G., T. Menigault, and D. Schwander: "Combined heat transfer in a semitransparent multilayer packed bed," *ASME Journal of Heat Transfer*, vol. 110, no. 2, pp. 463–467, 1988.
400. Tan, T., and Y. Chen: "Review of study on solid particle solar receivers," *Renewable and Sustainable Energy Reviews*, vol. 14, no. 1, pp. 265–276, 2010.
401. Maag, G., C. Falter, and A. Steinfeld: "Temperature of a quartz/sapphire window in a solar cavity-receiver," *ASME Journal of Solar Energy Engineering*, vol. 133, no. 1, p. 014501, 2011.
402. Yong, S., F.-Q. Wang, X. L. Xia, H. P. Tan, and Y.-C. Liang: "Radiative properties of a solar cavity receiver/reactor with quartz window," *International Journal of Hydrogen Energy*, vol. 36, no. 19, pp. 12148–12158, 2011.
403. Brock, W. H.: *The Norton History of Chemistry*, W. W. Norton & Company, Inc., New York, 1993.
404. Trombe, F., and M. Foex: "Essai de metallurgie du chrome par l'hydrogene au four solaire," *Revue de Métallurgie*, vol. 48, pp. 359–362, 1951.
405. Nakamura, T.: "Hydrogen production from water utilizing solar heat at high temperatures," *Solar Energy*, vol. 19, no. 5, pp. 467–475, 1977.
406. Palumbo, R., M. Keunecke, S. Möller, and A. Steinfeld: "Reflections on the design of solar thermal chemical reactors: Thoughts in transformation," *Energy*, vol. 29, pp. 727–744, 2004.
407. Lapp, J., J. H. Davidson, and W. Lipiński: "Efficiency of two-step solar thermochemical partial redox cycles with heat recovery," *Energy*, vol. 37, pp. 591–600, 2012.
408. Lipiński, W., D. Thommen, and A. Steinfeld: "Unsteady radiative heat transfer within a suspension of ZnO particles undergoing thermal dissociation," *Chemical Engineering Science*, vol. 61, pp. 7029–7035, 2006.

409. Abanades, S., P. Charvin, and G. Flamant: "Design and simulation of a solar chemical reactor for the thermal reduction of metal oxides: Case study of zinc oxide dissociation," *Chemical Engineering Science*, vol. 62, no. 22, pp. 6323–6333, 2007.
410. Müller, R., W. Lipiński, and A. Steinfeld: "Transient heat transfer in a directly-irradiated solar chemical reactor for the thermal dissociation of ZnO," *Applied Thermal Engineering*, vol. 28, pp. 524–531, 2008.
411. Schunk, L. O., W. Lipiński, and A. Steinfeld: "Ablative heat transfer in a shrinking packed-bed of ZnO undergoing solar thermal dissociation," *AIChE Journal*, vol. 55, pp. 1659–1666, 2009.
412. Dombrovsky, L. A., L. O. Schunk, W. Lipiński, and A. Steinfeld: "An ablation model for the thermal decomposition of porous zinc oxide layer heated by concentrated solar radiation," *International Journal of Heat and Mass Transfer*, vol. 52, pp. 2444–2452, 2009.
413. Villafán-Vidales, H. I., C. A. Arancibia-Bulnes, U. Dehesa-Carrasco, and H. Romero-Paredes: "Monte Carlo radiative transfer simulation of a cavity solar reactor for the reduction of cerium oxide," *International Journal of Hydrogen Energy*, vol. 34, no. 1, pp. 115–124, 2009.
414. Liang, Z., W. C. Chueh, K. Ganesan, S. M. Haile, and W. Lipiński: "Experimental determination of transmittance of porous cerium dioxide media in the spectral range 300–1,100 nm," *Experimental Heat Transfer*, vol. 24, pp. 285–299, 2011.
415. Ganesan, K., and W. Lipiński: "Experimental determination of spectral transmittance of porous cerium dioxide in the range 900–1,700 nm," *ASME Journal of Heat Transfer*, vol. 133, p. 104501, 2011.
416. Ganesan, K., L. A. Dombrovsky, and W. Lipiński: "A novel methodology to determine spectral radiative properties of ceria ceramics," in *Proceedings of the Eurotherm Seminar 95—Computational Thermal Radiation in Participating Media IV*, eds. P. Boulet and D. Lacroix, Nancy, 18–20 April 2012.
417. Haussener, S., and A. Steinfeld: "Effective heat and mass transport properties of anisotropic porous ceria for solar thermochemical fuel generation," *Materials*, vol. 5, pp. 192–209, 2012.
418. Lipiński, W., and A. Steinfeld: "Transient radiative heat transfer within a suspension of coal particles undergoing steam gasification," *Heat and Mass Transfer*, vol. 41, pp. 1021–1032, 2005.
419. Lipiński, W., A. Z'Graggen, and A. Steinfeld: "Transient radiation heat transfer within a nongray nonisothermal absorbing-emitting-scattering suspension of reacting particles undergoing shrinkage," *Numerical Heat Transfer – Part B: Fundamentals*, vol. 47, pp. 443–457, 2005.
420. Maag, G., S. Rodat, G. Flamant, and A. Steinfeld: "Heat transfer model and scale-up of an entrained-flow solar reactor for the thermal decomposition of methane," *International Journal of Hydrogen Energy*, vol. 35, no. 24, pp. 13232–13241, 2010.
421. Lipiński, W., and A. Steinfeld: "Heterogeneous thermochemical decomposition under direct irradiation," *International Journal of Heat and Mass Transfer*, vol. 47, pp. 1907–1916, 2004.
422. Dombrovsky, L. A., and W. Lipiński: "Transient temperature and thermal stress profiles in semi-transparent particles under high-flux irradiation," *International Journal of Heat and Mass Transfer*, vol. 50, pp. 2117–2123, 2007.

Problems

22.1 A vat of molten glass is heated from below by a gray, diffuse surface with $T = 1800\,\text{K}$ and $\epsilon = 0.8$. The glass layer is 1 m thick, and its top is exposed to free convection and radiation with an ambient space at 1000 K (heat transfer coefficient for free convection = $5\,\text{W/m}^2\,\text{K}$). Neglecting convection within the melt, estimate the temperature distribution within the glass, using the radiative properties of glass as given in Figs. 1-17 and 3-16. What is the total heat loss from the bottom surface?

22.2 Estimate the total heat flux for Problem 22.1, as well as the glass–air interface temperature, by using the additive solution method.

22.3 A glass sphere ($D = 4\,\text{cm}$) initially at uniform temperature $T_i = 300\,\text{K}$ is placed into a furnace, whose walls and inert gas are at a uniform $T_g = T_w = 1500\,\text{K}$. Assuming the glass to be gray and nonscattering ($\kappa = 1\,\text{cm}^{-1}$, $n = 1.5$, $k = 1.5\,\text{W/m K}$) and a sphere/furnace gas heat transfer coefficient of $10\,\text{W/m}^2\,\text{K}$, determine the sphere's temperature distribution as a function of time.

22.4 A 1 cm thick quartz window (assumed gray with $\kappa = 1\,\text{cm}^{-1}$ and $n = 1.5$) forms the barrier between a furnace and the ambient, resulting in face temperatures of $T_1 = 800\,\text{K}$ and $T_2 = 400\,\text{K}$. Estimate the conductive, radiative, and total heat fluxes passing through the window ($k = 1.5\,\text{W/m K}$).

22.5 Repeat Problem 5.36 for the case in which a gray, isotropically scattering, stationary gas ($\kappa = 2\,\text{cm}^{-1}$, $k = 0.04\,\text{W/m K}$) is filling the 1 cm thick gap between surface and shield.

22.6 A sheet of ice 20 cm thick is lying on top of black soil. Initially, ice and soil are at −10°C when the sun begins to shine, hitting the top of the ice with a strength of $800\,\text{W/m}^2$ (normal to the rays), at an off-normal angle of 30°. Assume the ground to be insulated, ice and water to have constant and equal

properties (k, ρ, c_p), a gray absorption coefficient (for solar light) of $\kappa \simeq 1\,\text{cm}^{-1}$, and a gray reflectance of 0.02. Neglecting emission from and scattering by the ice, as well as convection losses/gains at the surface, determine the transient temperature distribution within the ice/water until the time when all ice has melted.

22.7 Consider a gray medium separating an axle from its bearing. The gap is so narrow that the movement between axle and bearing may be approximated by Couette flow (two infinite parallel plates, one stationary, and the other moving at constant velocity U). The movement is so rapid that viscous dissipation must be considered [$\Phi = (\partial u/\partial y)^2$, where $u = u(y)$ is the velocity at a distance y from the lower, stationary plate]. The medium is gray and nonscattering with a constant absorption coefficient, and both surfaces are isothermal (at different temperatures) and gray-diffuse. Set up the necessary equations and boundary conditions to calculate the net heat transfer rates on the two surfaces.

22.8 Consider a solar water heater as shown in the adjacent sketch. A 5 mm thick layer of water is flowing down a black, insulated plate as shown while exposed to sunshine. The water is seeded with a fine powder that gives it a gray absorption coefficient of $\kappa = 5\,\text{cm}^{-1}$. The top of the water layer loses heat by free convection ($h = 10\,\text{W/m}^2\,\text{K}$) to the ambient at $T_{\text{amb}} = 300\,\text{K}$. At the top of the collector ($x = 0$) the water enters at a uniform temperature of $T_0 = 300\,\text{K}$. The velocity profile may be considered fully developed everywhere. Determine the cumulative collected solar energy as a function of x.

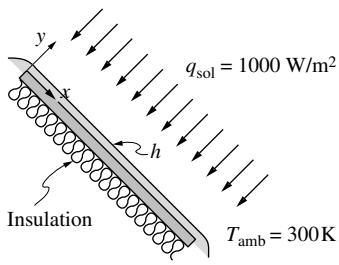

22.9 Consider a gas–particulate mixture flowing through an isothermal tube ($\epsilon_w = 1$, $T_w = 400\,\text{K}$). The gas is radiatively nonparticipating and has constant velocity u across the tube cross-section such that $\text{Pe} = \text{Re}\,\text{Pr} = uD/\alpha = 30{,}000$. The particles are very small, gray, and uniformly distributed such that $\kappa_p R = 5$ (no scattering) and $(\dot{m}\,c_p)_{\text{particles}}/(\dot{m}\,c_p)_{\text{gas}} = 2$. The particles are so small that they are essentially at the same temperature as the gas surrounding them. Using the diffusion approximation for the radiative heat transfer, set up the relevant equations and boundary conditions for the calculation of local bulk temperature and local total heat flux. Obtain a numerical solution (after neglecting axial conduction and radiation), and compare with Figs. 22-13 and 22-14.